A Strain Energy Function for Large Deformations of Curved Beams

by

Ian Mackenzie

A thesis

presented to the University of Waterloo

in fulfilment of the

thesis requirement for the degree of

Master of Applied Science

in

Systems Design Engineering

Waterloo, Ontario, Canada, 2008

I hereby declare that I am the sole author of this thesis. This is a true copy of the thesis, including any required final revisions, as accepted by my examiners. I understand that my thesis may be made electronically available to the public.

Abstract

This thesis develops strain and kinetic energy functions and a finite beam element useful for analyzing curved beams which go through large deflections, such as a hockey stick being swung and bent substantially as it hits the ice. The resulting beam model is demonstrated to be rotation invariant and capable of computing the correct strain energy and reaction forces for a specified deformation. A method is also described by which the model could be used to perform static or dynamic simulations of a beam.

Acknowledgements

I would like to thank my supervisor, Glenn Heppler, both for invaluable help guiding me through the research process and for allowing me the freedom to pursue many unusual (and several ultimately unworkable) ideas. I would also like to give thanks to Tim Lahey, for countless hours of discussion and debate over solid mechanics, LaTeX, MATLAB and so many other topics both before and during the Master's program. And, of course, to B., for patiently putting up with many late nights in the office trying to put everything together! Finally, I would like to thank my family for their constant support throughout my university career, and NSERC for providing the financial assistance that made this thesis possible.

Contents

List of Figures

List of Tables

Nomenclature

$(\cdot)^*$ — Value of a quantity $(\cdot)$ before deformation

$\dot{(\cdot)}$ — Derivative of a quantity $(\cdot)$ with respect to time

$\gamma_{x_c y_c}$, $\gamma_{x_c z_c}$ — Shear strains on a cross-section

ϵ — Column matrix of strains

$\epsilon_{x_c x_c}$ — Strain normal to a cross-section

θ_{A_0}, θ_{A_m}, θ_{A_1} — Cross-section angles with respect to spline Frenet frame

θ_A — Angle between $\vec{v}_A$ and $\vec{b}_A$

θ_B — Angle between $\vec{v}_B$ and $\vec{b}_B$

$\vec{b}_A$ — Normal vector to the plane in which $\vec{\ell}_A$ lies, or equivalently the binormal vector of the Frenet frame $\vec{\mathcal{F}}_\alpha$

$\vec{b}_B$ — Normal vector to the plane in which $\vec{\ell}_B$ lies, or equivalently the binormal vector of the Frenet frame $\vec{\mathcal{F}}_\beta$

θ_{A_0}, θ_{A_m}, θ_{A_1} — Control points for the scalar quadratic spline specifying the angle of cross-sections relative to the Frenet frame of first quadratic spline defining the locus of centroids

θ_{B_0}, θ_{B_m}, θ_{B_1} — Control points for the scalar quadratic spline specifying the angle of cross-sections relative to the Frenet frame of second quadratic spline defining the locus of centroids

θ_m	Angle between $\vec{\mathcal{F}}_{\beta_0}$ and $\vec{\mathcal{F}}_{\alpha_1}$
θ_{rel}	Net relative angle between cross-sections over the length of an element, measured with respect to the progressive frame $\vec{\mathcal{F}}_p$.
κ	Curvature of the deformed locus of centroids
κ_u, κ_v	Curvatures around the axes defined by $\vec{u}$ and $\vec{v}$ respectively (radians per unit length)
$\vec{\nu}$	Velocity of a point along the locus of centroids
$\vec{\nu}_A$	Velocity of the centroid of cross-section A
ξ	Rate of extension along the locus of centroids
ξ_A	Rate of extension along the locus of centroids at cross-section A
$\vec{\rho}(\tau, r_u, r_v)$	Position vector of a point within the beam
$\vec{\rho}_A$	Position vector of the centroid of cross-section A
$\vec{\rho}_m$	Mid control point, equal to the third control point of $\vec{\ell}_A$ and the first control point of $\vec{\ell}_B$
ϱ	Mass density per unit volume
$\sigma_{x_c x_c}$	Normal stress to a beam cross-section
$\sigma_{x_c z_c}, \sigma_{x_c y_c}$	Shear stresses on a beam cross-section
τ	Parameter describing the locus of centroids, in the range $[0, 1]$
τ_A, τ_B	Parameters in the range $[0, 1]$ describing the two splines making up the locus of centroids between cross-sections A and B
τ_c	Value of parameter τ at a specific cross-section
$\phi_{x_A}, \phi_{y_A}, \phi_{z_A}$	Rotation angles of cross-section A about the axes of $\vec{\mathcal{F}}_a$

$\phi_{x_B}, \phi_{y_B}, \phi_{z_B}$ Rotation angles of cross-section B about the axes of $\vec{\mathcal{F}}_a$

χ_{mn} Generalized moment of area of a cross-section

ψ Twist rate about the locus of centroids (radians per unit length)

ψ_A Rate of twist of cross-sections about the locus of centroids at cross-section A

$\vec{\omega}_A$ Angular velocity of cross-section A

$\Delta\xi$ Change in locus of centroids extension rate relative to the undeformed configuration, $\xi - \xi^*$

$\Delta(\xi\kappa_u), \Delta(\xi\kappa_v)$ Changes in locus of centroids extension-curvature products, $\xi\kappa_u - \xi^*\kappa_u^*$ and $\xi\kappa_v - \xi^*\kappa_v^*$

$\Delta(\xi\psi)$ Change in locus of centroids extension-twist product, $\xi\psi - \xi^*\psi^*$

A Cross-sectional area

$\vec{a}_1, \vec{a}_2, \vec{a}_3$ Unit basis vectors of $\vec{\mathcal{F}}_a$ defining the coordinate axes

$\vec{b}$ Unit binormal vector to the locus of centroids

$\mathbf{C}$ Material constitutive matrix

$\vec{c}_1$ First unit basis vector of $\vec{\mathcal{F}}_c$, equal to $\vec{t}$ of the cross-section associated with $\vec{\mathcal{F}}_c$

$\vec{c}_2$ Second unit basis vector of $\vec{\mathcal{F}}_c$, equal to $\vec{u}$ of the the cross-section associated with $\vec{\mathcal{F}}_c$

$\vec{c}_3$ Third unit basis vector of $\vec{\mathcal{F}}_c$, equal to $\vec{v}$ of the the cross-section associated with $\vec{\mathcal{F}}_c$

$\vec{c}_A$ Second control point of $\vec{\ell}_A(\tau_A)$

$\vec{c}_B$ Second control point of $\vec{\ell}_B(\tau_B)$

d_{00}, d_{01}, d_{11} Dot products of spline control legs

$\vec{d}_0, \vec{d}_1$ Quadratic spline control legs

E Modulus of elasticity

$\mathbf{F}$ $3{\times}3$ deformation gradient giving derivatives of coordinates x_c, y_c, z_c with respect to undeformed (original) coordinates x_c^*, y_c^*, z_c^*

F Internal axial force in the beam

$\vec{\mathcal{F}}_{\alpha_0}$ Frenet frame at the start of $\vec{\ell}_A$, made up of $\vec{t}_A$, $\vec{n}_{A_0}$, and $\vec{b}_A$

$\vec{\mathcal{F}}_{\alpha_1}$ Frenet frame at the end of $\vec{\ell}_A$, made up of $\vec{t}_m$, $\vec{n}_{A_1}$, and $\vec{b}_A$

$\vec{\mathcal{F}}_{\alpha}$ Frenet frame of $\vec{\ell}_A$

$\vec{\mathcal{F}}_{\beta_0}$ Frenet frame at the end of $\vec{\ell}_B$, made up of $\vec{t}_B$, $\vec{n}_{B_1}$, and $\vec{b}_B$

$\vec{\mathcal{F}}_{\beta_0}$ Frenet frame at the start of $\vec{\ell}_B$, made up of $\vec{t}_m$, $\vec{n}_{B_0}$, and $\vec{b}_B$

$\vec{\mathcal{F}}_{\beta}$ Frenet frame of $\vec{\ell}_B$

$\vec{\mathcal{F}}_a$ Global, fixed, Cartesian frame

$\vec{\mathcal{F}}_{A_0}$ Frame of cross-section A, made up of $\vec{t}_A$, $\vec{n}_{A_0}$ and $\vec{b}_A$

$\vec{\mathcal{F}}_b$ Cartesian frame, originally aligned with $\vec{\mathcal{F}}_a$, which is attached to a specific cross-section of the beam and rotates with that cross-section

$\vec{\mathcal{F}}_{B_1}$ Frame of cross-section B, made up of $\vec{t}_B$, $\vec{n}_{B_1}$ and $\vec{b}_B$

$\vec{\mathcal{F}}_c$ A Cartesian frame attached to a specific beam cross-section

$\vec{\mathcal{F}}_p$ Progressive frame defined along both splines making up the locus of centroids

G Shear modulus

I_{mn} Indexed moment of area of a cross-section

L Lagrangian of one element

$\vec{\ell}(\tau)$ Position vector of a point along the locus of centroids

$\vec{\ell}_A(\tau_A), \vec{\ell}_B(\tau_B)$ Position vectors of points on the two quadratic splines making up the locus of centroids between cross-sections A and B

M_t Internal twisting moment in the beam (about an axis aligned with $\vec{t}$

M_u Internal bending moment in the beam about an axis aligned with $\vec{u}$

M_v Internal bending moment in the beam about an axis aligned with $\vec{v}$

$\vec{n}$ Unit principal normal vector to the locus of centroids

$\vec{n}_{A_0}$ Principal normal vector at the start of $\vec{\ell}_A$ (at the cross-section A)

$\vec{n}_{A_1}$ Principal normal vector at the end of $\vec{\ell}_A$ (where it meets $\vec{\ell}_B$)

$\vec{n}_{B_0}$ Principal normal vector at the start of $\vec{\ell}_B$ (where it meets $\vec{\ell}_A$)

$\vec{n}_{B_1}$ Principal normal vector at the end of $\vec{\ell}_B$ (at the cross-section B)

$\vec{p}_0, \vec{p}_1, \vec{p}_2$ Quadratic spline control points

Q_i Generalized force corresponding to coordinate q_i, *i.e.* the partial derivative of work W with respect to that coordinate

q_i Generalized coordinates describing one beam element

q_{A_k} Parameters describing the beam half element associated with cross-section A

$\mathbf{R}_{A_0}$ Rotation matrix giving the orientation of $\vec{\mathcal{F}}_{A_0}$ from the Frenet frame $\vec{\mathcal{F}}_{\alpha_0}$

$\mathbf{R}_{B_1}$ Rotation matrix giving the orientation of $\vec{\mathcal{F}}_{B_1}$ from the Frenet frame $\vec{\mathcal{F}}_{\beta_1}$

$\mathbf{R}_m$	Rotation matrix giving the orientation of $\vec{\mathcal{F}}_{\beta_0}$ with respect to $\vec{\mathcal{F}}_{\alpha_1}$
$\mathbf{R}_{p_A}$	Rotation matrix defining the orientation of $\vec{\mathcal{F}}_p$ relative to $\vec{\mathcal{F}}_\alpha$
$\mathbf{R}_{p_B}$	Rotation matrix defining the orientation of $\vec{\mathcal{F}}_p$ relative to $\vec{\mathcal{F}}_\beta$
r_u	Distance within a beam cross-section from the cross-section centroid, in the direction of $\vec{u}$
r_v	Distance within a beam cross-section from the cross-section centroid, in the direction of $\vec{v}$
s	Arc length along the locus of centroids
$\vec{t}$	Unit tangent vector to the locus of centroids
T	Kinetic energy of a beam element
T_A	Kinetic energy of the half-element corresponding to cross-section A
T_B	Kinetic energy of the half-element corresponding to cross-section B
$\vec{t}_A, \vec{u}_A, \vec{v}_A$	Cross-section normal (tangent to the locus of centroids) and principal axis vectors of cross-section A, describing its orientation
$\vec{t}_m$	Common tangent vector to both splines where they meet in the middle of the element
U	Strain energy of a beam element
U_A	Strain energy of the half-element corresponding to cross-section A
U_B	Strain energy of the half-element corresponding to cross-section B
u_a, v_a, w_a	Displacements in the 1-, 2- and 3-directions of $\vec{\mathcal{F}}_a$ respectively
$\vec{u}, \vec{v}$	Unit normal vectors to the locus of centroids defining the directions of the principal axes of a cross-section

$\mathrm{d}V$ — Differential volume element

W — Work done on the element by applied forces and moments

$x_{A_0}, y_{A_0}, z_{A_0}$ — Coordinates of the first spline control point with respect to the global fixed Cartesian frame $\vec{\mathcal{F}}_a$

$x_{A_m}, y_{A_m}, z_{A_m}$ — Coordinates of the middle spline control point with respect to $\vec{\mathcal{F}}_a$

$x_{A_1}, y_{A_1}, z_{A_1}$ — Coordinates of the last spline control point with respect to $\vec{\mathcal{F}}_a$

x_A, y_A, z_A — Coordinates of the centroid of cross-section A with respect to the global fixed Cartesian frame $\vec{\mathcal{F}}_a$

x_a, y_a, z_a — Coordinates in the 1-, 2- and 3-directions of $\vec{\mathcal{F}}_a$ respectively

x_B, y_B, z_B — Coordinates of the centroid of cross-section B with respect to the global fixed Cartesian frame $\vec{\mathcal{F}}_a$

x_c, y_c, z_c — Coordinates in the 1-, 2-, and 3-directions of $\vec{\mathcal{F}}_c$ respectively

Note: Throughout the text, when a symbol is first introduced, it is described in a table set off by horizontal lines above and below.

1

Introduction

Long, slender beams are commonly used in engineering applications, and it is therefore valuable to understand how they deform when forces are applied to them. For the common case of a straight beam that undergoes some small deformation, the well-known Euler-Bernoulli beam model (see section 3.1) can be used to efficiently simulate the behaviour of the beam.

In several cases, however, an Euler-Bernoulli model cannot be used; an object such as a fishing rod goes through large rotations and deformations, and an object such as a hockey stick does the same but has the added complexity of having some initial curvature. In these cases, one can simulate the behaviour of the object by converting it to a mesh of simple, generic 'elements' (*e.g.*, trapezoidal shapes) and applying a 3D finite element analysis. In this situation, however, a large set of linear equations must be solved to simulate the behaviour of the beam (with the number of variables and equations proportional to the number of elements used). If properties of the shape of the object can be exploited somehow to use a small number of specialized elements instead of a large number of generic ones, simulation can be made much more efficient. Long, slender beams are common examples of shapes that can be simulated efficiently using this approach.

1.1 Beam models

A beam is a "slender structural member" [1] such as an I-beam used in building construction, or a fishing rod or hockey stick as mentioned above. The shape of a straight beam can be defined by a single reference line along with a description of the shape of the beam at every point along that line (*i.e.*, its cross-sectional shape at that point). This reference line frequently coincides with the beam's locus of centroids (a line passing through the centroids of all of the beam's cross-sections). Similarly, curved beams can be described by a single reference *curve* and a description of the cross-sectional shape at every point on the curve; the reference curve often coincides with the beam's (curved) locus of centroids.

It is also usually possible to make simplifying assumptions about the behaviour of beam cross-sections; for instance, a common assumption is that each cross-section's shape remains constant [1]. If this is true, then the deformation of the beam's reference curve is frequently all that is required to define the deformation of the beam as a whole. In some cases (for an example see section 2.3) it may be necessary to define other quantities along the reference curve, but in all cases beam models are characterized by quantities that vary with respect to only one variable. For instance, displacements of points along a parametric reference curve $\vec{p}(t)$ would be a function of t only. This can be contrasted to modelling the deformation of a plate, where displacements of points within the plate might vary with respect to two parameters such as the horizontal and vertical position within the plate.

The goal of this work is to create an efficient beam model that can be used to simulate curved and twisted beams which may go through large displacements. One possible application would be to simulate the behaviour of a hockey stick as it hits a puck. In dynamic simulations like this, it is important to have a very efficient model since the deformation of the stick is different at every instant, so possibly thousands of different analyses, each corresponding to a different point in time, will have to be done. Similarly, while a single structural beam in a building may

2

only require one static analysis to determine whether it is capable of withstanding a given load, a more efficient beam model may allow for more interesting dynamic simulations of the building.

1.2 Assumptions

There are several assumptions currently made about the motion of the beam to be analyzed:

Small strain The strain at any point within the beam will always be small, *i.e.*, the strain at any point on the beam remains in the linear elastic range. This allows cases such as the fishing rod example above (where at any one point on the rod, the strains are small) but rules out a case such as a rubber band being stretched to twice its length.

Negligible shear When determining the overall deformation of the beam, transverse shear is small compared to bending so that all cross-sections remain perpendicular to the locus of centroids.

No in-plane deformation Any cross-section of the beam perpendicular to its locus of centroids remains the same shape, *i.e.*, the effects of Poisson's ratio can be ignored and there is no normal strain in the plane of the cross-section.

No warping Under torsion, the beam behaves like a circular beam, *i.e.*, torsion results only in shear and not in warping of the cross-section.

Although the assumption of zero warping for a non-circular beam is not accurate, the effects of warping can be approximated for a given shape by adjusting the values of the shear modulus G and polar moment of area J; see for example Timoshenko [2], pp. 289-290.

Note that it is not assumed that the beam is initially straight, or that it has a constant cross-section. Also note that small displacements are not assumed, so the beam may go through large displacements and rotations. This not only means

that the beam as a whole may go through large motions (*e.g.*, a helicopter blade spinning), but that one end of the beam may have large displacements relative to the other end (*e.g.*, a fishing rod being bent into a semicircle). However, the assumption of small strain disallows the possibility of large relative displacements between *nearby* points in the beam.

1.3   Prior work

Although there exist many articles which discuss curved beams, many focus exclusively on two-dimensional shapes, *e.g.*, Noor *et al.* [3] who present a nonlinear approach for planar arches.

There do exist several papers which discuss the deformation of three-dimensional beams. Zupan and Saje [4] discuss a method for the deformations of arbitrarily curved and twisted three-dimensional beams; however, the deformation is restricted to be small, and so the method cannot be applied to beams which (as well as pure rigid-body motion) may have large end-to-end deformation.

Tabarrok *et al.* [5] develop a model for three-dimensional, curved and twisted beams which may go through moderate displacements. However, defining the orientation of beam cross-sections is done case-by-case for specific beam shapes (*e.g.*, a twisted beam with a straight locus of centroids or a helical rod) which have a 'natural', stable method of definining orientation. Similarly, Sandhu *et al.* [6] derives a finite element for curved and twisted three-dimensional beams, but uses the Frenet frame of the locus of centroids to define orientation; as discussed in section 5.1, the Frenet frame can be an unstable reference for several interesting beam shapes.

Much of the literature relevant to defining a generic, stable reference for cross-section orientation can be found in the discipline of computer graphics instead of engineeering, where the goal is to interpolate the orientation of an object or camera during an animation. One very common approach is interpolating orientations by representing them as quaternions [7, 8]. However, quaternion interpolation func-

tions are fairly complex, so they can be inefficient to evaluate. More importantly, derivatives of these functions are quite complex [9], so several important operations from a solid mechanics viewpoint (such as attempting to enforce continuity between finite elements or taking derivatives to compute strains) can be very difficult.

Chapter 5 describes how planar quadratic splines form a good reference for measuring an angle of orientation, but interpolating angles is more complex than positions because a given orientation can be described by an infinite number of different angles (*e.g.*, θ, $\theta + 2\pi$, $\theta + 4\pi$, $\theta - 2\pi$...). Park and Ravani [10] derive a conceptually very elegant method of interpolating orientations using matrices instead of angles. While several of their ideas were used when developing the orientation interpolant of section 5.2, and in fact several intermediate steps use matrices instead of angles, it was ultimately more efficient to interpolate the angle directly.

2

Shape Description

A common method for simulating the behaviour of deformable bodies is the finite element method (see Kaliakin [11] or Shames & Dym [12]). This involves taking the continuous body in question and defining its position and shape by a set of smaller elements, each described by discrete nodes. For different types of body shapes and different modes of deformation, different types of elements be used.

2.1 The Euler-Bernoulli model

The deformed shape of an initially straight, prismatic (*i.e.*, constant cross-section) beam may be defined by the vertical displacements w_i of several points along a suitably chosen reference line (usually the beam's locus of centroids) as well as the slope w_i' of the locus of centroids at each point [12]. Given a suitable displacement interpolation function between those points, the initial positions, the displacements and the slope values at those points completely define the shape of the deformed locus of centroids.

If the beam is assumed to act like an Euler-Bernoulli beam (cross-sections remain plane and normal to the locus of centroids, and the effects of Poisson's ratio can be ignored), then defining the shape of the locus of centroids completely defines the shape of the beam, as illustrated in Figure 2.1. In this way, the continuous shape of the beam is defined in terms of a discrete set of nodes along the beam,

(a) Original

(b) Deformed
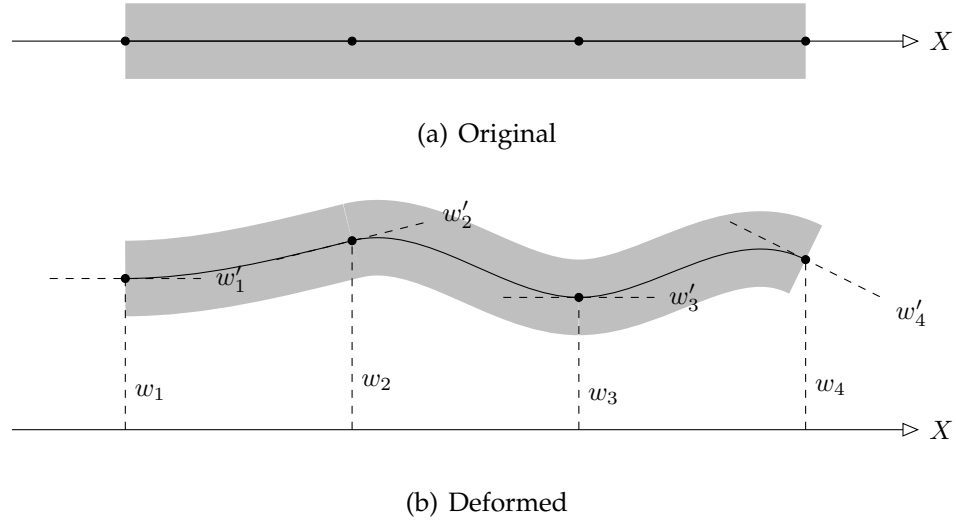
Figure 2.1: Euler-Bernoulli beam deformation.

with position and slope being defined at each node. Each section of the beam between two nodes is considered one element of the beam.

If the cross-sectional shape of the beam is not constant, then the shape parameters (*e.g.,* height, width, radius) must also be interpolated along the beam. For instance, in addition to definitions for the vertical displacement and slope of the locus of centroids, the shape parameters and their derivatives could be specified at each node and be interpolated between nodes in a similar way as for the displacements and slopes.

2.2   Planar curved beams

Straight beams such as those described in the previous section can often be assumed to deform only in a direction perpendicular to their initial reference curve (*e.g.,* vertically, if the beam is initially horizontal). In the case of a planar, curved beam (such as a circular arch), each point on the beam must in general have two deformation degrees of freedom instead of one (*i.e.,* points can deform horizontally as well as vertically, or in directions tangential and normal to the reference curve). Also, the direction of the reference curve at each point may have to be specified by a tangent vector instead of a slope (since, for example, the slope would be infinite

at any point where the beam was vertical).

Figure 2.2 shows one method of specifying the original and deformed shapes of a planar, curved beam with constant cross-section by specifying positions and tangent vectors at the nodes. There, a * superscript denotes position vectors and tangents as they exist in the original, undeformed configuration of the beam. For small displacements of the beam, it may be convenient to describe the deformation by displacements of the geometric nodes and changes of the tangent vector at each node

$$\Delta \vec{p}_i = \vec{p}_i - \vec{p}_i^* \tag{2.1}$$

$$\Delta \vec{t}_i = \vec{t}_i - \vec{t}_i^* \tag{2.2}$$

$(\cdot)^*$ Value of a quantity $(\cdot)$ before deformation

and then derive some expression for the strain energy of each element in terms of $\Delta \vec{p}_i$ and $\Delta \vec{t}_i$.

However, as will be discussed in Chapter 3, it can be more effective (especially when displacements may be large) to not consider changes in $\vec{p}$ or $\vec{t}$ directly, but instead consider changes in some derived quantities. For instance, if the geometric interpolants between nodes in Figure 2.2 were circular arcs, it may be more effective to compute the change in curvature and arc length of each arc instead of the changes of the arc endpoints $\vec{p}_i$ directly. In this case, the actual displacement $\Delta \vec{p}_i$ is meaningless.

If necessary, more complex shapes could be created by using more nodes, as illustrated in Figure 2.3.

2.3   Three-dimensional curved beams

The most complex beam case is that of one which may have an arbitrary shape and deform in an arbitrary way in three dimensions. In the case of a hockey stick (or similar cases), such complexity is unavoidable – a hockey stick curves in multiple directions, and goes through both large rigid-body motions (swinging the stick)

(a) Original   (b) Deformed
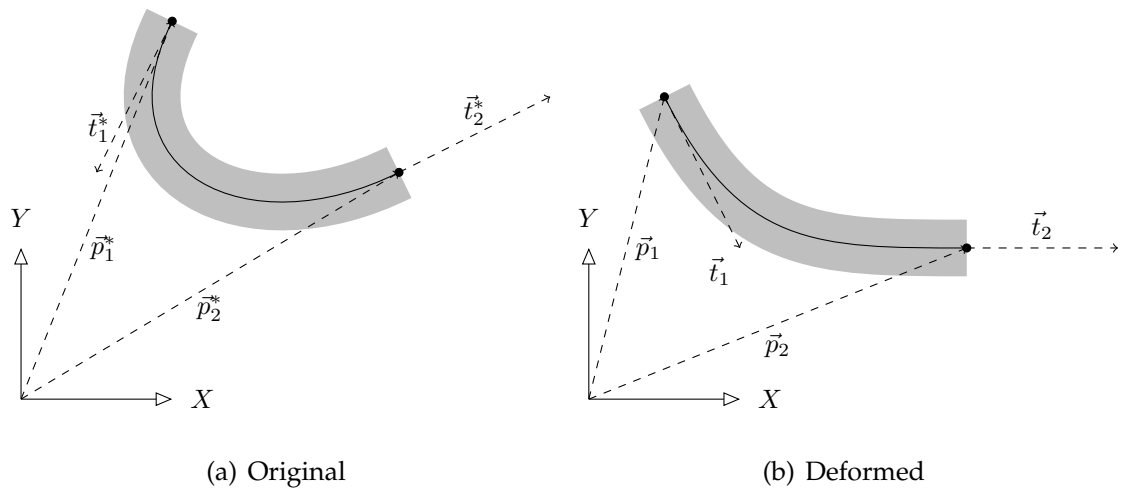
Figure 2.2: Planar curved beam deformation.
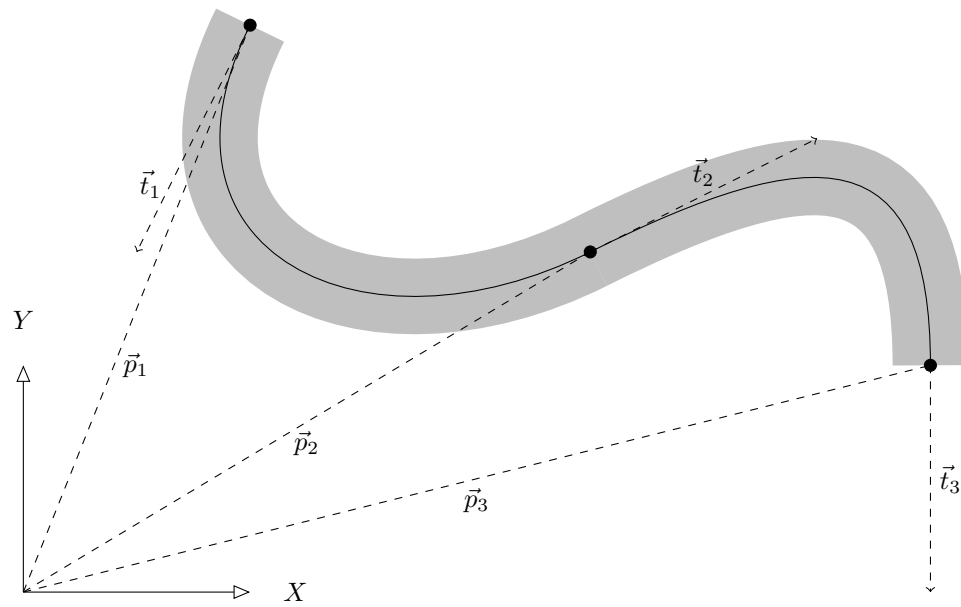
Figure 2.3: Multiple planar sections joined together to create a complex beam shape.

and large deformations (the stick is bent substantially when it hits the ice, and to a lesser extent when it hits the puck). To form a finite element model of such a beam, several quantities must be defined:

Locus of centroids As in the previous cases, the locus of centroids can be defined as some form of geometric interpolant between specified points. These points are geometric nodes at which the local geometry of the locus of centroids is specified. Here, however, the locus of centroids does not necessarily lie in a plane, so describing and interpolating it is more difficult.

Cross-section shape Again as in previous cases, the shape of the cross-section (width, height, radius, etc.) must be interpolated between the geometric nodes.

Cross-section orientation Note that in the planar cases, the orientations of cross-sections are completely defined by the requirement that they should be locally normal to the locus of centroids, since all deformation is assumed to be in-plane. In the fully three-dimensional case, however, cross-sections may also twist about the locus of centroids; this twist must also be somehow defined at the geometric nodes and interpolated between them.

In general, motion of the beam is modelled by motion of individual cross-sections, along with a displacement interpolation function between cross-sections; each cross-section has six degrees of freedom (three translational and three rotational) corresponding to rigid-body motion. To interpolate the beam geometry between cross-sections, a locus of centroids is first interpolated between cross-section centroids.

Once the locus of centroids has been interpolated, it is necessary to interpolate the shape and orientation of the cross-section at every point along it. Shape parameters (which are dependent on the shape chosen for the cross-section, *e.g.*, width and height for a rectangular cross-section or radius for a circular cross-section) must be interpolated between cross-sections. The orientation of any cross-section

is mostly defined (two out of three degrees of freedom) by the requirement that it should be locally normal to the locus of centroids; the third degree of freedom corresponds to rotation about the local tangent to the locus of centroids. This rotation must also be interpolated between given cross-sections.

Each portion of the beam between two successive cross-sections (corresponding to two successive geometric nodes) forms one element of the beam for purposes of finite element analysis. The geometric interpolation functions used between cross-sections (geometric nodes) must satisfy two requirements: continuity and completeness [12]. It is important for the beam as a whole not to have any sharp edges or discontinuities; the geometric interpolation functions must therefore be designed to have C^1 continuity (continuity of the first derivative) between elements. Also, the geometric interpolants must be complete: they must be able to describe all of the desired behaviours of the beam. For instance, geometric interpolation functions that did not take twist into account would not be able to accurately simulate a case where, in reality, the beam would indeed twist.

Figures 2.4 and 2.5 show how the locus of centroids and intermediate cross-section shapes and orientations are geometrically interpolated between given rectangular cross-sections; the details of the geometric interpolation are presented in Chapter 5. Note that the facets seen in Figure 2.5 are rendering artifacts (the entire shape shown is actually one continuous element), and the element is actually solid (it is rendered as hollow for simplicity and to allow the reference curve to be visible). Also note that the cross-section does indeed get larger and twist about the reference curve over the length of the element.
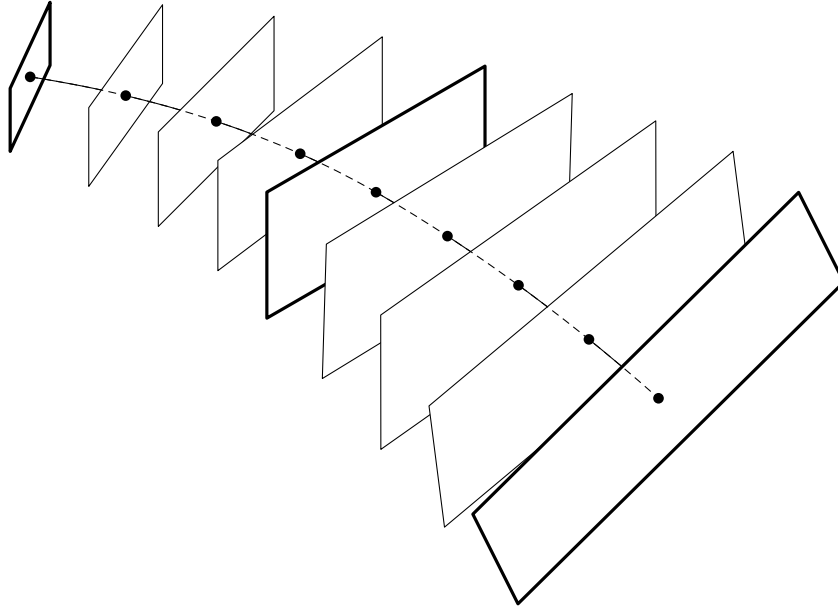
Figure 2.4: Sample geometric interpolation between given (bold) cross-sections.
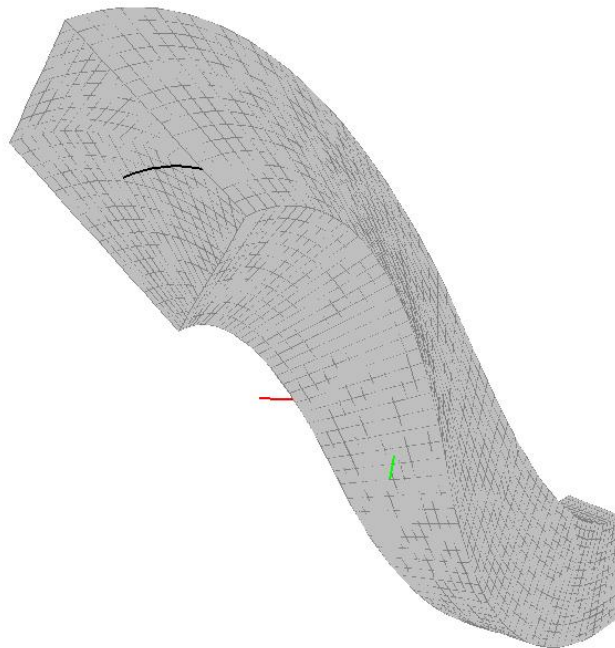
Figure 2.5: Actual interpolated beam element between two cross-sections.

3

Model Development

To be able to use a finite element approach in simulating the dynamics of a flexible beam, it must be possible to find an expression for the strain energy of a beam element given an original and a deformed shape. In general, the strain energy is given by [13]

$$U = \frac{1}{2} \int_V \epsilon^T \mathbf{C} \epsilon \, \mathrm{d}V \tag{3.1}$$

U	Strain energy of a beam element
ϵ	Column matrix of strains
$\mathbf{C}$	Material constitutive matrix
$\mathrm{d}V$	Differential volume element

However, in many cases, this expression for strain energy can be simplified by making assumptions about the shape of the body and the sort of deformation it undergoes. The following sections will describe successively more complex beam models, and finally introduce a model for three-dimensional, initially curved beams going through large deformations which will be derived in detail in Chapter 4.

(a) Initial   (b) Deformed
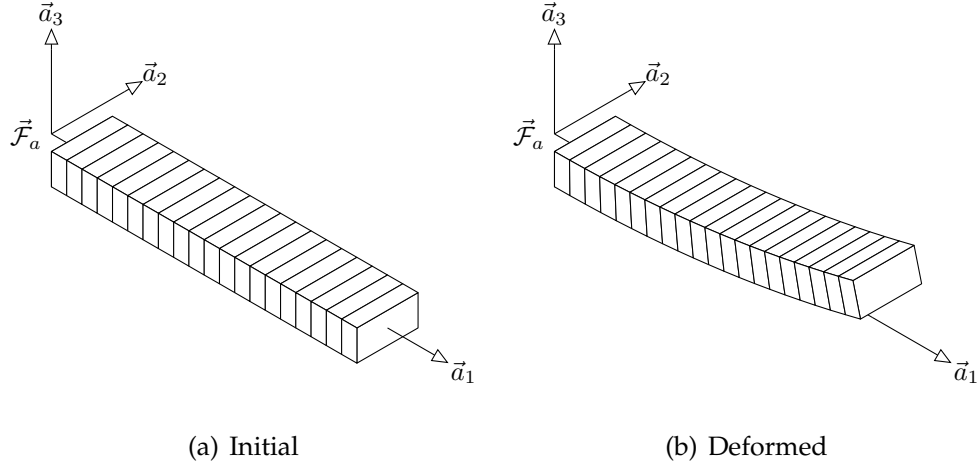
Figure 3.1: Euler-Bernoulli beam.

3.1 The Euler-Bernoulli model

A common example of a set of assumptions used to simplify equation (3.1) is that of a prismatic Euler-Bernoulli beam [12] as shown in Figure 3.1. This model assumes a straight beam where deformation is described by the cross-section centroids being displaced vertically, with all cross-sections remaining planar and normal to the locus of centroids. This corresponds to the assumptions

$$x_a(x_a^*, y_a^*, z_a^*) - x_a^* = u_a(x_a^*, y_a^*, z_a^*) = -z_a^* \frac{\mathrm{d}w_a}{\mathrm{d}x_a^*} \tag{3.2}$$

$$y_a(x_a^*, y_a^*, z_a^*) - y_a^* = v_a(x_a^*, y_a^*, z_a^*) = 0 \tag{3.3}$$

$$z_a(x_a^*, y_a^*, z_a^*) - z_a^* = w_a(x_a^*, y_a^*, z_a^*) = w_a(x_a^*) \tag{3.4}$$

$\vec{\mathcal{F}}_a$	Global, fixed, Cartesian frame
$\vec{a}_1, \vec{a}_2, \vec{a}_3$	Unit basis vectors of $\vec{\mathcal{F}}_a$ defining the coordinate axes
x_a, y_a, z_a	Coordinates in the 1-, 2- and 3-directions of $\vec{\mathcal{F}}_a$ respectively
u_a, v_a, w_a	Displacements in the 1-, 2- and 3-directions of $\vec{\mathcal{F}}_a$ respectively

i.e., the vertical displacement w_a of a point is only a function of its undeformed axial coordinate x_a^*, there is no (out-of-plane) deformation ($v_a = 0$), and horizontal

displacement u_a occurs only due to the rotation of beam cross-sections (*e.g.*, if the beam is bent upwards, then points at the top of the beam will swing backwards and points at the bottom of the beam will swing forwards). See Appendix A for an overview of the $\vec{\mathcal{F}}_a$ vectrix notation.

The normal strain (the only non-zero strain) is then

$$\epsilon_{x_a x_a} = \frac{\mathrm{d}u_a}{\mathrm{d}x_a^*} = -z_a \frac{\mathrm{d}^2 w_a}{\mathrm{d}x_a^{*2}} \tag{3.5}$$

This uses a linear method of computing strain, which is only valid if the displacements w_a are small [14]. In this case, equation (3.1) can be greatly simplified because $\epsilon = \epsilon^T = \epsilon_{x_a x_a}$ and $\mathbf{C} = E$, so that

$$
\begin{aligned}
U &= \frac{1}{2} \int_V \epsilon^T \mathbf{C} \epsilon \, \mathrm{d}V \\
&= \frac{1}{2} \int_V E \epsilon_{x_a x_a}^2 \, \mathrm{d}V \\
&= \frac{1}{2} \int_V E \left(-z_a^* \frac{\mathrm{d}^2 w_a}{\mathrm{d}x_a^{*2}} \right)^2 \mathrm{d}V \\
&= \frac{1}{2} \int_{x_a^*=0}^L \int_A E z_a^{*2} \left(\frac{\mathrm{d}^2 w_a}{\mathrm{d}x_a^{*2}} \right)^2 \mathrm{d}A \, \mathrm{d}x_a^* \\
&= \frac{1}{2} \int_{x_a^*=0}^L E \left(\int_A z_a^{*2} \mathrm{d}A \right) \left(\frac{\mathrm{d}^2 w_a}{\mathrm{d}x_a^{*2}} \right)^2 \mathrm{d}x_a^* \\
&= \frac{1}{2} \int_{x_a^*=0}^L E I \left(\frac{\mathrm{d}^2 w_a}{\mathrm{d}x_a^{*2}} \right)^2 \mathrm{d}x_a^* \tag{3.6}
\end{aligned}
$$

E Modulus of elasticity

By separating the integration into integration along the length of the beam and integration over its cross-sectional area, this approach allows a three-dimensional integral over the volume of the beam to be replaced by a one-dimensional integral along the length of the beam. In this case, the integral over the cross-sectional area can be replaced by I, the second moment of area of the beam cross-section about an axis parallel to $\vec{a}_2$. The following sections will illustrate how to apply the same concept to more complex deformation models and beam shapes.

(a) Initial   (b) Deformed
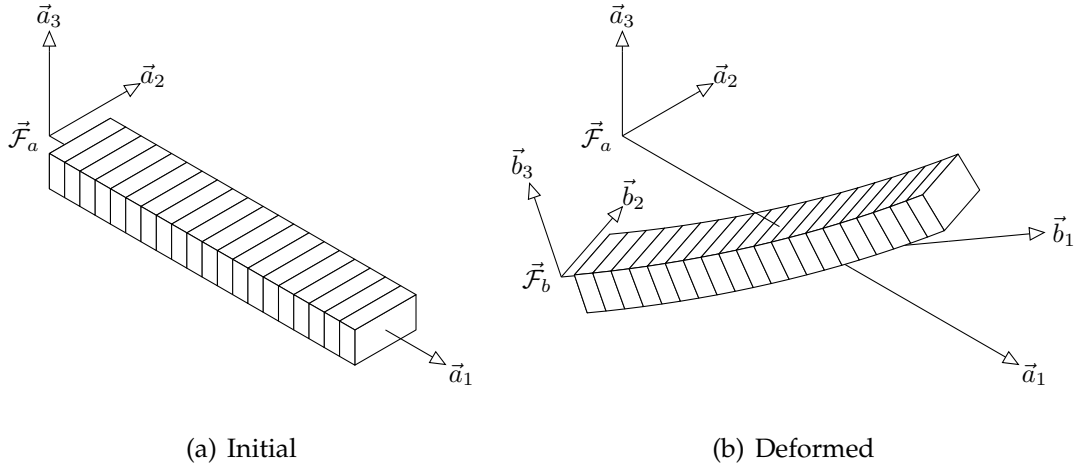
Figure 3.2: Euler-Bernoulli beam with rigid-body motion.

3.2 Rigid body motion

In a case such as that illustrated in Figure 3.2, the motion of the beam cannot be approximated by small vertical displacements $w_a(x_a^*)$, as the displacements with respect to the fixed $\vec{\mathcal{F}}_a$ frame are large. However, assuming that the motion of the beam can be approximated as a single rigid-body motion (for which $U = 0$) plus some small deformation (for which $U \neq 0$), equation (3.6) can be used if displacements are expressed in a frame $\vec{\mathcal{F}}_b$ attached to the beam:

$$U = \frac{1}{2} \int_{x_b^*=0}^{L} EI \left(\frac{\mathrm{d}^2 w_b}{\mathrm{d}x_b^{*2}} \right)^2 \mathrm{d}x_b^* \tag{3.7}$$

$\vec{\mathcal{F}}_b$	Cartesian frame, originally aligned with $\vec{\mathcal{F}}_a$, which is attached to a specific cross-section of the beam and rotates with that cross-section

Coordinates x_b, y_b, z_b and displacements u_b, v_b, w_b are defined similarly to their $\vec{\mathcal{F}}_a$ counterparts. Note that choosing to place the $\vec{\mathcal{F}}_b$ frame at one end of the beam is arbitrary; it could also be at the other end or at some point within the beam (whichever is most convenient).

(a) Initial   (b) Deformed
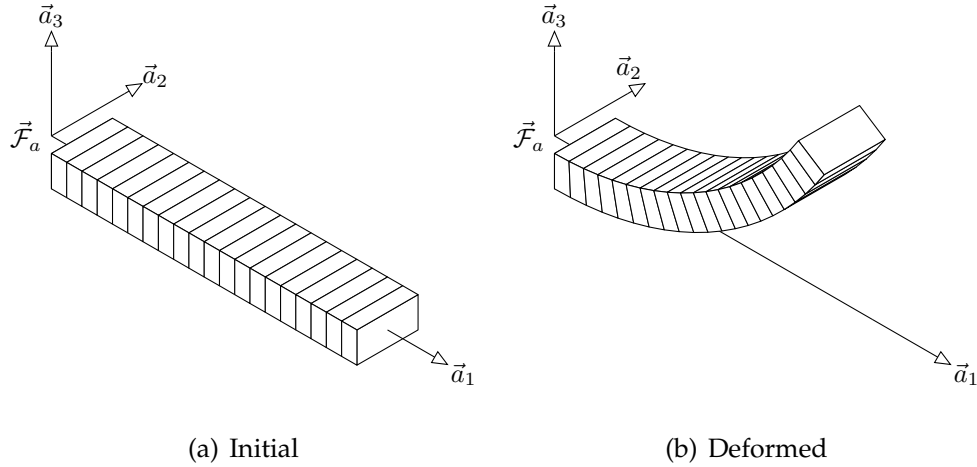
Figure 3.3: Beam with large end-to-end deformation.

3.3 End-to-end deformation

In a case such as that illustrated in Figure 3.3, where a long slender beam has some large relative displacement between its two ends, there is no single frame that can be attached to the beam such that all beam displacements are small relative to that frame. In this case, one approach is to use a strain measure that is valid for large displacements, such as the Lagrangian strain tensor [14]:

$$\epsilon_{ij} = L_{ij} = \frac{1}{2}\left(\frac{\partial u_i}{\partial x_j^*} + \frac{\partial u_j}{\partial x_i^*} + \sum_{k=1}^{3}\frac{\partial u_k}{\partial x_i^*}\frac{\partial u_k}{\partial x_j^*}\right) \tag{3.8}$$

where the x_i^* are the global coordinates x_a, y_a, and z_a, and the u_i are the global displacements u_a, v_a and w_a. However, the nonlinearity in equation (3.8) makes it expensive to compute and unwieldy to integrate, as well as conceptually more difficult to visualize and reason about.

To develop a simpler approach, note that the second derivative $\mathrm{d}^2 w_a / \mathrm{d} x_a^{*2}$ used in equation (3.6) is only an approximation to the (negative of) beam curvature (and is not applicable when displacements w_a are large). More accurately, it is an approximation to the *change* in beam curvature; for the case of a straight beam with zero initial curvature, the change in curvature is equal to the final (deformed) curvature. Equation (3.6) can be written in terms of the final, deformed curvature

17

as:

$$U = \frac{1}{2} \int_{s=0}^{L} EI\kappa^2 \mathrm{d}s \qquad (3.9)$$

κ Curvature of the deformed locus of centroids

s Arc length along the locus of centroids

---

which is valid as long as the deformation curvature at any point is small. By re-placing the second derivative $\mathrm{d}^2 w_a / \mathrm{d} x_a^{*2}$ with curvature κ and position x_a^* with arc length s, the Euler-Bernoulli model can be adapted to beams with large end-to-end deformation.

The problem now becomes that of determining κ at every point along the locus of centroids, and of finding a way to integrate with respect to arc length; this is dependent on what basis functions are used to interpolate the deformed shape of the beam. A convenient choice for three-dimensional beams will be shown to be quadratic splines, as covered in Chapter 5.

3.4   Multiple curvatures and twist

For a beam undergoing 3D deformation (*i.e.*, not just in-plane deformation), a single curvature value is not sufficient to describe the deformation at any point along the beam; in general, the deformed beam may curve about two different axes and may also twist. The overall approach, however, is the same as the previous section.

In this case, there exist two different curvatures κ_u and κ_v about the two principal axes of a cross-section, as well as a twist rate ψ in radians per unit length about the locus of centroids. The strain energy equation (3.9) then becomes

$$U = \frac{1}{2} \int_{s=0}^{L} EI_{uu}\kappa_u^2 + EI_{vv}\kappa_v^2 + GJ\psi^2 \mathrm{d}s \qquad (3.10)$$

G Shear modulus

---

where instead of a single term involving curvature κ and second moment of area I, there are three separate terms involving curvatures κ_u and κ_v and moments of

18
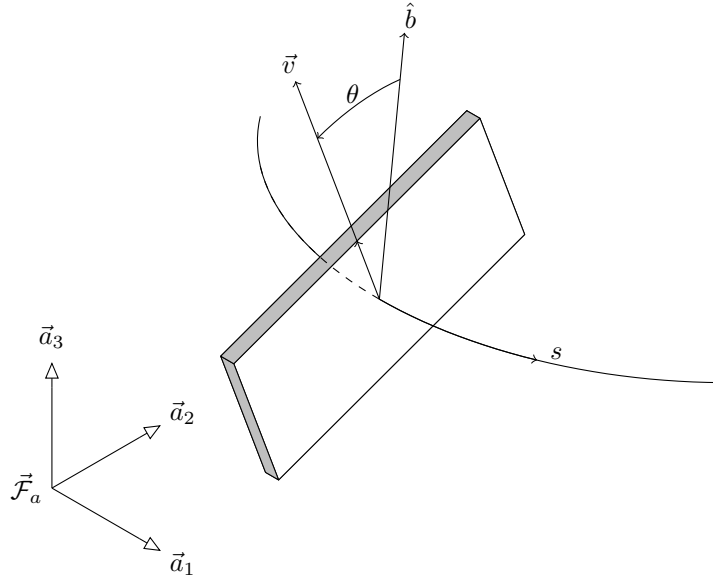
Figure 3.4: Orientation of cross-section relative to locus of centroids.

area I_{uu} and I_{vv} about the two principal axes of the cross-section, as well as twist rate ψ and the polar moment of area J of the cross-section. (The u and v subscripts denoting the two cross-section principal axes are here somewhat arbitrary, but are used in anticipation of the notation used in Chapter 4.)

Note that here a method of determining the cross-section orientation relative to the locus of centroids is required as well as a description of the locus of centroids itself. For example, this could take the form of an expression for the angle between a principal axis vector $\vec{v}$ and the unit binormal $\vec{b}$ to the locus of centroids, as illustrated in Figure 3.4, in which case

$$\kappa_u = \kappa \sin \theta$$

$$\kappa_v = \kappa \cos \theta$$

$$\psi = \frac{\mathrm{d}\theta}{\mathrm{d}s}$$

$\vec{b}$	Unit binormal vector to the locus of centroids

(a) Initial (b) Deformed
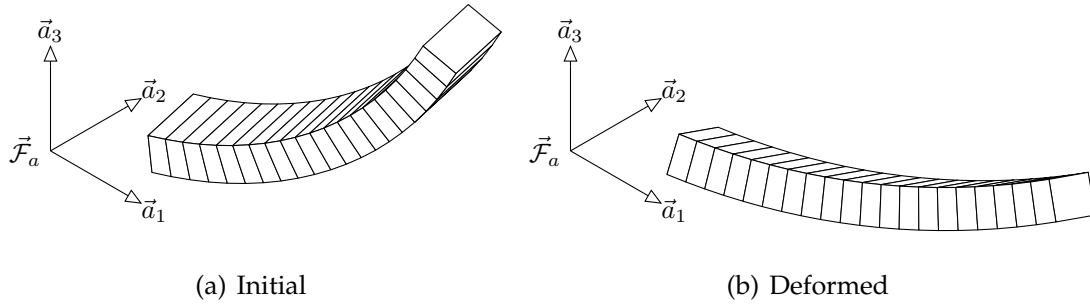
Figure 3.5: Beam with initial curvature.

3.5 Initial curvature

Finally, the problem of finding the strain energy of a deformed beam becomes more complex if the beam has some initial curvature, as shown in Figure 3.5. First, since the beam may have non-zero initial curvatures and twists, the parameters in the strain energy expression must be *changes* in curvatures and twists instead of actual values.

Second, since a differential 'slice' of the beam (corresponding to a differential change in arc length s along the locus of centroids) no longer has constant thickness, the calculation of strain energy becomes more complex. This initial beam curvature leads to a coupling between bending and extension, so it can no longer be assumed that the locus of centroids remains the same length and a new parameter ξ must be introduced which describes the rate of extension of the locus of centroids. Finally, and most importantly, the initial curvature of the beam affects its bending and torsional stiffnesses; it will be shown in Chapter 4 that the second moments and polar moments of area in equation (3.10) are replaced by generalized moments of area which depend on the initial curvatures.

4

Model Derivation

4.1 Shape definition

As described in section 2.3, the description of a 3D curved beam element must take into account the shape of the locus of centroids, the shape of each cross-section, and the orientation of each cross-section. First, define the locus of centroids by a parametric curve, as shown in Figure 4.1:
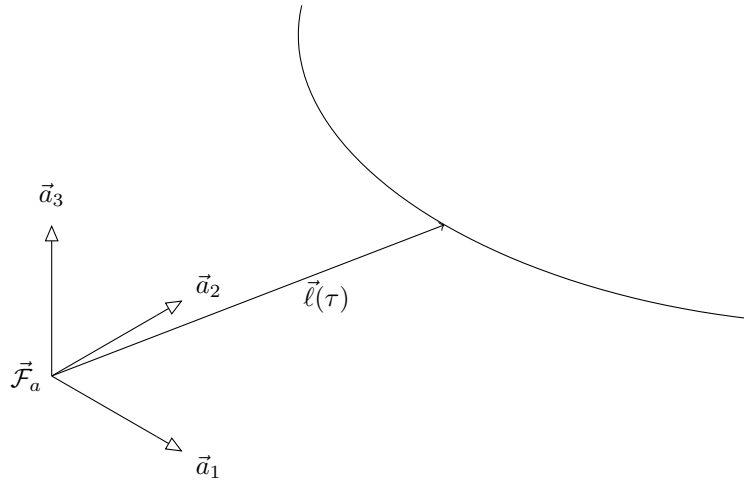
Figure 4.1: The locus of centroids.
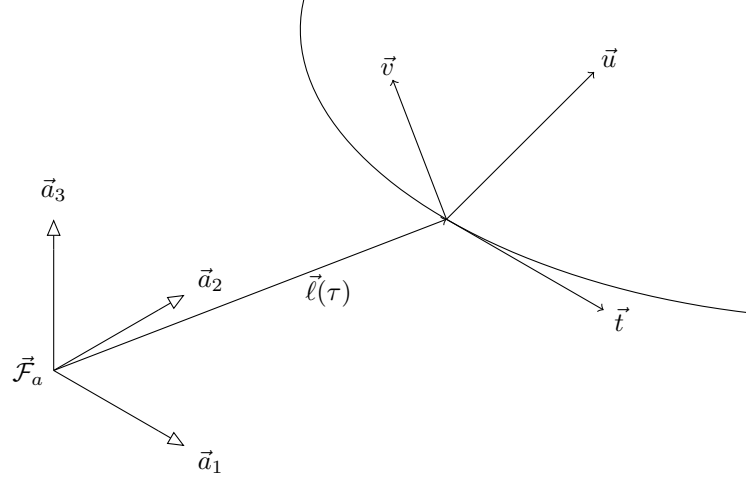
Figure 4.2: Unit vectors defined along the locus of centroids

τ	Parameter describing the locus of centroids, in the range $[0,1]$
$\vec{\ell}(\tau)$	Position vector of a point along the locus of centroids

Next, define three unit vectors which specify the orientation of a cross-section at any point along the locus of centroids, as shown in Figure 4.2:

$\vec{t}$	Unit tangent vector to the locus of centroids
$\vec{u}, \vec{v}$	Unit normal vectors to the locus of centroids defining the directions of the principal axes of a cross-section

Finally, the position vector of points within the beam can be defined in terms of the locus of centroids parameter τ and two radial distances r_u and r_v, as shown in Figure 4.3:

$$\vec{\rho}(\tau, r_u, r_v) = \vec{\ell}(\tau) + r_u\vec{u} + r_v\vec{v} \qquad (4.1)$$

$\vec{\rho}(\tau, r_u, r_v)$	Position vector of a point within the beam
r_u	Distance within a beam cross-section from the cross-section centroid, in the direction of $\vec{u}$
r_v	Distance within a beam cross-section from the cross-section centroid, in the direction of $\vec{v}$

22
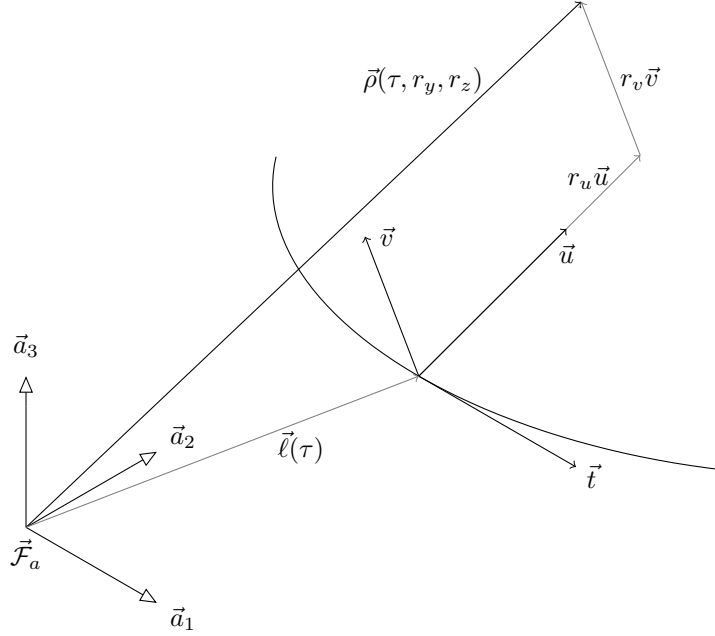
Figure 4.3: Position of a point within the beam.

4.2   Cross-sectional coordinates

Strains within a cross-section can be calculated using a simple linear method if the deformation is described as changes in point coordinates in a Cartesian frame [14]. A curvilinear coordinate system can also be used, but in this case the expressions for strain become more complex [13].

If, for any point, the reference frame for the purposes of strain calculation is chosen to be a cross-sectional frame $\vec{\mathcal{F}}_c$ corresponding to the cross-section (to which $\vec{t}$ is normal) in which that point exists, then all displacements with respect to $\vec{\mathcal{F}}_c$ can be assumed to be small and a linear method of strain computation can be used. Conceptually, for every beam cross-section, a frame $\vec{\mathcal{F}}_c$ is formed, the displacements of all neighbouring points are computed with respect to that frame, and a simple linear strain calculation is performed to find the strain at every point on the cross-section.

The key notion is that to use a linear method of computing strain, point displacements with respect to the reference frame must be small; it does not matter

23
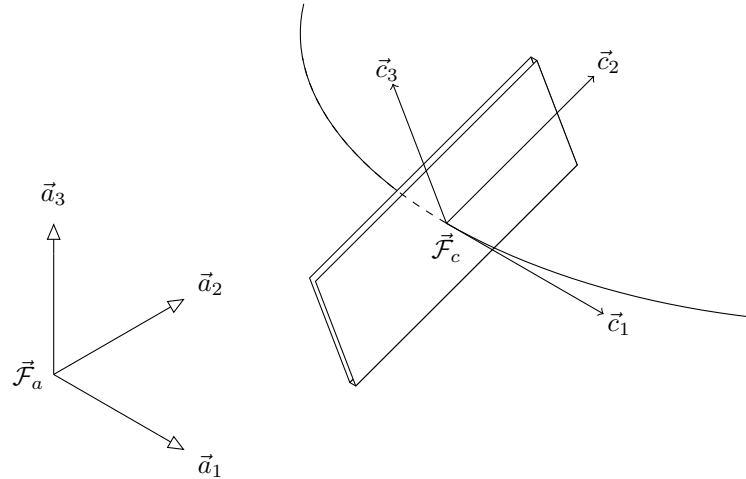
Figure 4.4: Cross-sectional frame

if different reference frames are used for different points if all that is ultimately required is an expression for total strain energy which is frame independent.

4.2.1 Cross-sectional frame

The unit vectors $\vec{t}$, $\vec{u}$ and $\vec{v}$ introduced in the previous section define the orientation of the cross-section at any point; they can also be used to define a frame of reference. At any point along the locus of centroids, the cross-sectional frame $\vec{\mathcal{F}}_c$ is attached to the cross-section at that point and its unit basis vectors are equal to the unit vectors described above, as shown in Figure 4.4:

$\vec{\mathcal{F}}_c$	A Cartesian frame attached to a specific beam cross-section
$\vec{c}_1$	First unit basis vector of $\vec{\mathcal{F}}_c$, equal to $\vec{t}$ of the cross-section associated with $\vec{\mathcal{F}}_c$
$\vec{c}_2$	Second unit basis vector of $\vec{\mathcal{F}}_c$, equal to $\vec{u}$ of the the cross-section associated with $\vec{\mathcal{F}}_c$
$\vec{c}_3$	Third unit basis vector of $\vec{\mathcal{F}}_c$, equal to $\vec{v}$ of the the cross-section associated with $\vec{\mathcal{F}}_c$
x_c, y_c, z_c	Coordinates in the 1-, 2-, and 3-directions of $\vec{\mathcal{F}}_c$ respectively

The cross-sectional frame $\vec{\mathcal{F}}_c$ is different from the previously discussed frames $\vec{\mathcal{F}}_a$ and $\vec{\mathcal{F}}_b$ in that there is a different frame $\vec{\mathcal{F}}_c$ for every point along the beam's locus of centroids instead of one frame for the whole beam.

Note that *at* any cross-section, $\vec{c}_1$, $\vec{c}_2$ and $\vec{c}_3$ are equal to $\vec{t}$, $\vec{u}$ and $\vec{v}$, so in many cases the two sets of vectors are interchangeable. However, when working with points *in the neighbourhood of* a specific cross-section, $\vec{c}_1$, $\vec{c}_2$ and $\vec{c}_3$ are fixed while $\vec{t}$, $\vec{u}$ and $\vec{v}$ change as the locus of centroids bends and as the beam twists about the locus of centroids. Therefore, when discussing a certain point within the beam, $\vec{t}$, $\vec{u}$ and $\vec{v}$ will always refer to the normal vectors of the cross-section in which that point exists, while $\vec{c}_1$, $\vec{c}_2$ and $\vec{c}_3$ may refer to the normal vectors of a different, pre-determined cross-section.

4.2.2 Computation

Note that the coordinates x_c, y_c, and z_c of a point relative to the origin of the $\vec{\mathcal{F}}_c$ frame can be expressed as the dot product of the vector $\vec{\rho}(\tau, r_u, r_v) - \vec{\ell}(\tau_c)$ with the basis vectors of $\vec{\mathcal{F}}_c$, as shown in Figure 4.5:

$$x_c = \left(\vec{\rho}(\tau, r_u, r_v) - \vec{\ell}(\tau_c) \right) \cdot \vec{c}_1 \tag{4.2}$$

$$y_c = \left(\vec{\rho}(\tau, r_u, r_v) - \vec{\ell}(\tau_c) \right) \cdot \vec{c}_2 \tag{4.3}$$

$$z_c = \left(\vec{\rho}(\tau, r_u, r_v) - \vec{\ell}(\tau_c) \right) \cdot \vec{c}_3 \tag{4.4}$$
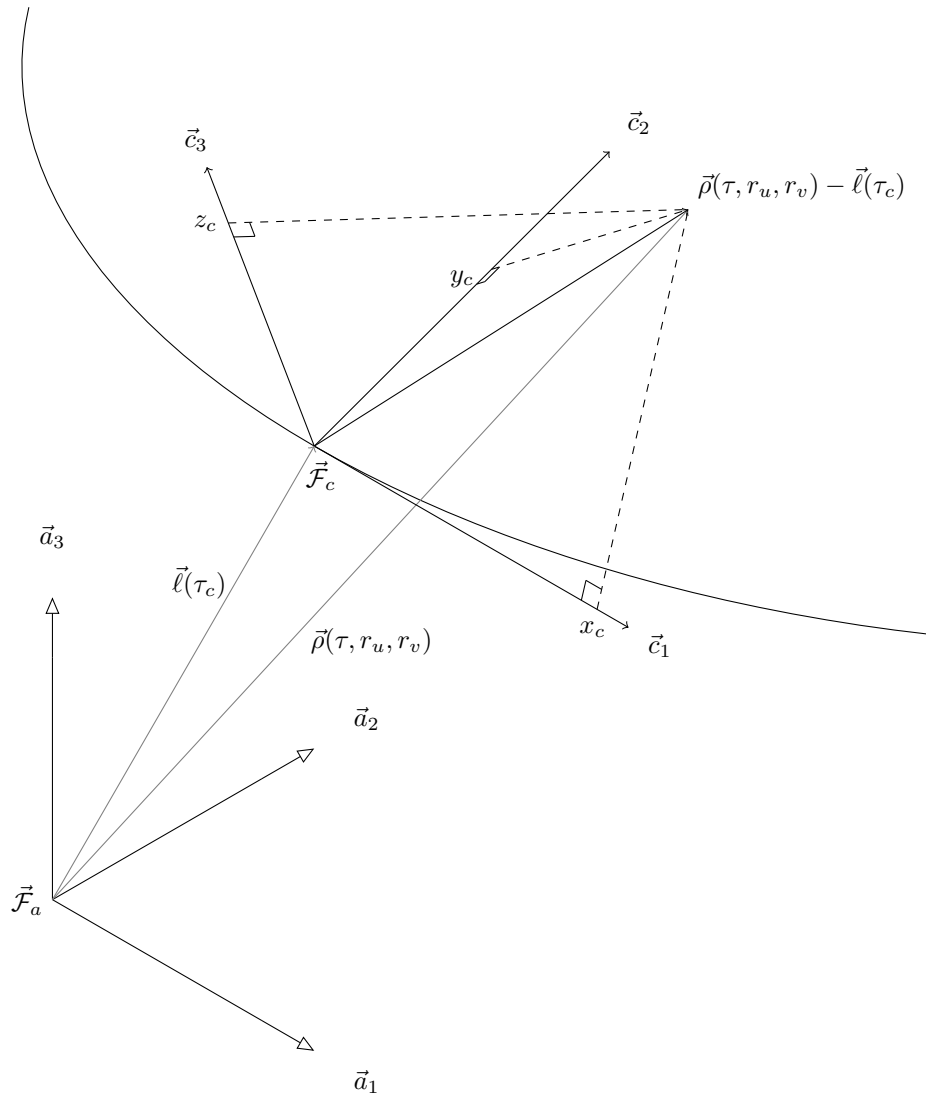
Figure 4.5: Cross-sectional coordinates

Equation (4.1) can be substituted into equations (4.2)–(4.4) to obtain

$$x_c = \left(\vec{\ell}(\tau) - \vec{\ell}(\tau_c) + r_u\vec{u} + r_v\vec{v}\right) \cdot \vec{c}_1 \tag{4.5}$$

$$y_c = \left(\vec{\ell}(\tau) - \vec{\ell}(\tau_c) + r_u\vec{u} + r_v\vec{v}\right) \cdot \vec{c}_2 \tag{4.6}$$

$$z_c = \left(\vec{\ell}(\tau) - \vec{\ell}(\tau_c) + r_u\vec{u} + r_v\vec{v}\right) \cdot \vec{c}_3 \tag{4.7}$$

4.2.3   Differentiation

Equations (4.5), (4.6) and (4.7) can be differentiated with respect to τ, r_u and r_v. Note that since $\vec{u}$ and $\vec{v}$ are constant within any cross-section, they vary only with respect to τ and not with r_u or r_v. Also, the only derivatives that will be of interest will be those evaluated at points on the given cross-section, where $\{\vec{c}_1, \vec{c}_2, \vec{c}_3\} = \{\vec{t}, \vec{u}, \vec{v}\}$:

$$\frac{\mathrm{d}x_c}{\mathrm{d}\tau} = \left(\frac{\mathrm{d}\vec{\ell}}{\mathrm{d}\tau} + r_u\frac{\mathrm{d}\vec{u}}{\mathrm{d}\tau} + r_v\frac{\mathrm{d}\vec{v}}{\mathrm{d}\tau}\right) \cdot \vec{c}_1 \tag{4.8}$$

$$\frac{\mathrm{d}x_c}{\mathrm{d}r_u} = \vec{u} \cdot \vec{c}_1 = \vec{u} \cdot \vec{t} = 0 \tag{4.9}$$

$$\frac{\mathrm{d}x_c}{\mathrm{d}r_v} = \vec{v} \cdot \vec{c}_1 = \vec{v} \cdot \vec{t} = 0 \tag{4.10}$$

$$\frac{\mathrm{d}y_c}{\mathrm{d}\tau} = \left(\frac{\mathrm{d}\vec{\ell}}{\mathrm{d}\tau} + r_u\frac{\mathrm{d}\vec{u}}{\mathrm{d}\tau} + r_v\frac{\mathrm{d}\vec{v}}{\mathrm{d}\tau}\right) \cdot \vec{c}_2 \tag{4.11}$$

$$\frac{\mathrm{d}y_c}{\mathrm{d}r_u} = \vec{u} \cdot \vec{c}_2 = \vec{u} \cdot \vec{u} = 1 \tag{4.12}$$

$$\frac{\mathrm{d}y_c}{\mathrm{d}r_v} = \vec{v} \cdot \vec{c}_2 = \vec{v} \cdot \vec{u} = 0 \tag{4.13}$$

$$\frac{\mathrm{d}z_c}{\mathrm{d}\tau} = \left(\frac{\mathrm{d}\vec{\ell}}{\mathrm{d}\tau} + r_u\frac{\mathrm{d}\vec{u}}{\mathrm{d}\tau} + r_v\frac{\mathrm{d}\vec{v}}{\mathrm{d}\tau}\right) \cdot \vec{c}_3 \tag{4.14}$$

$$\frac{\mathrm{d}z_c}{\mathrm{d}r_u} = \vec{u} \cdot \vec{c}_3 = \vec{u} \cdot \vec{v} = 0 \tag{4.15}$$

$$\frac{\mathrm{d}z_c}{\mathrm{d}r_v} = \vec{v} \cdot \vec{c}_3 = \vec{v} \cdot \vec{v} = 1 \tag{4.16}$$

In order to form a rotation-invariant beam model equations (4.8), (4.11) and (4.14) need to be expressed with respect to rotation-invariant parameters.

4.2.4 Extension

Define ξ as the magnitude of $\mathrm{d}\vec{\ell}/\mathrm{d}\tau$, which is equal to the rate of change of arc length along the locus of centroids:

$$\xi = \left| \frac{\mathrm{d}\vec{\ell}}{\mathrm{d}\tau} \right| = \frac{\mathrm{d}s}{\mathrm{d}\tau} \tag{4.17}$$

ξ Rate of extension along the locus of centroids

Note that since $\vec{t}$ is a unit vector tangent to the locus of centroids $\vec{\ell}$,

$$\frac{\mathrm{d}\vec{\ell}}{\mathrm{d}\tau} = \frac{\mathrm{d}s}{\mathrm{d}\tau}\frac{\mathrm{d}\vec{\ell}}{\mathrm{d}s} = \xi\frac{\mathrm{d}\vec{\ell}}{\mathrm{d}s} = \xi\vec{t} \tag{4.18}$$

4.2.5 Curvature and twist

To find the derivatives of $\vec{u}$ and $\vec{v}$ with respect to τ, define a curvature vector $\vec{\kappa}$ which defines the change in orientation of cross-sections with respect to s:

$$\vec{\kappa} = \psi\vec{t} + \kappa_u\vec{u} + \kappa_v\vec{v} \tag{4.19}$$

ψ Twist rate about the locus of centroids (radians per unit length)

κ_u, κ_v Curvatures around the axes defined by $\vec{u}$ and $\vec{v}$ respectively (radians per unit length)

Then for an arbitrary vector $\vec{q}$ attached to a cross-section the derivative of $\vec{q}$ with respect to arc length s is

$$\frac{\mathrm{d}\vec{q}}{\mathrm{d}s} = \vec{\kappa} \times \vec{q} \tag{4.20}$$

and, using equation (4.17), its derivative with respect to τ is

$$\begin{aligned}
\frac{\mathrm{d}\vec{q}}{\mathrm{d}\tau} &= \frac{\mathrm{d}\vec{q}}{\mathrm{d}s}\frac{\mathrm{d}s}{\mathrm{d}\tau} \\
&= \xi\frac{\mathrm{d}\vec{q}}{\mathrm{d}s} \\
&= \xi\vec{\kappa} \times \vec{q} \\
&= \xi(\psi\vec{t} + \kappa_u\vec{u} + \kappa_v\vec{v}) \times \vec{q}
\end{aligned} \tag{4.21}$$

Therefore,

$$
\frac{\mathrm{d}\vec{t}}{\mathrm{d}\tau} = \xi(\psi\vec{t} + \kappa_u\vec{u} + \kappa_v\vec{v}) \times \vec{t}
$$

$$
= \xi(\kappa_v\vec{u} - \kappa_u\vec{v}) \tag{4.22}
$$

$$
\frac{\mathrm{d}\vec{u}}{\mathrm{d}\tau} = \xi(\psi\vec{t} + \kappa_u\vec{u} + \kappa_v\vec{v}) \times \vec{u}
$$

$$
= \xi(-\kappa_v\vec{t} + \psi\vec{v}) \tag{4.23}
$$

$$
\frac{\mathrm{d}\vec{v}}{\mathrm{d}\tau} = \xi(\psi\vec{t} + \kappa_u\vec{u} + \kappa_v\vec{v}) \times \vec{v}
$$

$$
= \xi(\kappa_u\vec{t} - \psi\vec{u}) \tag{4.24}
$$

4.2.6 Rotation invariance

By substituting equations (4.18), (4.23) and (4.24) into equations (4.8), (4.11), and (4.14), the three derivatives with respect to τ can be expressed in a completely rotation-invariant way:

$$
\frac{\mathrm{d}x_c}{\mathrm{d}\tau} = \left(\xi\vec{t} + r_u\xi(-\kappa_v\vec{t} + \psi\vec{v}) + r_v\xi(\kappa_u\vec{t} - \psi\vec{u})\right) \cdot \vec{c}_1
$$

$$
= \xi\left((1 - r_u\kappa_v + r_v\kappa_u)\vec{t} - r_v\psi\vec{u} + r_u\psi\vec{v}\right) \cdot \vec{c}_1
$$

$$
= \xi(1 - r_u\kappa_v + r_v\kappa_u) \tag{4.25}
$$

$$
\frac{\mathrm{d}y_c}{\mathrm{d}\tau} = \left(\xi\vec{t} + r_u\xi(-\kappa_v\vec{t} + \psi\vec{v}) + r_v\xi(\kappa_u\vec{t} - \psi\vec{u})\right) \cdot \vec{c}_2
$$

$$
= \xi\left((1 - r_u\kappa_v + r_v\kappa_u)\vec{t} - r_v\psi\vec{u} + r_u\psi\vec{v}\right) \cdot \vec{c}_2
$$

$$
= -\xi r_v\psi \tag{4.26}
$$

$$
\frac{\mathrm{d}z_c}{\mathrm{d}\tau} = \left(\xi\vec{t} + r_u\xi(-\kappa_v\vec{t} + \psi\vec{v}) + r_v\xi(\kappa_u\vec{t} - \psi\vec{u})\right) \cdot \vec{c}_3
$$

$$
= \xi\left((1 - r_u\kappa_v + r_v\kappa_u)\vec{t} - r_v\psi\vec{u} + r_u\psi\vec{v}\right) \cdot \vec{c}_3
$$

$$
= \xi r_u\psi \tag{4.27}
$$

Therefore,

$$
\begin{bmatrix} \mathrm{d}x_c \\ \mathrm{d}y_c \\ \mathrm{d}z_c \end{bmatrix} = \begin{bmatrix} \frac{\mathrm{d}x_c}{\mathrm{d}\tau} & \frac{\mathrm{d}x_c}{\mathrm{d}r_u} & \frac{\mathrm{d}x_c}{\mathrm{d}r_v} \\ \frac{\mathrm{d}y_c}{\mathrm{d}\tau} & \frac{\mathrm{d}y_c}{\mathrm{d}r_u} & \frac{\mathrm{d}y_c}{\mathrm{d}r_v} \\ \frac{\mathrm{d}z_c}{\mathrm{d}\tau} & \frac{\mathrm{d}z_c}{\mathrm{d}r_u} & \frac{\mathrm{d}z_c}{\mathrm{d}r_v} \end{bmatrix} \begin{bmatrix} \mathrm{d}\tau \\ \mathrm{d}r_u \\ \mathrm{d}r_v \end{bmatrix}
$$

$$
\begin{bmatrix} \mathrm{d}x_c \\ \mathrm{d}y_c \\ \mathrm{d}z_c \end{bmatrix} = \begin{bmatrix} \xi(1 - r_u\kappa_v + r_v\kappa_u) & 0 & 0 \\ -\xi r_v\psi & 1 & 0 \\ \xi r_u\psi & 0 & 1 \end{bmatrix} \begin{bmatrix} \mathrm{d}\tau \\ \mathrm{d}r_u \\ \mathrm{d}r_v \end{bmatrix} \tag{4.28}
$$

Equation (4.28) relates changes in cross-sectional coordinates x_c, y_c and z_c to changes in curvilinear coordinates τ, r_u and r_v entirely by parameters that are rotation invariant; if the beam goes through some arbitrary rigid body motion, its extension rate ξ, curvatures κ_u and κ_v and twist rate ψ remain exactly the same.

4.3 Deformation

Positions of points within the original, undeformed beam are given by

$$
\vec{\rho}^*(\tau, r_u, r_v) = \vec{\ell}^*(\tau) + r_u\vec{u}^* + r_v\vec{v}^* \tag{4.29}
$$

Similarly to (4.28), differential changes in the undeformed coordinates x_c^*, y_c^* and z_c^* with respect to the curvilinear coordinates τ, r_u and r_v are given by

$$
\begin{bmatrix} \mathrm{d}x_c^* \\ \mathrm{d}y_c^* \\ \mathrm{d}z_c^* \end{bmatrix} = \begin{bmatrix} \xi^*(1 - r_u\kappa_v^* + r_v\kappa_u^*) & 0 & 0 \\ -\xi^* r_v\psi^* & 1 & 0 \\ \xi^* r_u\psi^* & 0 & 1 \end{bmatrix} \begin{bmatrix} \mathrm{d}\tau \\ \mathrm{d}r_u \\ \mathrm{d}r_v \end{bmatrix} \tag{4.30}
$$

or inversely

$$
\begin{bmatrix} \mathrm{d}\tau \\ \mathrm{d}r_u \\ \mathrm{d}r_v \end{bmatrix} = \begin{bmatrix} \frac{1}{\xi^*(1 - r_u\kappa_v^* + r_v\kappa_u^*)} & 0 & 0 \\ \frac{r_v\psi^*}{(1 - r_u\kappa_v^* + r_v\kappa_u^*)} & 1 & 0 \\ -\frac{r_u\psi^*}{(1 - r_u\kappa_v^* + r_v\kappa_u^*)} & 0 & 1 \end{bmatrix} \begin{bmatrix} \mathrm{d}x_c \\ \mathrm{d}y_c \\ \mathrm{d}z_c \end{bmatrix} \tag{4.31}
$$

Strains within the beam can then be computed by comparing the local behaviour of the beam before and after deformation, described by equations (4.30) and (4.28) respectively.

4.3.1 Strains

For a linear computation of strain, it is first necessary to find the deformation gradient $\mathbf{F}$ [14]:

$$\begin{bmatrix} \mathrm{d}x_c \\ \mathrm{d}y_c \\ \mathrm{d}z_c \end{bmatrix} = \mathbf{F} \begin{bmatrix} \mathrm{d}x_c^* \\ \mathrm{d}y_c^* \\ \mathrm{d}z_c^* \end{bmatrix} \tag{4.32}$$

$\mathbf{F}$ 3×3 deformation gradient giving derivatives of coordinates x_c, y_c, z_c with respect to undeformed (original) coordinates x_c^*, y_c^*, z_c^*

Substituting equations (4.30) and (4.28) into equation (4.32),

$$\begin{bmatrix} \xi(1 - r_u\kappa_v + r_v\kappa_u) & 0 & 0 \\ -\xi r_v\psi & 1 & 0 \\ \xi r_u\psi & 0 & 1 \end{bmatrix} \begin{bmatrix} \mathrm{d}\tau \\ \mathrm{d}r_u \\ \mathrm{d}r_v \end{bmatrix} = \mathbf{F} \begin{bmatrix} \xi^*(1 - r_u\kappa_v^* + r_v\kappa_u^*) & 0 & 0 \\ -\xi^* r_v\psi^* & 1 & 0 \\ \xi^* r_u\psi^* & 0 & 1 \end{bmatrix} \begin{bmatrix} \mathrm{d}\tau \\ \mathrm{d}r_u \\ \mathrm{d}r_v \end{bmatrix} \tag{4.33}$$

This must be true for arbitrary $\mathrm{d}\tau$, $\mathrm{d}r_u$, $\mathrm{d}r_v$, so it can be concluded that

$$\begin{bmatrix} \xi(1 - r_u\kappa_v + r_v\kappa_u) & 0 & 0 \\ -\xi r_v\psi & 1 & 0 \\ \xi r_u\psi & 0 & 1 \end{bmatrix} = \mathbf{F} \begin{bmatrix} \xi^*(1 - r_u\kappa_v^* + r_v\kappa_u^*) & 0 & 0 \\ -\xi^* r_v\psi^* & 1 & 0 \\ \xi^* r_u\psi^* & 0 & 1 \end{bmatrix} \tag{4.34}$$

and therefore

$$\begin{aligned} \mathbf{F} &= \begin{bmatrix} \xi(1 - r_u\kappa_v + r_v\kappa_u) & 0 & 0 \\ -\xi r_v\psi & 1 & 0 \\ \xi r_u\psi & 0 & 1 \end{bmatrix} \begin{bmatrix} \xi^*(1 - r_u\kappa_v^* + r_v\kappa_u^*) & 0 & 0 \\ -\xi^* r_v\psi^* & 1 & 0 \\ \xi^* r_u\psi^* & 0 & 1 \end{bmatrix}^{-1} \\[2mm] &= \begin{bmatrix} \xi(1 - r_u\kappa_v + r_v\kappa_u) & 0 & 0 \\ -\xi r_v\psi & 1 & 0 \\ \xi r_u\psi & 0 & 1 \end{bmatrix} \begin{bmatrix} \frac{1}{\xi^*(1 - r_u\kappa_v^* + r_v\kappa_u^*)} & 0 & 0 \\ \frac{r_v\psi^*}{1 - r_u\kappa_v^* + r_v\kappa_u^*} & 1 & 0 \\ \frac{-r_u\psi^*}{1 - r_u\kappa_v^* + r_v\kappa_u^*} & 0 & 1 \end{bmatrix} \\[2mm] &= \begin{bmatrix} \frac{\xi(1 - r_u\kappa_v + r_v\kappa_u)}{\xi^*(1 - r_u\kappa_v^* + r_v\kappa_u^*)} & 0 & 0 \\ \frac{-r_v(\xi\psi - \xi^*\psi*)}{\xi^*(1 - r_u\kappa_v^* + r_v\kappa_u^*)} & 1 & 0 \\ \frac{r_u(\xi\psi - \xi^*\psi^*)}{\xi^*(1 - r_u\kappa_v^* + r_v\kappa_u^*)} & 0 & 1 \end{bmatrix} \end{aligned} \tag{4.35}$$

It is then possible to form the material displacement gradient [14]

$$
\mathbf{F} - \mathbf{I} =
\begin{bmatrix}
\frac{\xi(1-r_u\kappa_v+r_v\kappa_u)}{\xi^*(1-r_u\kappa_v^*+r_v\kappa_u^*)} & 0 & 0 \\
\frac{-r_v(\xi\psi-\xi^*\psi*)}{\xi^*(1-r_u\kappa_v^*+r_v\kappa_u^*)} & 1 & 0 \\
\frac{r_u(\xi\psi-\xi^*\psi^*)}{\xi^*(1-r_u\kappa_v^*+r_v\kappa_u^*)} & 0 & 1
\end{bmatrix}
-
\begin{bmatrix}
1 & 0 & 0 \\
0 & 1 & 0 \\
0 & 0 & 1
\end{bmatrix}
$$

$$
=
\begin{bmatrix}
\frac{\xi(1-r_u\kappa_v+r_v\kappa_u)-\xi^*(1-r_u\kappa_v^*+r_v\kappa_u^*)}{\xi^*(1-r_u\kappa_v^*+r_v\kappa_u^*)} & 0 & 0 \\
\frac{-r_v(\xi\psi-\xi^*\psi^*)}{\xi^*(1-r_u\kappa_v^*+r_v\kappa_u^*)} & 0 & 0 \\
\frac{r_u(\xi\psi-\xi^*\psi^*)}{\xi^*(1-r_u\kappa_v^*+r_v\kappa_u^*)} & 0 & 0
\end{bmatrix}
$$

$$
=
\begin{bmatrix}
\frac{(\xi-\xi^*)-r_u(\xi\kappa_v-\xi^*\kappa_v^*)+r_v(\xi\kappa_u-\xi^*\kappa_u^*)}{\xi^*(1-r_u\kappa_v^*+r_v\kappa_u^*)} & 0 & 0 \\
\frac{-r_v(\xi\psi-\xi^*\psi^*)}{\xi^*(1-r_u\kappa_v^*+r_v\kappa_u^*)} & 0 & 0 \\
\frac{r_u(\xi\psi-\xi^*\psi^*)}{\xi^*(1-r_u\kappa_v^*+r_v\kappa_u^*)} & 0 & 0
\end{bmatrix}
\tag{4.36}
$$

from which the three non-zero strains can be extracted:

$$
\epsilon_{x_c x_c} = \frac{\Delta\xi - r_u\Delta(\xi\kappa_v) + r_v\Delta(\xi\kappa_u)}{\xi^*(1 - r_u\kappa_v^* + r_v\kappa_u^*)}
\tag{4.37}
$$

$$
\gamma_{x_c y_c} = \frac{-r_v\Delta(\xi\psi)}{\xi^*(1 - r_u\kappa_v^* + r_v\kappa_u^*)}
\tag{4.38}
$$

$$
\gamma_{x_c z_c} = \frac{r_u\Delta(\xi\psi)}{\xi^*(1 - r_u\kappa_v^* + r_v\kappa_u^*)}
\tag{4.39}
$$

$\epsilon_{x_c x_c}$	Strain normal to a cross-section
$\gamma_{x_c y_c}, \gamma_{x_c z_c}$	Shear strains on a cross-section
$\Delta\xi$	Change in locus of centroids extension rate relative to the undeformed configuration, $\xi - \xi^*$
$\Delta(\xi\kappa_u), \Delta(\xi\kappa_v)$	Changes in locus of centroids extension-curvature products, $\xi\kappa_u - \xi^*\kappa_u^*$ and $\xi\kappa_v - \xi^*\kappa_v^*$
$\Delta(\xi\psi)$	Change in locus of centroids extension-twist product, $\xi\psi - \xi^*\psi^*$

4.3.2 Strain energy integral

Given equations (4.37)–(4.39), it is possible to integrate over the volume of an element to find the total strain energy [14]:

$$
dU = \frac{1}{2} \begin{bmatrix} \epsilon_{x_c x_c} & \gamma_{x_c y_c} & \gamma_{x_c z_c} \end{bmatrix} \begin{bmatrix} E & 0 & 0 \\ 0 & G & 0 \\ 0 & 0 & G \end{bmatrix} \begin{bmatrix} \epsilon_{x_c x_c} \\ \gamma_{x_c y_c} \\ \gamma_{x_c z_c} \end{bmatrix} dV
$$

$$
dU = \frac{1}{2}(E\epsilon_{x_c x_c}^2 + G(\gamma_{x_c y_c}^2 + \gamma_{x_c z_c}^2))dV
$$

$$
U = \frac{1}{2}\int_V E\epsilon_{x_c x_c}^2 + G(\gamma_{x_c y_c}^2 + \gamma_{x_c z_c}^2)\, dV \tag{4.40}
$$

Using equation (4.30),

$$
dV = dx_c^* dy_c^* dz_c^*
$$

$$
= \begin{vmatrix} \xi^*(1 - r_u\kappa_v^* + r_v\kappa_u^*) & 0 & 0 \\ -\xi^* r_v\psi^* & 1 & 0 \\ \xi^* r_u\psi^* & 0 & 1 \end{vmatrix} d\tau dr_u dr_v
$$

$$
= \xi^*(1 - r_u\kappa_v^* + r_v\kappa_u^*)d\tau dr_u dr_v \tag{4.41}
$$

Substituting equations (4.37)–(4.39) and (4.41) into equation (4.40), and splitting the integration through the volume of the element into integration along the locus

33

of centroids and integration over the cross-sectional area, yields

$$U = \frac{1}{2} \int_{\tau=0}^{1} \int_{A} \left(E \left(\frac{\Delta\xi - r_u\Delta(\xi\kappa_v) + r_v\Delta(\xi\kappa_u)}{\xi^*(1 - r_u\kappa_v^* + r_v\kappa_u^*)} \right)^2 \right.$$

$$\left. + G \left(\left(\frac{-r_v\Delta(\xi\psi)}{\xi^*(1 - r_u\kappa_v^* + r_v\kappa_u^*)} \right)^2 + \left(\frac{r_u\Delta(\xi\psi)}{\xi^*(1 - r_u\kappa_v^* + r_v\kappa_u^*)} \right)^2 \right) \right)$$

$$\xi^*(1 - r_u\kappa_v^* + r_v\kappa_u^*) \, \mathrm{d}r_u \, \mathrm{d}r_v \, \mathrm{d}\tau \tag{4.42}$$

$$= \frac{1}{2} \int_{\tau=0}^{1} \int_{A} \left(\frac{E(\Delta\xi)^2}{\xi^{*2}(1 - r_u\kappa_v^* + r_v\kappa_u^*)^2} - \frac{2Er_u\Delta\xi\Delta(\xi\kappa_v)}{\xi^{*2}(1 - r_u\kappa_v^* + r_v\kappa_u^*)^2} \right.$$

$$+ \frac{2Er_v\Delta\xi\Delta(\xi\kappa_v)}{\xi^{*2}(1 - r_u\kappa_v^* + r_v\kappa_u^*)^2} + \frac{Er_u^2(\Delta(\xi\kappa_v))^2}{\xi^{*2}(1 - r_u\kappa_v^* + r_v\kappa_u^*)^2}$$

$$- \frac{2Er_ur_v\Delta(\xi\kappa_v)\Delta(\xi\kappa_u)}{\xi^{*2}(1 - r_u\kappa_v^* + r_v\kappa_u^*)^2} + \frac{Er_v^2(\Delta(\xi\kappa_u))^2}{\xi^{*2}(1 - r_u\kappa_v^* + r_v\kappa_u^*)^2}$$

$$+ \left. \frac{G\left(r_v^2(\Delta(\xi\psi))^2 + r_u^2(\Delta(\xi\psi))^2\right)}{\xi^{*2}(1 - r_u\kappa_v^* + r_v\kappa_u^*)^2} \right)$$

$$\xi^*(1 - r_u\kappa_v^* + r_v\kappa_u^*) \, \mathrm{d}r_u \, \mathrm{d}r_v \, \mathrm{d}\tau \tag{4.43}$$

Separating by powers of r_u and r_v, and bringing outside of the area integral any terms that are constant over the cross-section,

$$U = \frac{1}{2} \int_{\tau=0}^{1} \left((\Delta\xi)^2 \left[\frac{E}{\xi^*} \int_{A} \frac{1}{1 - r_u\kappa_v^* + r_v\kappa_u^*} \mathrm{d}r_u \mathrm{d}r_v \right] \right.$$

$$- \Delta\xi\Delta(\xi\kappa_v) \left[\frac{2E}{\xi^*} \int_{A} \frac{r_u}{1 - r_u\kappa_v^* + r_v\kappa_u^*} \mathrm{d}r_u \mathrm{d}r_v \right]$$

$$+ \Delta\xi\Delta(\xi\kappa_u) \left[\frac{2E}{\xi^*} \int_{A} \frac{r_v}{1 - r_u\kappa_v^* + r_v\kappa_u^*} \mathrm{d}r_u \mathrm{d}r_v \right]$$

$$+ (\Delta(\xi\kappa_v))^2 \left[\frac{E}{\xi^*} \int_{A} \frac{r_u^2}{1 - r_u\kappa_v^* + r_v\kappa_u^*} \mathrm{d}r_u \mathrm{d}r_v \right]$$

$$- \Delta(\xi\kappa_v)\Delta(\xi\kappa_u) \left[\frac{2E}{\xi^*} \int_{A} \frac{r_ur_v}{1 - r_u\kappa_v^* + r_v\kappa_u^*} \mathrm{d}r_u \mathrm{d}r_v \right]$$

$$+ (\Delta(\xi\kappa_u))^2 \left[\frac{E}{\xi^*} \int_{A} \frac{r_v^2}{1 - r_u\kappa_v^* + r_v\kappa_u^*} \mathrm{d}r_u \mathrm{d}r_v \right]$$

$$+ (\Delta(\xi\psi))^2 \left[\frac{G}{\xi^*} \int_{A} \frac{r_v^2}{1 - r_u\kappa_v^* + r_v\kappa_u^*} \mathrm{d}r_u \mathrm{d}r_v \right]$$

$$+ (\Delta(\xi\psi))^2 \left[\frac{G}{\xi^*} \int_{A} \frac{r_u^2}{1 - r_u\kappa_v^* + r_v\kappa_u^*} \mathrm{d}r_u \mathrm{d}r_v \right] \right) \mathrm{d}\tau \tag{4.44}$$

34

Note that none of the terms enclosed in square brackets in equation (4.44) depend on any post-deformation quantities, so they can be evaluated once and then used throughout the course of a dynamic beam simulation. This is conceptually similar to separating out an area integral to obtain the second moment of area I as in section 3.1, although in this case the area integrals are more complex.

4.3.3 Generalized moments

In order to simplify equation (4.44), first define

$$I_{mn} = \int_A r_u^m r_v^n \mathrm{d}A = \int_A r_u^m r_v^n \mathrm{d}r_u \mathrm{d}r_v \tag{4.45}$$

I_{mn} Indexed moment of area of a cross-section

Note that area, first moments of area, and second, product, and polar moments of area can all be expressed as indexed moments of area:

$$A = \int_A \mathrm{d}A = I_{00} \tag{4.46}$$

$$Q_u = \int_A r_v \mathrm{d}A = I_{01} \tag{4.47}$$

$$Q_v = \int_A r_u \mathrm{d}A = I_{10} \tag{4.48}$$

$$I_{uu} = \int_A r_v^2 \mathrm{d}A = I_{02} \tag{4.49}$$

$$I_{uv} = \int_A r_v r_u \mathrm{d}A = I_{11} \tag{4.50}$$

$$I_{vv} = \int_A r_u^2 \mathrm{d}A = I_{20} \tag{4.51}$$

$$J = \int_A (r_u^2 + r_v^2)\mathrm{d}A = I_{02} + I_{20} \tag{4.52}$$

Next, define

$$\chi_{mn} = \chi_{mn}(\tau) = \int_A \frac{r_u^m r_v^n}{1 - r_u \kappa_v^* + r_v \kappa_u^*}\mathrm{d}r_u \mathrm{d}r_v \tag{4.53}$$

χ_{mn} Generalized moment of area of a cross-section

If the original beam curvatures $\kappa_u^* = \kappa_v^* = 0$,

$$\chi_{mn} = \int_A \frac{r_u^m r_v^n}{1 - r_u(0) + r_v(0)}\mathrm{d}r_u \mathrm{d}r_v = \int_A r_u^m r_v^n \mathrm{d}r_u \mathrm{d}r_v = I_{mn} \tag{4.54}$$

so that the generalized moments χ_{mn} are equal to the indexed moments I_{mn} for an initially straight beam.

In order to evaluate the integral in equation (4.53), use a negative binomial series [15]:

$$(1 - (a - b))^{-1} = \sum_{i=0}^{\infty} (-1)^i (a - b)^i \tag{4.55}$$

$$(a - b)^i = \sum_{k=0}^{i} \binom{i}{k} (-1)^k a^{i-k} b^k \tag{4.56}$$

$$
\begin{aligned}
(1 - (a - b))^{-1} &= \sum_{i=0}^{\infty} (-1)^i \left(\sum_{k=0}^{i} \binom{i}{k} (-1)^k a^{i-k} b^k \right) \\
&= \sum_{i=0}^{\infty} \sum_{k=0}^{i} (-1)^{i+k} \binom{i}{k} a^{i-k} b^k \\
&= \sum_{i=0}^{\infty} \sum_{k=0}^{i} (-1)^{i-k} \binom{i}{i-k} a^{i-k} b^k \qquad \text{Since } (-1)^{i-k} = (-1)^{i+k} \\
&= \sum_{i=0}^{\infty} \sum_{j=0}^{i} (-1)^j \binom{i}{j} a^j b^{i-j} \qquad \text{Substituting } j = i - k \quad (4.57)
\end{aligned}
$$

Using equation (4.57), equation (4.53) becomes

$$
\begin{aligned}
\chi_{mn} &= \int_A \frac{r_u^m r_v^n}{1 - r_u \kappa_v^* + r_v \kappa_u^*} \mathrm{d}r_u \mathrm{d}r_v \\
&= \int_A r_u^m r_v^n \left(1 - (r_u \kappa_v^* - r_v \kappa_u^*) \right)^{-1} \mathrm{d}r_u \mathrm{d}r_v \\
&= \int_A r_u^m r_v^n \left(\sum_{i=0}^{\infty} \sum_{j=0}^{i} (-1)^j \binom{i}{j} (r_u \kappa_v^*)^j (r_v \kappa_u^*)^{i-j} \right) \mathrm{d}r_u \mathrm{d}r_v \\
&= \sum_{i=0}^{\infty} \sum_{j=0}^{i} (-1)^j \binom{i}{j} \kappa_u^{*\,i-j} \kappa_v^{*\,j} \int_A r_u^{j+m} r_v^{i-j+n} \mathrm{d}r_u \mathrm{d}r_v \tag{4.58} \\
&= \sum_{i=0}^{\infty} \sum_{j=0}^{i} (-1)^j \binom{i}{j} \kappa_u^{*\,i-j} \kappa_v^{*\,j} I_{j+m,i-j+n} \tag{4.59}
\end{aligned}
$$

Therefore, to evaluate a generalized moment of area of a cross-section, the only requirement is that the indexed moments I_{mn} are able to be evaluated over the cross-section, and the generalized moments χ_{mn} can be computed from equation (4.59).

36

4.3.4 Strain energy

Using equation (4.53), equation (4.44) becomes

$$
\begin{aligned}
U = \frac{1}{2} \int_{\tau=0}^{1} \Bigg(& (\Delta\xi)^2 \left[\frac{E}{\xi^*}\chi_{00}\right] - \Delta\xi\Delta(\xi\kappa_v)\left[\frac{2E}{\xi^*}\chi_{10}\right] + \Delta\xi\Delta(\xi\kappa_u)\left[\frac{2E}{\xi^*}\chi_{01}\right] \\
& + (\Delta(\xi\kappa_v))^2\left[\frac{E}{\xi^*}\chi_{20}\right] - \Delta(\xi\kappa_v)\Delta(\xi\kappa_u)\left[\frac{2E}{\xi^*}\chi_{11}\right] + (\Delta(\xi\kappa_u))^2\left[\frac{E}{\xi^*}\chi_{02}\right] \\
& + (\Delta(\xi\psi))^2\left[\frac{G}{\xi^*}(\chi_{20}+\chi_{02})\right] \Bigg) \mathrm{d}\tau
\end{aligned}
\tag{4.60}
$$

where the generalized moments χ_{mn} are computed from equation (4.59). Although this can be computationally expensive depending on how many terms of the infinite series are evaluated, it only has to be performed once for a given beam instead of having to be updated at every time step in a simulation.

4.3.5 Internal force

The internal force in the beam can be obtained by integrating the normal stress $\sigma_{x_c x_c}$ over the cross-sectional area [1]:

$$
\begin{aligned}
F &= \int_A \sigma_{x_c x_c} \mathrm{d}A \\
&= \int_A E\epsilon_{x_c x_c} \mathrm{d}A \\
&= E \int_A \epsilon_{x_c x_c} \mathrm{d}A
\end{aligned}
\tag{4.61}
$$

F	Internal axial force in the beam
$\sigma_{x_c x_c}$	Normal stress to a beam cross-section

Using equation (4.37),

$$
\begin{aligned}
F &= E \int_A \frac{\Delta\xi - r_u\Delta(\xi\kappa_v) + r_v\Delta(\xi\kappa_u)}{\xi^*(1 - r_u\kappa_v^* + r_v\kappa_u^*)} \mathrm{d}A \\
&= \frac{E\Delta\xi}{\xi^*} \int_A \frac{1}{1 - r_u\kappa_v^* + r_v\kappa_u^*}\mathrm{d}A - \frac{E\Delta(\xi\kappa_v)}{\xi^*} \int_A \frac{r_u}{1 - r_u\kappa_v^* + r_v\kappa_u^*}\mathrm{d}A \\
&\quad + \frac{E\Delta(\xi\kappa_u)}{\xi^*} \int_A \frac{r_v}{1 - r_u\kappa_v^* + r_v\kappa_u^*}\mathrm{d}A \\
&= \frac{E}{\xi^*}\Big(\Delta\xi\chi_{00} - \Delta(\xi\kappa_v)\chi_{10} + \Delta(\xi\kappa_u)\chi_{01}\Big)
\end{aligned}
\tag{4.62}
$$

4.3.6 Internal bending moments

The internal bending moment in the beam about an axis aligned with $\vec{u}$ can be obtained by integrating the product of normal stress $\sigma_{x_c x_c}$ and cross-sectional coordinate r_v over the cross-sectional area [1]:

$$
\begin{aligned}
M_u &= \int_A r_v \sigma_{x_c x_c} \, \mathrm{d}A \\
&= \int_A E r_v \epsilon_{x_c x_c} \, \mathrm{d}A \\
&= E \int_A r_v \epsilon_{x_c x_c} \, \mathrm{d}A
\end{aligned}
\tag{4.63}
$$

M_u Internal bending moment in the beam about an axis aligned with $\vec{u}$

Once again substituting in equation (4.37),

$$
\begin{aligned}
M_u &= E \int_A r_v \frac{\Delta \xi - r_u \Delta(\xi \kappa_v) + r_v \Delta(\xi \kappa_u)}{\xi^* (1 - r_u \kappa_v^* + r_v \kappa_u^*)} \, \mathrm{d}A \\
&= \frac{E \Delta \xi}{\xi^*} \int_A \frac{r_v}{1 - r_u \kappa_v^* + r_v \kappa_u^*} \, \mathrm{d}A - \frac{E \Delta(\xi \kappa_v)}{\xi^*} \int_A \frac{r_u r_v}{1 - r_u \kappa_v^* + r_v \kappa_u^*} \, \mathrm{d}A \\
&\quad + \frac{E \Delta(\xi \kappa_u)}{\xi^*} \int_A \frac{r_v^2}{1 - r_u \kappa_v^* + r_v \kappa_u^*} \, \mathrm{d}A \\
&= \frac{E}{\xi^*} \Big(\Delta \xi \chi_{01} - \Delta(\xi \kappa_v) \chi_{11} + \Delta(\xi \kappa_u) \chi_{02} \Big)
\end{aligned}
\tag{4.64}
$$

Similarly,

$$
M_v = \frac{E}{\xi^*} \Big(\Delta \xi \chi_{10} - \Delta(\xi \kappa_v) \chi_{20} + \Delta(\xi \kappa_u) \chi_{11} \Big)
\tag{4.65}
$$

M_v Internal bending moment in the beam about an axis aligned with $\vec{v}$

4.3.7 Internal twisting moment

The internal twisting moment in the beam can be obtained by integrating the products of shear stresses and cross-sectional coordinates over the cross-section [1]:

$$
\begin{aligned}
M_t &= \int_A r_u \sigma_{x_c z_c} - r_v \sigma_{x_c y_c} \mathrm{d}A \\
&= \int_A r_u G \gamma_{x_c z_c} - r_v G \gamma_{x_c y_c} \mathrm{d}A \\
&= G \left(\int_A r_u \gamma_{x_c z_c} \mathrm{d}A - \int_A r_v \gamma_{x_c y_c} \mathrm{d}A \right)
\end{aligned}
\tag{4.66}
$$

M_t	Internal twisting moment in the beam (about an axis aligned with $\vec{t}$
$\sigma_{x_c z_c}, \sigma_{x_c y_c}$	Shear stresses on a beam cross-section

Using equations (4.38) and (4.39),

$$
\begin{aligned}
M_t &= G \left(\int_A r_u \frac{r_u \Delta(\xi \psi)}{\xi^*(1 - r_u \kappa_v^* + r_v \kappa_u^*)} \mathrm{d}A - \int_A r_v \frac{-r_v \Delta(\xi \psi)}{\xi^*(1 - r_u \kappa_v^* + r_v \kappa_u^*)} \mathrm{d}A \right) \\
&= \frac{G \Delta(\xi \psi)}{\xi^*} \left(\int_A \frac{r_u^2}{1 - r_u \kappa_v^* + r_v \kappa_u^*} \mathrm{d}A + \int_A \frac{r_v^2}{1 - r_u \kappa_v^* + r_v \kappa_u^*} \mathrm{d}A \right) \\
&= \frac{G \Delta(\xi \psi)}{\xi^*} (\chi_{20} + \chi_{02})
\end{aligned}
\tag{4.67}
$$

4.4 Motion

For a dynamic simulation where the inertia of the beam is significant, it is necessary to compute the kinetic energy of the beam as well as its strain energy at any instant. As with strain energy, the calculation of kinetic energy can be simplified by making assumptions about the shape of the beam.

Specifically, since beams are very long compared to their width, their kinetic energy can be closely approximated by assuming that all of the mass is distributed only along the locus of centroids and not throughout the beam. For any cross-section, this has the effect of ignoring the contribution to kinetic energy of that cross-section's angular velocity, *i.e.*, ignoring the small variation in velocity across

$$I = \tfrac{1}{12}m(3r^2 + L^2) \qquad\qquad\qquad I = \tfrac{1}{12}mL^2$$

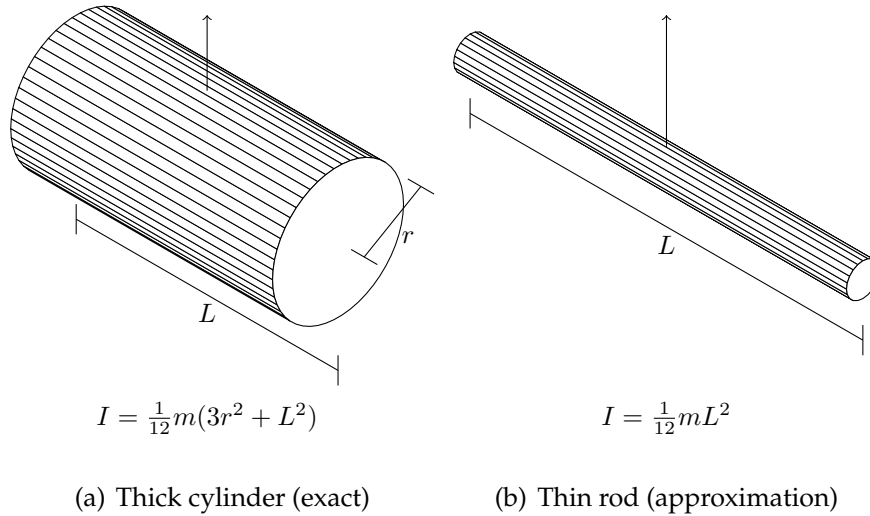(a) Thick cylinder (exact)　　　　(b) Thin rod (approximation)

Figure 4.6: Moment of inertia approximation

the cross-section and assuming that all points are concentrated at the cross-section centroid.

For long, slender beams this contribution is small, the error being on the order of the difference between calculating the moment of inertia for a thick cylinder and thin rod, as illustrated in Figure 4.6. When $L \gg r$, the expression for moment of inertia of the cylinder is very close to the rod approximation.

One situation where the assumption that all mass is concentrated along the line of centroids breaks down is the case of a straight rod being spun about its own axis; in this case the *only* contribution to kinetic energy is from the angular velocity of cross-sections about the locus of centroids. In this case a more specialized rod model should be used instead of the generic curved-beam model developed here.

4.4.1 Kinetic energy

The kinetic energy of a beam element is given by integrating along the locus of centroids,

$$T = \frac{1}{2} \int_{\tau=0}^{1} \vec{\nu} \cdot \vec{\nu} \, \mathrm{d}m \tag{4.68}$$

The mass of a differential slice of the beam element is obtained by integrating across the cross-sectional area:

$$\mathrm{d}m = \int_A \varrho \mathrm{d}V \tag{4.69}$$

ϱ Mass density per unit volume

Using equation (4.41),

$$\begin{aligned}
\mathrm{d}m &= \int_A \varrho\xi^*(1 - r_u\kappa_v^* + r_v\kappa_u^*)\mathrm{d}\tau \mathrm{d}r_u \mathrm{d}r_v \\
&= \varrho\xi^*\left(\int_A \mathrm{d}r_u\mathrm{d}r_v - \kappa_v^*\int_A r_u\mathrm{d}r_u\mathrm{d}r_v + \kappa_u^*\int_A r_v\mathrm{d}r_u\mathrm{d}r_v\right)\mathrm{d}\tau \\
&= \varrho\xi^*(A - \kappa_v^* I_{10} + \kappa_u^* I_{01})\mathrm{d}\tau
\end{aligned} \tag{4.70}$$

A Cross-sectional area

But since r_u and r_v are measured from the cross-section centroid, $I_{10} = I_{01} = 0$ by definition, so that

$$\mathrm{d}m = \varrho A\xi^*\mathrm{d}\tau \tag{4.71}$$

Substituting equation (4.71) into equation (4.68),

$$T = \frac{1}{2}\int_{\tau=0}^1 \varrho A(\vec{\nu}\cdot\vec{\nu})\xi^*\mathrm{d}\tau \tag{4.72}$$

5

Finite Element Construction

Equations (4.60) and (4.72) define the strain and kinetic energies for an abstract beam element; to use them, an element must be defined for which all the quantities in those expressions can be evaluated. To compute the strain energy, the locus of centroid quantities ξ, κ_u, κ_v and ψ and generalized moments χ_{mn} must be evaluated; to compute the kinetic energy, the area A and velocity $\vec{\nu}$ must be evaluated.

A convenient way of describing elements of a beam is by specifying the behaviour of specific cross-sections within the beam, and defining a geometric interpolant that describes the shape of the beam in between those cross-sections, as discussed in section 2.3. In this way, the first and second cross-sections define the first element, the second and third cross-sections define the second element, and so on, as illustrated in Figure 2.4. For the elements to be C^1, all the behaviour up to first order must be specified at each cross-section.

For a given cross-section A, the following quantities must be defined:

$\vec{\rho}_A$	Position vector of the centroid of cross-section A
$\vec{t}_A, \vec{u}_A, \vec{v}_A$	Cross-section normal (tangent to the locus of centroids) and principal axis vectors of cross-section A, describing its orientation
ξ_A	Rate of extension along the locus of centroids at cross-section A
ψ_A	Rate of twist of cross-sections about the locus of centroids at cross-section A
$\vec{\nu}_A$	Velocity of the centroid of cross-section A
$\vec{\omega}_A$	Angular velocity of cross-section A

Shape parameters (*e.g.*, radius of a circle or width and height of a rectangle) and their derivatives must also be defined at each cross-section.

Each element of the beam is defined by two cross-sections A and B. From section 2.3, an element for a three-dimensional curved beam is geometrically defined by the locus of centroids, the orientation of cross-sections relative to the locus of centroids, and the area properties of cross-sections along the locus of centroids.

5.1   Locus of centroids

For each element, a locus of centroids must be defined that starts and ends at the centroids $\vec{\rho}_A$ and $\vec{\rho}_B$ of the element's two defining cross-sections. The derivatives at each end must also equal $\xi_A \vec{t}_A$ and $\xi_B \vec{t}_B$; it is important to specify the rate of extension along the locus of centroids since a change in the rate of extension is what gives rise to extensional strain and, in turn, internal force, as discussed in section 4.3. This geometric interpolation between cross-sections is illustrated in Figure 5.1.

Ideally, it should be easy to evaluate position, extension rate, and curvature along the locus of centroids; crucially, it must also be possible to effectively define cross-section orientation relative to the locus of centroids.

One relatively straightforward approach to defining orientation would be to
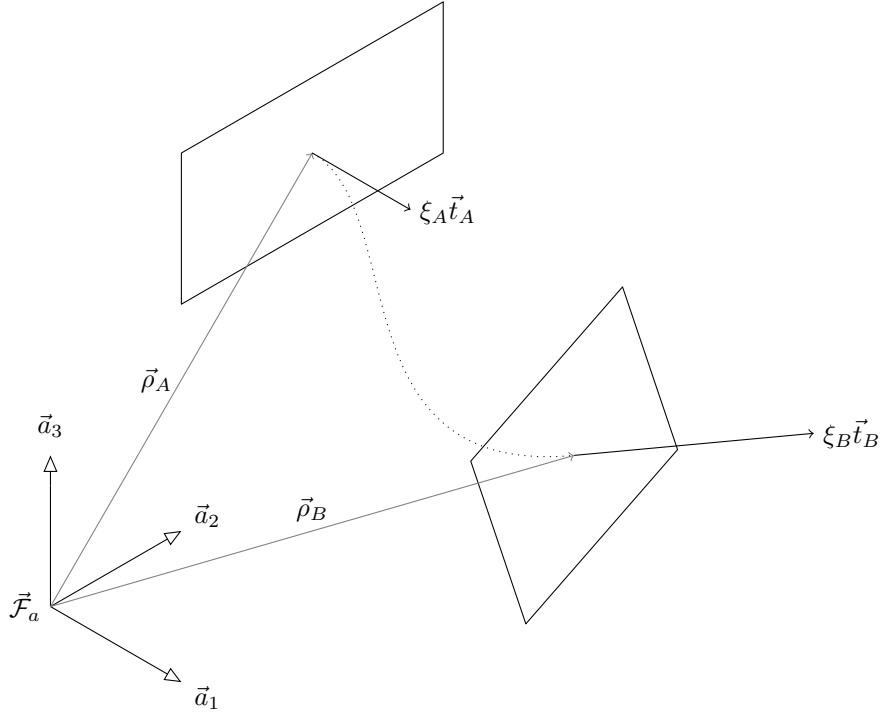
Figure 5.1: Interpolation of the locus of centroids.

use the locus of centroid's Frenet frame [16], which is composed of the unit tangent, principal normal and binormal vectors. However, the Frenet frame can be, numerically, a very unstable reference, as illustrated in Figure 5.2. There, the principal normal to the measured locus of centroids of a hockey stick blade varies quite significantly, as compared to a 'progressive normal' (which is defined to have zero twist about the locus of centroids).

For a planar curve, this problem does not exist; the binormal is constant and equal to the normal of the plane in which the curve lies, and the tangent and normal vectors always lie in the same plane. The Frenet frame can then form a stable reference for measuring orientation (perhaps as shown earlier in Figure 3.4, where the orientation of the cross-section is defined as an angle between the vector $\vec{v}$ and the curve binormal $\vec{b}$).

Unfortunately, the interpolation illustrated in Figure 5.1 is impossible to perform in general with a planar curve, since it is not necessarily true that both points

44
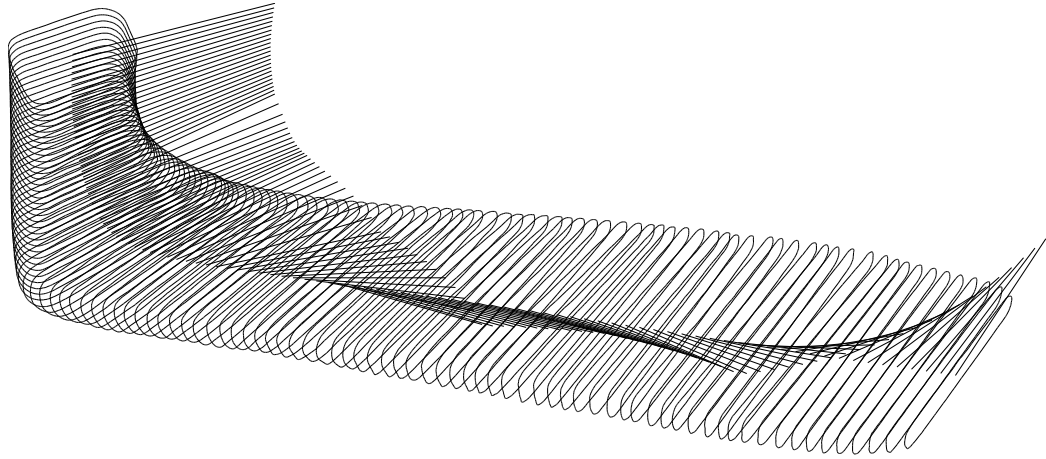
(a) Principal normal
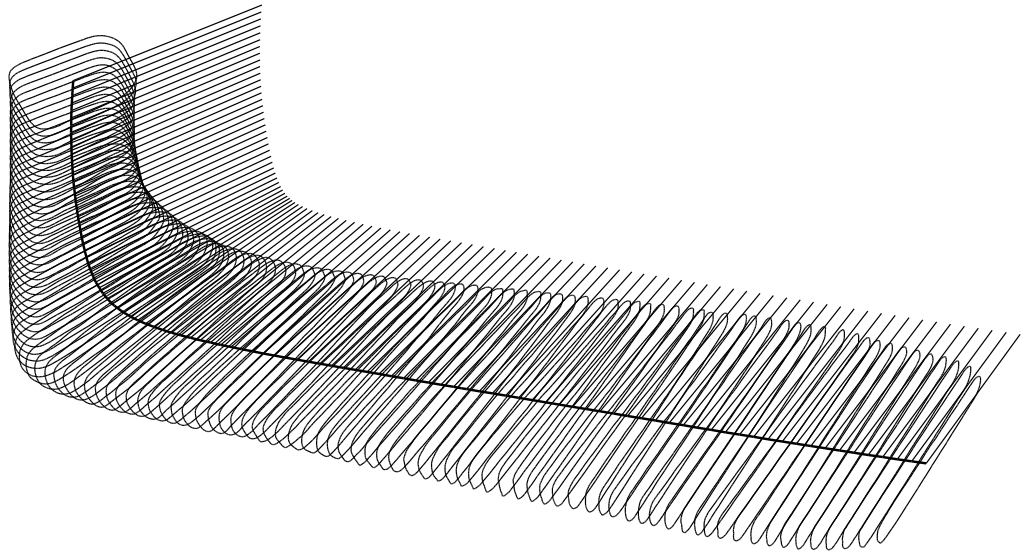
(b) Progressive normal

Figure 5.2: Instability of the Frenet frame.
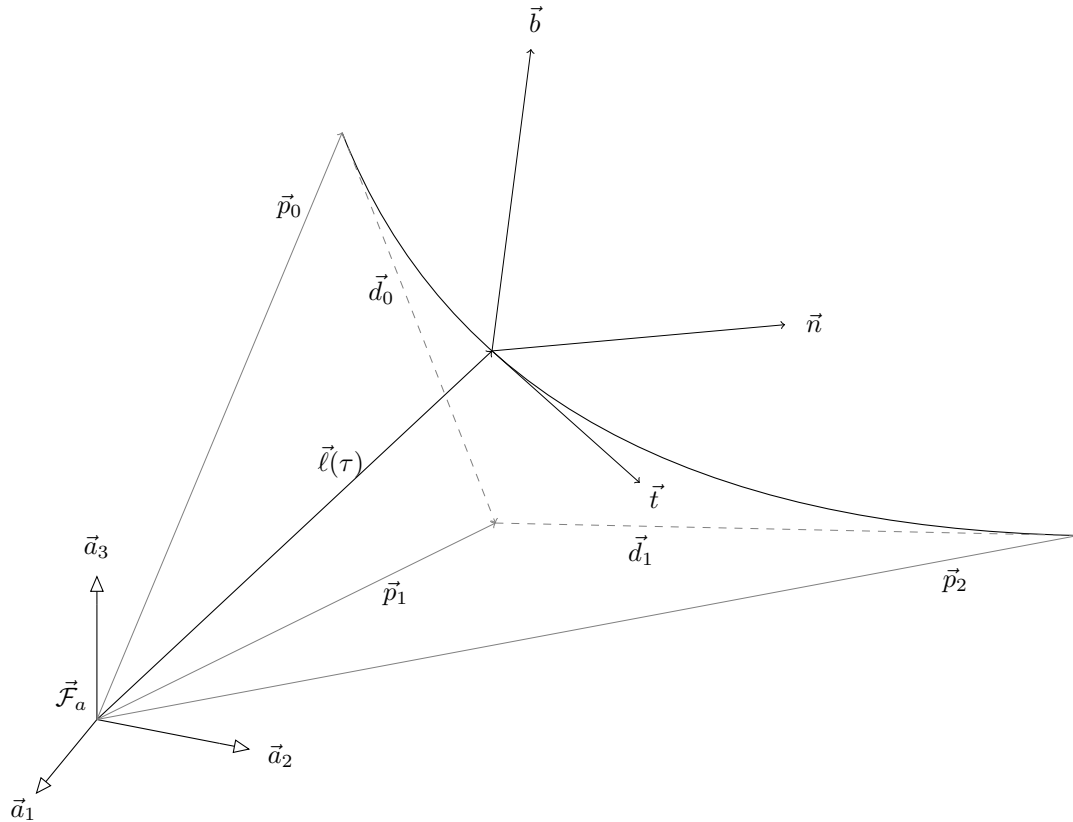
Figure 5.3: Quadratic spline

and both tangent vectors all lie in the same plane.

While constructing a single planar curve between two cross-sections is not generally possible, it *is* possible to construct a piecewise, C^1 curve composed of two sections, each of which are planar (but in different planes); this will be shown by construction in section 5.1.2.

A convenient choice for the two curves are quadratic splines [16] (which are always planar) since their representation by polynomials allows efficient evaluation and differentiation.

46

5.1.1 Quadratic splines

A quadratic spline is formed from three control points, as shown in Figure 5.3. Points on a quadratic spline are given by [16]

$$\vec{\ell}(\tau) = (1-\tau)^2\vec{p}_0 + 2\tau(1-\tau)\vec{p}_1 + (1-\tau)^2\vec{p}_2 \tag{5.1}$$

$\vec{p}_0, \vec{p}_1, \vec{p}_2$ Quadratic spline control points

and its first derivative (with respect to τ) is

$$
\begin{aligned}
\frac{\mathrm{d}\vec{\ell}}{\mathrm{d}\tau} &= 2\big((1-\tau)(\vec{p}_1 - \vec{p}_0) + \tau(\vec{p}_2 - \vec{p}_1)\big) \\
&= 2\big((1-\tau)\vec{d}_0 + \tau\vec{d}_1\big)
\end{aligned}
\tag{5.2}
$$

where

$$\vec{d}_0 = \vec{p}_1 - \vec{p}_0 \tag{5.3}$$

$$\vec{d}_1 = \vec{p}_2 - \vec{p}_1 \tag{5.4}$$

$\vec{d}_0, \vec{d}_1$ Quadratic spline control legs

The magnitude of the first derivative is the rate of extension ξ, and is equal to the rate of change of arc length s with respect to the parameter τ:

$$
\begin{aligned}
\xi = \frac{\mathrm{d}s}{\mathrm{d}\tau} &= \left|\frac{\mathrm{d}\vec{\ell}}{\mathrm{d}\tau}\right| \\
&= \sqrt{\frac{\mathrm{d}\vec{\ell}}{\mathrm{d}\tau} \cdot \frac{\mathrm{d}\vec{\ell}}{\mathrm{d}\tau}} \\
&= 2\sqrt{\big((1-\tau)\vec{d}_0 + \tau\vec{d}_1\big) \cdot \big((1-\tau)\vec{d}_0 + \tau\vec{d}_1\big)} \\
&= 2\sqrt{(1-\tau)^2 d_{00} + 2\tau(1-\tau)d_{01} + \tau^2 d_{11}}
\end{aligned}
\tag{5.5}
$$

where

$$d_{00} = \vec{d}_0 \cdot \vec{d}_0 \tag{5.6}$$

$$d_{01} = \vec{d}_0 \cdot \vec{d}_1 \tag{5.7}$$

$$d_{11} = \vec{d}_1 \cdot \vec{d}_1 \tag{5.8}$$

---
d_{00}, d_{01}, d_{11} Dot products of spline control legs

The first derivative of $\vec{\ell}$ with respect to s, *i.e.*, the unit tangent vector $\vec{t}$, is then

$$
\begin{aligned}
\vec{t} &= \frac{\mathrm{d}\vec{\ell}}{\mathrm{d}s} \\
&= \frac{\mathrm{d}\vec{\ell}}{\mathrm{d}\tau}\frac{\mathrm{d}\tau}{\mathrm{d}s} \\
&= \frac{1}{\xi}\frac{\mathrm{d}\vec{\ell}}{\mathrm{d}\tau}
\end{aligned}
\tag{5.9}
$$

the unit binormal to the spline is

$$
\vec{b} = \frac{\vec{d_0} \times \vec{d_1}}{\left|\vec{d_0} \times \vec{d_1}\right|}
\tag{5.10}
$$

(since $\vec{d_0}$ and $\vec{d_1}$ define the plane of the spline) and the unit normal vector can be constructed from $\vec{t}$ and $\vec{b}$ [16]:

$$
\vec{n} = \vec{b} \times \vec{t}
\tag{5.11}
$$

$\vec{n}$ Unit principal normal vector to the locus of centroids
---

From Appendix B, the curvature of the spline is

$$
\kappa = \frac{4\sqrt{d_{00}d_{11} - d_{01}^2}}{\xi^3}
$$

5.1.2   Locus construction

To construct a locus of centroids consisting of two planar quadratic splines, three control points must be defined for each spline. The resulting piecewise curve must satisfy the requirements of section 5.1, and must be C^1 where the two halves meet. The two halves will be referred to as $\vec{\ell}_A(\tau_A)$ and $\vec{\ell}_B(\tau_B)$ respectively:

τ_A, τ_B Parameters in the range $[0, 1]$ describing the two splines making up the locus of centroids between cross-sections A and B

$\vec{\ell}_A(\tau_A), \vec{\ell}_B(\tau_B)$ Position vectors of points on the two quadratic splines making up the locus of centroids between cross-sections A and B

Note that $\tau_A = 0$ at the cross-section A and $\tau_B = 1$ at the cross-section B.

In order to start and end at the two cross-section centroids, the first control point of the first spline $\vec{\ell}_A(\tau_A)$ must be $\vec{\rho}_A$ and the last control point of the second spline $\vec{\ell}_B(\tau_B)$ must be $\vec{\rho}_B$.

In order for $\vec{\ell}_A(\tau_A)$ to have the required first derivative $\xi_A \vec{t}_A$ at the cross-section A, note that from equation (5.2),

$$\left. \frac{d\vec{\ell}_A}{d\tau_A} \right|_{\tau_A = 0} = 2(\vec{c}_A - \vec{\rho}_A) = \xi_A \vec{t}_A \tag{5.12}$$

$$\begin{array}{c|c} \vec{c}_A & \text{Second control point of } \vec{\ell}_A(\tau_A) \end{array}$$

Therefore,

$$\vec{c}_A = \vec{\rho}_A + \frac{1}{2}\xi_A \vec{t}_A \tag{5.13}$$

Similarly,

$$\left. \frac{d\vec{\ell}_B}{d\tau_B} \right|_{\tau_B = 1} = 2(\vec{\rho}_B - \vec{c}_B) = \xi_B \vec{t}_B \tag{5.14}$$

$$\begin{array}{c|c} \vec{c}_B & \text{Second control point of } \vec{\ell}_B(\tau_B) \end{array}$$

and so

$$\vec{c}_B = \vec{\rho}_B - \frac{1}{2}\xi_B \vec{t}_B \tag{5.15}$$

In order for the two splines $\vec{\ell}_A(\tau_A)$ and $\vec{\ell}_B(\tau_B)$ to meet, the third control point of $\vec{\ell}_A$ must be equal to the first control point of $\vec{\ell}_B$:

$$\begin{array}{c|c} \vec{\rho}_m & \text{Mid control point, equal to the third control point of } \vec{\ell}_A \\ & \text{and the first control point of } \vec{\ell}_B \end{array}$$

To have C^1 continuity between the two splines, the derivatives of each must be equal where they meet:

$$\left. \frac{d\vec{\ell}_A}{d\tau_A} \right|_{\tau_A = 1} = \left. \frac{d\vec{\ell}_B}{d\tau_B} \right|_{\tau_B = 0}$$

$$2(\vec{\rho}_m - \vec{c}_A) = 2(\vec{c}_B - \vec{\rho}_m)$$

$$2\vec{\rho}_m = \vec{c}_A + \vec{c}_B$$

$$\vec{\rho}_m = \frac{\vec{c}_A + \vec{c}_B}{2} \tag{5.16}$$

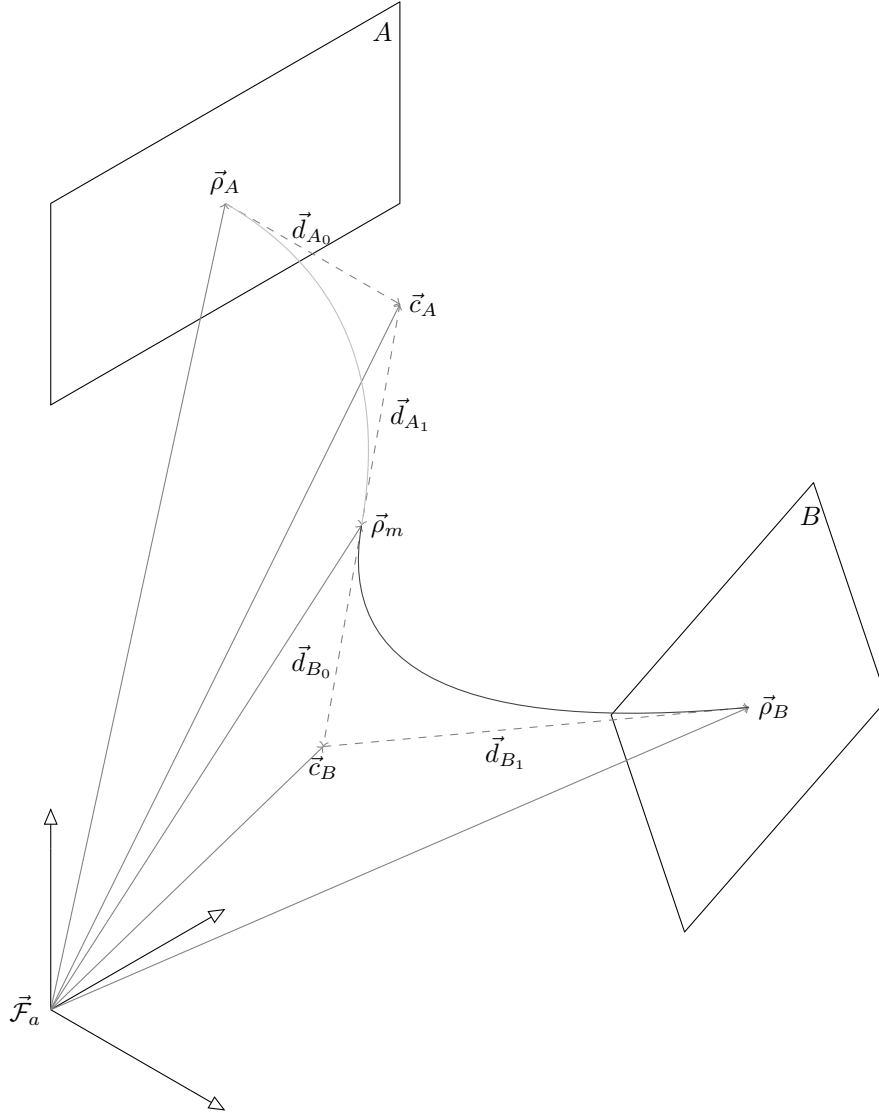Figure 5.4: Quadratic spline construction.

The spline $\vec{\ell}_A(\tau_A)$ can then be constructed from the control points $\vec{\rho}_A$, $\vec{c}_A$, and $\vec{\rho}_m$, and the spline $\vec{\ell}_B(\tau_B)$ can then be constructed from the control points $\vec{\rho}_m$, $\vec{c}_B$, and $\vec{\rho}_B$, as shown in Figure 5.4.
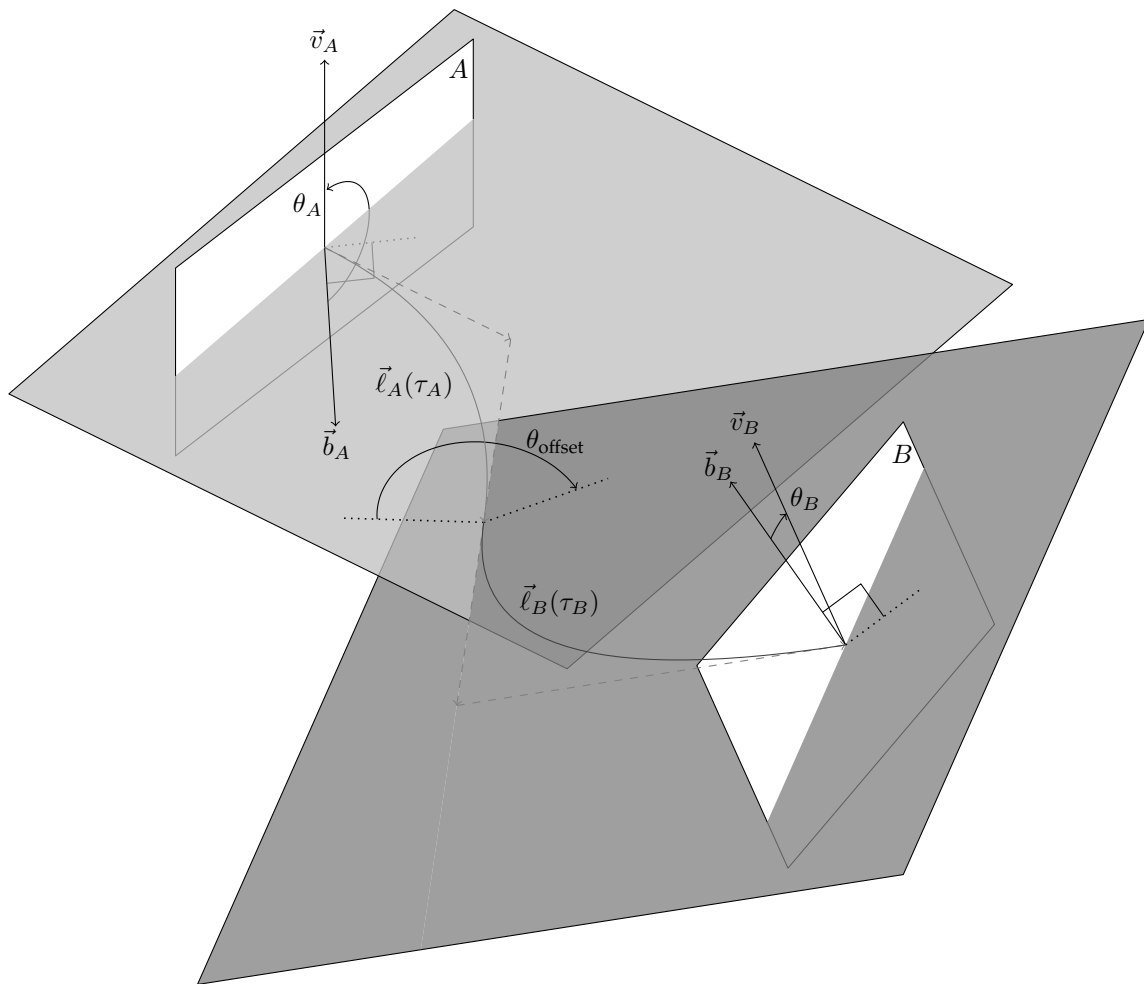
Figure 5.5: Cross-section orientation measured from spline planes.

5.2 Cross-section orientation

Having defined two quadratic splines $\vec{\ell}_A$ and $\vec{\ell}_B$, each defines a plane and a set of Frenet frames $\vec{\mathcal{F}}_\alpha$ and $\vec{\mathcal{F}}_\beta$ from which to define the orientations of individual cross-sections. The orientation can then be defined by measuring the angle of the cross-sectional vector $\vec{v}$ from binormal $\vec{b}$ of the appropriate Frenet frame, as shown in Figure 5.5. Note that if the two planes were the same, then interpolating cross-section orientation between the cross-sections A and B would be a straightforward matter of interpolating between θ_A and θ_B with (for example) a scalar spline. However, since the two planes may have a (potentially large) offset angle θ_{offset} between them, a more sophisticated approach is needed.

$\vec{\mathcal{F}}_\alpha$	Frenet frame of $\vec{\ell}_A$
$\vec{\mathcal{F}}_\beta$	Frenet frame of $\vec{\ell}_B$
$\vec{b}_A$	Normal vector to the plane in which $\vec{\ell}_A$ lies, or equivalently the binormal vector of the Frenet frame $\vec{\mathcal{F}}_\alpha$
$\vec{b}_B$	Normal vector to the plane in which $\vec{\ell}_B$ lies, or equivalently the binormal vector of the Frenet frame $\vec{\mathcal{F}}_\beta$
θ_A	Angle between $\vec{v}_A$ and $\vec{b}_A$
θ_B	Angle between $\vec{v}_B$ and $\vec{b}_B$

Figure 5.6 shows the Frenet frames $\vec{\mathcal{F}}_\alpha$ and $\vec{\mathcal{F}}_\beta$ (omitting the tangent vector $\vec{t}$) at several points along both quadratic splines which make up the locus of centroids for one element, as well as the cross-sectional frames $\vec{\mathcal{F}}_{A_0}$ and $\vec{\mathcal{F}}_{B_0}$ at each end. Note that the curve binormal $\vec{b}$ to each spline remains constant, while the principal curve normal $\vec{n}$ varies but remains in the same plane.

$\vec{n}_{A_0}$	Principal normal vector at the start of $\vec{\ell}_A$ (at the cross-section A)
$\vec{n}_{A_1}$	Principal normal vector at the end of $\vec{\ell}_A$ (where it meets $\vec{\ell}_B$)
$\vec{n}_{B_0}$	Principal normal vector at the start of $\vec{\ell}_B$ (where it meets $\vec{\ell}_A$)
$\vec{n}_{B_1}$	Principal normal vector at the end of $\vec{\ell}_B$ (at the cross-section B)
$\vec{t}_m$	Common tangent vector to both splines where they meet in the middle of the element
$\vec{\mathcal{F}}_{\alpha_0}$	Frenet frame at the start of $\vec{\ell}_A$, made up of $\vec{t}_A$, $\vec{n}_{A_0}$, and $\vec{b}_A$
$\vec{\mathcal{F}}_{\alpha_1}$	Frenet frame at the end of $\vec{\ell}_A$, made up of $\vec{t}_m$, $\vec{n}_{A_1}$, and $\vec{b}_A$
$\vec{\mathcal{F}}_{\beta_0}$	Frenet frame at the start of $\vec{\ell}_B$, made up of $\vec{t}_m$, $\vec{n}_{B_0}$, and $\vec{b}_B$
$\vec{\mathcal{F}}_{\beta_0}$	Frenet frame at the end of $\vec{\ell}_B$, made up of $\vec{t}_B$, $\vec{n}_{B_1}$, and $\vec{b}_B$
$\vec{\mathcal{F}}_{A_0}$	Frame of cross-section A, made up of $\vec{t}_A$, $\vec{n}_{A_0}$ and $\vec{b}_A$
$\vec{\mathcal{F}}_{B_1}$	Frame of cross-section B, made up of $\vec{t}_B$, $\vec{n}_{B_1}$ and $\vec{b}_B$

Note that at any point, the orientation of the cross-sectional frame $\vec{\mathcal{F}}_c$ can be defined by a single rotation matrix about the local 1-axis (corresponding to $\vec{t}$) of $\vec{\mathcal{F}}_{F_A}$ or $\vec{\mathcal{F}}_{F_B}$. Also note that where the two splines meet, $\vec{\mathcal{F}}_\beta$ can also be expressed as a single rotation about the 1-axis of $\vec{\mathcal{F}}_\alpha$ (or vice versa) since at that point the tangents of both splines are equal to $\vec{t}_m$.

The rotation matrix giving the orientation of the cross-sectional frame $\vec{\mathcal{F}}_{A_0}$ with respect to the Frenet frame $\vec{\mathcal{F}}_{\alpha_0}$ is (as discussed in Appendix A)

$$\mathbf{R}_{A_0} = \vec{\mathcal{F}}_{A_0} \cdot \vec{\mathcal{F}}_{\alpha_0}^T = \begin{bmatrix} \vec{t}_{A_0} \\ \vec{u}_{A_0} \\ \vec{v}_{A_0} \end{bmatrix} \cdot [\vec{t}_{A_0} \ \vec{n}_{A_0} \ \vec{b}_A] = \begin{bmatrix} 1 & 0 & 0 \\ 0 & \cos(\theta_A) & \sin(\theta_A) \\ 0 & -\sin(\theta_A) & \cos(\theta_A) \end{bmatrix} \qquad (5.17)$$

$\mathbf{R}_{A_0}$	Rotation matrix giving the orientation of $\vec{\mathcal{F}}_{A_0}$ from the Frenet frame $\vec{\mathcal{F}}_{\alpha_0}$

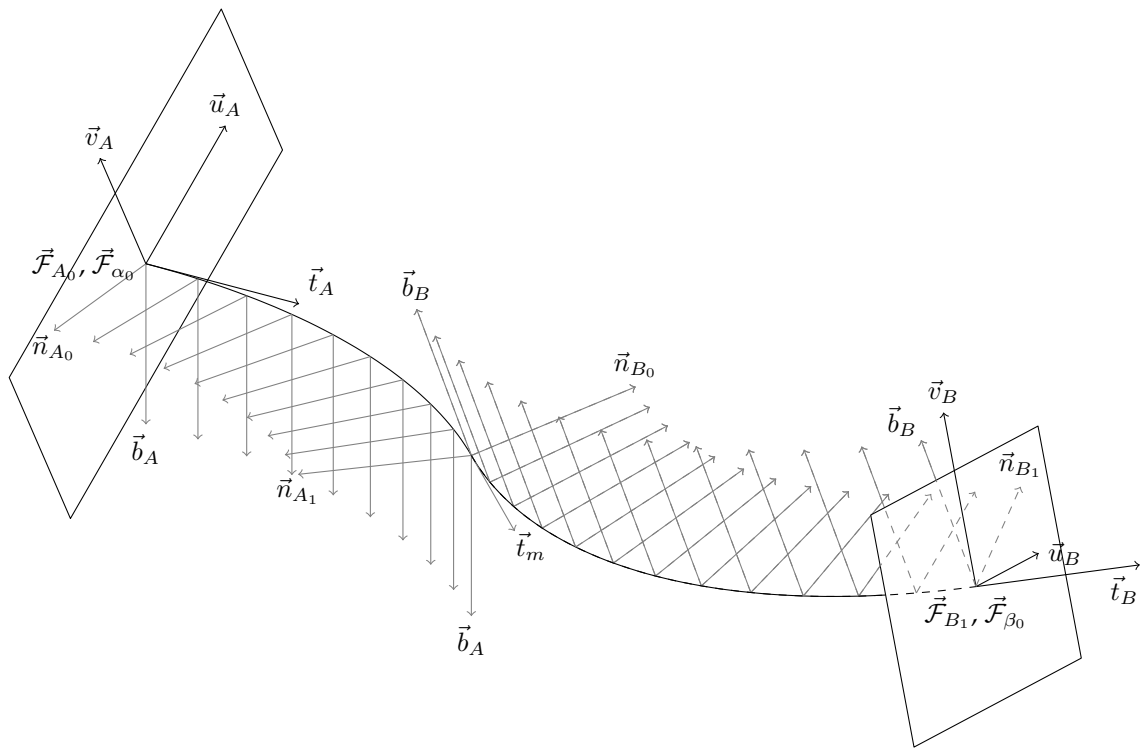Figure 5.6: Frenet (gray) and cross-sectional frames on an element.

Note that while $\mathbf{R}_{A_0}$ is uniquely defined, the angle θ_A is not. However, given a rotation matrix $\mathbf{R}$ (assumed to be about the 1-axis, *i.e.* having the same form as $\mathbf{R}_{A_0}$), a solution for the corresponding angle θ can be found. Noting that $R_{23} = \sin(\theta)$ and $R_{32} = -\sin(\theta)$, one solution for θ is

$$\theta = \sin^{-1}\left(\frac{R_{23} - R_{32}}{2}\right) \tag{5.18}$$

where the resulting value for θ will lie in the range $-\frac{\pi}{2} \le \theta \le \frac{\pi}{2}$.

A similar expression could be formed using an inverse cosine on the R_{22} and R_{33} elements, resulting in a value for θ in the range $0 \le \theta \le \pi$; however, using an inverse sine is the better choice because it distinguishes between small positive and small negative angles (later on, this method will be used to calculate angles which are likely to be small, but may be positive or negative). Also note that equation (5.18) could have been written to use either only R_{32} *or* only R_{23}; however, averaging both values will tend to minimize numerical noise.

Similarly to $\mathbf{R}_{A_0}$, the rotation matrix $\mathbf{R}_{B_1}$ can also be calculated:

$$\mathbf{R}_{B_1} = \vec{\mathcal{F}}_{B_1} \cdot \vec{\mathcal{F}}_{\beta_1}^T = \begin{bmatrix} \vec{t}_{B_1} \\ \vec{u}_{B_1} \\ \vec{v}_{B_1} \end{bmatrix} \cdot [\vec{t}_{B_1} \ \vec{n}_{B_1} \ \vec{b}_B] = \begin{bmatrix} 1 & 0 & 0 \\ 0 & \cos(\theta_B) & \sin(\theta_B) \\ 0 & -\sin(\theta_B) & \cos(\theta_B) \end{bmatrix} \tag{5.19}$$

$\mathbf{R}_{B_1}$ Rotation matrix giving the orientation of $\vec{\mathcal{F}}_{B_1}$ from the Frenet frame $\vec{\mathcal{F}}_{\beta_1}$

Finally, it is possible to find a rotation matrix giving the orientation of $\vec{\mathcal{F}}_{\beta_0}$ with respect to $\vec{\mathcal{F}}_{\alpha_1}$:

$$\mathbf{R}_m = \vec{\mathcal{F}}_{\beta_0} \cdot \vec{\mathcal{F}}_{\alpha_1}^T = \begin{bmatrix} \vec{t}_m \\ \vec{n}_{B_0} \\ \vec{b}_B \end{bmatrix} \cdot [\vec{t}_m \ \vec{n}_{A_1} \ \vec{b}_A] = \begin{bmatrix} 1 & 0 & 0 \\ 0 & \cos(\theta_m) & \sin(\theta_m) \\ 0 & -\sin(\theta_m) & \cos(\theta_m) \end{bmatrix} \tag{5.20}$$

$\mathbf{R}_m$ Rotation matrix giving the orientation of $\vec{\mathcal{F}}_{\beta_0}$ with respect to $\vec{\mathcal{F}}_{\alpha_1}$

θ_m Angle between $\vec{\mathcal{F}}_{\beta_0}$ and $\vec{\mathcal{F}}_{\alpha_1}$
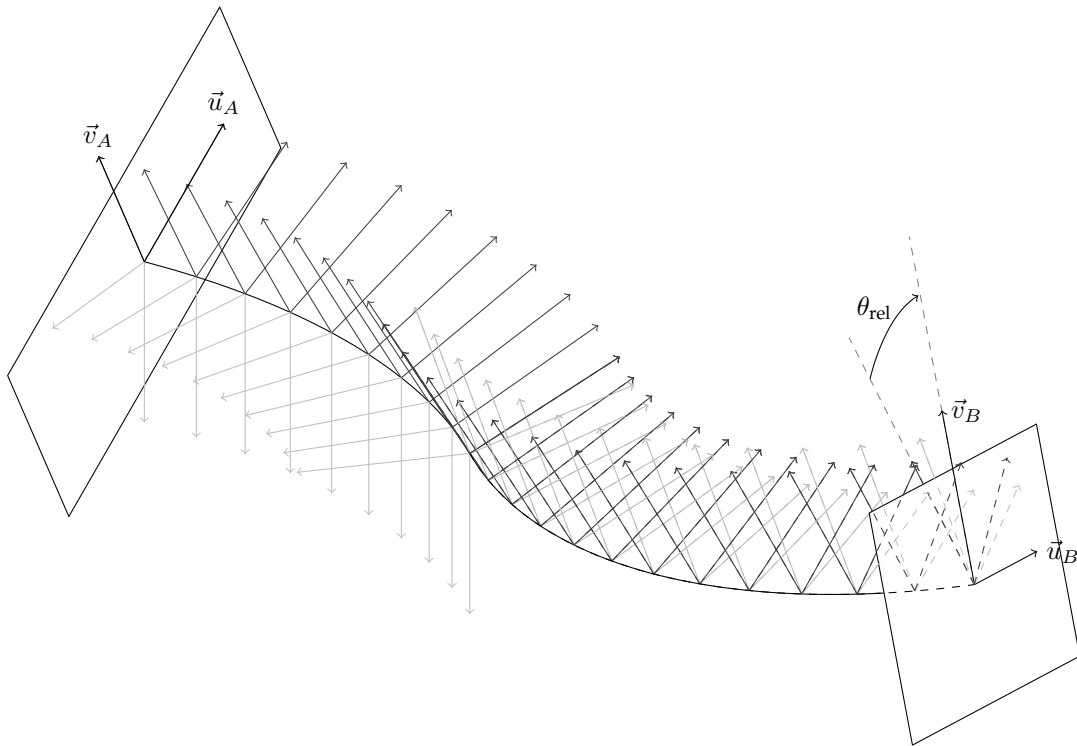

Figure 5.7: Relative angle measured with respect to progressive frame $\vec{\mathcal{F}}_p$.

Now, consider an imaginary 'progressive' frame $\vec{\mathcal{F}}_p$ that starts aligned with the frame of section A and progresses along the first spline $\vec{\ell}_A$ maintaining a constant angle from $\vec{\mathcal{F}}_\alpha$, then progresses along the second spline $\vec{\ell}_B$ maintaining a constant angle from $\vec{\mathcal{F}}_\beta$, as illustrated in Figure 5.7. That is, at any point along $\vec{\ell}_A$ the frame $\vec{\mathcal{F}}_p$ is related to the Frenet frame $\vec{\mathcal{F}}_\alpha$ by a constant rotation matrix $\mathbf{R}_{p_A}$, and similarly for $\vec{\ell}_B$:

$$\vec{\mathcal{F}}_p = \begin{cases} \mathbf{R}_{p_A}\vec{\mathcal{F}}_\alpha & \text{along } \vec{\ell}_A \\ \mathbf{R}_{p_B}\vec{\mathcal{F}}_\beta & \text{along } \vec{\ell}_B \end{cases} \tag{5.21}$$

$\vec{\mathcal{F}}_p$	Progressive frame defined along both splines making up the locus of centroids
$\mathbf{R}_{p_A}$	Rotation matrix defining the orientation of $\vec{\mathcal{F}}_p$ relative to $\vec{\mathcal{F}}_\alpha$
$\mathbf{R}_{p_B}$	Rotation matrix defining the orientation of $\vec{\mathcal{F}}_p$ relative to $\vec{\mathcal{F}}_\beta$

If all cross-section orienation angles were measured with respect to $\vec{\mathcal{F}}_p$, interpolation would be a relatively straightforward matter of interpolating an angle from zero (since $\vec{\mathcal{F}}_p$ was defined to start oriented with the cross-section A), ending at the relative angle θ_{rel} between $\vec{\mathcal{F}}_p$ and $\vec{\mathcal{F}}_{B_1}$, and having specific derivatives at each end (specified by the values of ψ as described at the start of this chapter).

θ_{rel}	Net relative angle between cross-sections over the length of an element, measured with respect to the progressive frame $\vec{\mathcal{F}}_p$.

Even if angles were to be measured from the Frenet frames $\vec{\mathcal{F}}_\alpha$ and $\vec{\mathcal{F}}_\beta$ of each spline, this method can be used; since for both splines, the progressive frame is at a constant angle from the Frenet frame, the cross-section angle can be interpolated with respect to the progressive frame, then split into two separate functions, each shifted up or down by some constant to give the correct angles θ_A and θ_B (measured with respect to the Frenet frame) at the cross-sections A and B.

To find the relative angle θ_{rel}, the relative rotation matrix $\mathbf{R}_{\text{rel}}$ (which describes the orientation of $\vec{\mathcal{F}}_{B_1}$ relative to the progressive frame $\vec{\mathcal{F}}_p$ at the cross-section B) must first be found:

$$\vec{\mathcal{F}}_{B_1} = \mathbf{R}_{\text{rel}}\vec{\mathcal{F}}_p \tag{5.22}$$

First, note that at the cross-section A, the progressive frame $\vec{\mathcal{F}}_p$ is defined to be equal to the cross-sectional frame $\vec{\mathcal{F}}_{A_0}$, so that (using equations (5.17) and (5.21))

$$\vec{\mathcal{F}}_p = \vec{\mathcal{F}}_{A_0}$$
$$\mathbf{R}_{p_A}\vec{\mathcal{F}}_{\alpha_0} = \mathbf{R}_{A_0}\vec{\mathcal{F}}_{\alpha_0}$$
$$\mathbf{R}_{p_A} = \mathbf{R}_{A_0} \tag{5.23}$$

Where the two splines $\vec{\ell}_A$ and $\vec{\ell}_B$ meet,

$$\vec{\mathcal{F}}_p = \mathbf{R}_{p_A}\vec{\mathcal{F}}_{\alpha_1} \tag{5.24}$$

but also

$$\vec{\mathcal{F}}_p = \mathbf{R}_{p_B}\vec{\mathcal{F}}_{\beta_0} \tag{5.25}$$

Therefore,

$$\mathbf{R}_{p_A}\vec{\mathcal{F}}_{\alpha_1} = \mathbf{R}_{p_B}\vec{\mathcal{F}}_{\beta_0}$$
$$\mathbf{R}_{p_B} = \mathbf{R}_{p_A}\vec{\mathcal{F}}_{\alpha_1} \cdot \vec{\mathcal{F}}_{\beta_0}^T$$
$$\mathbf{R}_{p_B} = \mathbf{R}_{p_A}\left(\vec{\mathcal{F}}_{\beta_0} \cdot \vec{\mathcal{F}}_{\alpha_1}^T\right)^T$$

and using equations (5.23) and (5.20),

$$\mathbf{R}_{p_B} = \mathbf{R}_{A_0}\mathbf{R}_m^T \tag{5.26}$$

Finally, at the cross-section B (using equations (5.22) and (5.19)),

$$\vec{\mathcal{F}}_{B_1} = \mathbf{R}_{\text{rel}}\vec{\mathcal{F}}_p$$
$$\mathbf{R}_{B_1}\vec{\mathcal{F}}_{\beta_1} = \mathbf{R}_{\text{rel}}\mathbf{R}_{p_B}\vec{\mathcal{F}}_{\beta_1}$$
$$\mathbf{R}_{B_1} = \mathbf{R}_{\text{rel}}\mathbf{R}_{A_0}\mathbf{R}_m^T$$
$$\mathbf{R}_{\text{rel}} = \mathbf{R}_{B_1}\mathbf{R}_m\mathbf{R}_{A_0}^T \tag{5.27}$$

The relative angle $\theta_{\rm rel}$ can then be extracted from $\mathbf{R}_{\rm rel}$ using equation (5.18). The initial interpolation for θ can then be expressed as a piecewise quadratic spline in the same way as the locus of centroids, by defining two control points based on derivatives at the ends, and a mid control point chosen to ensure C^1 continuity. (A single cubic spline or similar interpolant could also be used, but using two quadratic splines is convenient because they will have to be split up anyways.) To find the control points, note that

$$\left.\frac{\mathrm{d}\theta}{\mathrm{d}\tau_A}\right|_A = \left.\frac{\mathrm{d}\theta}{\mathrm{d}s}\right|_A \left.\frac{\mathrm{d}s}{\mathrm{d}\tau_A}\right|_A = \psi_A\xi_A \tag{5.28}$$

$$\left.\frac{\mathrm{d}\theta}{\mathrm{d}\tau_B}\right|_B = \left.\frac{\mathrm{d}\theta}{\mathrm{d}s}\right|_B \left.\frac{\mathrm{d}s}{\mathrm{d}\tau_B}\right|_B = \psi_B\xi_B \tag{5.29}$$

and therefore, similar to equations (5.13) and (5.15),

$$\theta_{c_A} = \frac{1}{2}\psi_A\xi_A \tag{5.30}$$

$$\theta_{c_B} = \theta_{\rm rel} - \frac{1}{2}\psi_B\xi_B \tag{5.31}$$

noting that the initial control point is zero and the final control point is $\theta_{\rm rel}$. The mid control point is then

$$\theta_m = \frac{\theta_{c_A} + \theta_{c_B}}{2} \tag{5.32}$$

The two quadratic splines just formed are then shifted by θ_A and $\theta_B - \theta_{\rm rel}$ respectively so that the first control point of the first spline is θ_A and the last control point of the second spline is θ_B, as required (so that the angles are now with respect to each spline's Frenet frame instead of the progressive frame). The control points of the first spline are therefore

$$\theta_{A_0} = \theta_A \tag{5.33}$$

$$\theta_{A_m} = \theta_A + \theta_{c_A} \tag{5.34}$$

$$\theta_{A_1} = \theta_A + \theta_m \tag{5.35}$$

$\theta_{A_0}, \theta_{A_m}, \theta_{A_1}$ Control points for the scalar quadratic spline specifying the angle of cross-sections relative to the Frenet frame of first quadratic spline defining the locus of centroids

---

and the control points of the second spline are

$$\theta_{B_0} = \theta_m + (\theta_{\text{rel}} - \theta_B) \tag{5.36}$$

$$\theta_{B_m} = \theta_{c_B} + (\theta_{\text{rel}} - \theta_B) \tag{5.37}$$

$$\theta_{B_1} = \theta_B \tag{5.38}$$

$\theta_{B_0}, \theta_{B_m}, \theta_{B_1}$	Control points for the scalar quadratic spline specifying the angle of cross-sections relative to the Frenet frame of second quadratic spline defining the locus of centroids

as illustrated in Figure 5.8. The angle θ at any point in the element is then given by

$$\theta = \begin{cases} (1 - \tau_A)^2 \theta_{A_0} + 2\tau_A(1 - \tau_A)\theta_{A_m} + \tau^2 \theta_{A_1} & \text{along } \vec{\ell}_A(\tau_A) \\ (1 - \tau_B)^2 \theta_{B_0} + 2\tau_B(1 - \tau_B)\theta_{B_m} + \tau^2 \theta_{B_1} & \text{along } \vec{\ell}_B(\tau_B) \end{cases} \tag{5.39}$$

In this way, the expression for angle θ is discontinuous but the cross-section orientations are geometrically continuous.

5.3 Shape properties

Just as with the orientation angle, any necessary shape parameters (radius, width, height etc.) can be interpolated between cross-sections using pairs of quadratic splines, without the added complexity of having to account for the offset angle described in the previous section.

For instance, given radii r_A and r_B of circular cross-sections A and B, and derivatives with respect to arc length r'_A and r'_B, it is possible to define

$$r_{c_A} = r_A + \frac{1}{2}\xi_A r'_A$$

$$r_{c_B} = r_B - \frac{1}{2}\xi_B r'_B$$

$$r_m = \frac{r_{c_A} + r_{c_B}}{2}$$

leading to an expression for radius over the element

$$r = \begin{cases} (1 - \tau_A)^2 r_A + 2\tau_A(1 - \tau_A)r_{c_A} + \tau^2 r_m & \text{along } \vec{\ell}_A(\tau_A) \\ (1 - \tau_B)^2 r_m + 2\tau_B(1 - \tau_B)r_{c_B} + \tau^2 r_B & \text{along } \vec{\ell}_B(\tau_B) \end{cases} \tag{5.40}$$
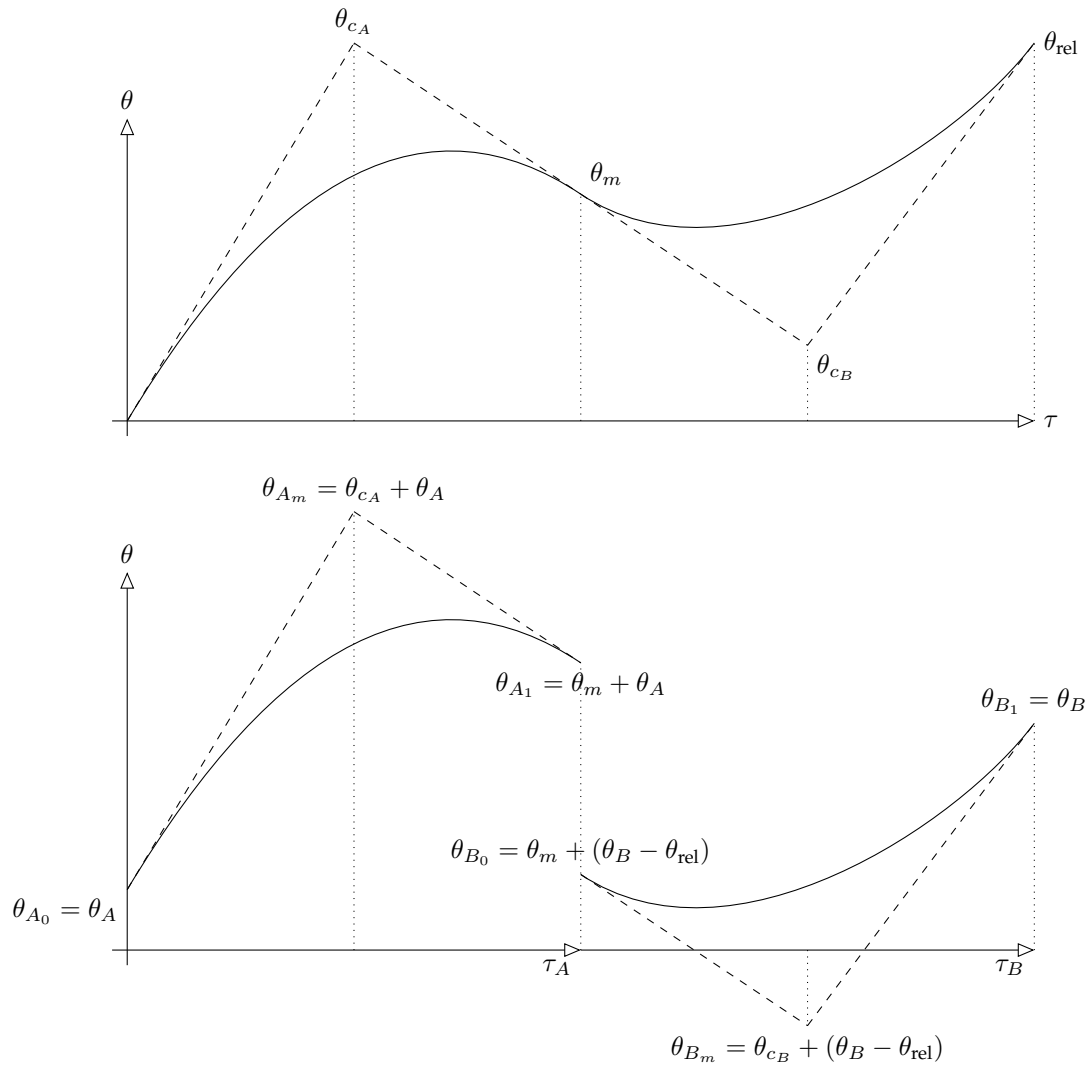
Figure 5.8: Angle interpolant split into two halves.

6

Finite Element Analysis

Chapter 4 introduced expressions for the strain and kinetic energies of an arbitrary curved beam element, and Chapter 5 developed a specific element formed from quadratic splines. By combining the two, the strain and kinetic energies of an element derived in Chapter 4 can be evaluated in terms of the discrete cross-sectional parameters described in Chapter 5.

The general approach to analyzing the beam as a whole is to construct the undeformed beam from cross-sections with the above parameters specified. The beam is then allowed to deform, as shown in Figure 6.1. The strain energy of the deformed beam can be evaluated by computing the differences in ξ, κ_u, κ_v and ψ along the deformed and undeformed beams; the kinetic energy of the beam can be evaluated by computing the velocity $\vec{\nu}$ along the deformed beam.

6.1   Strain energy

To evaluate the strain energy expression in equation (4.60), first note that the various χ_{mn} quantities are functions of the locus of centroids parameter τ, but they do not change when the beam is deformed since they are functions of the area properties and original curvatures only. One very efficient way of evaluating the integral is therefore with weighted Gaussian integration [17], which can be used to
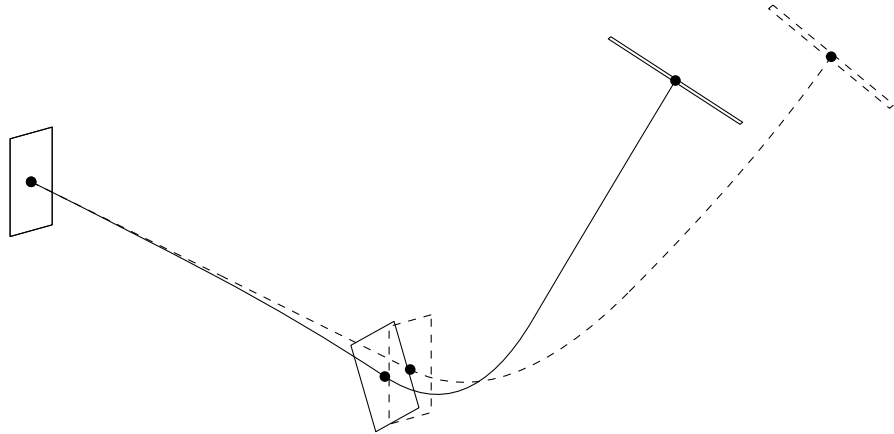
(a) Original (dashed) and deformed (solid) cross-sections.
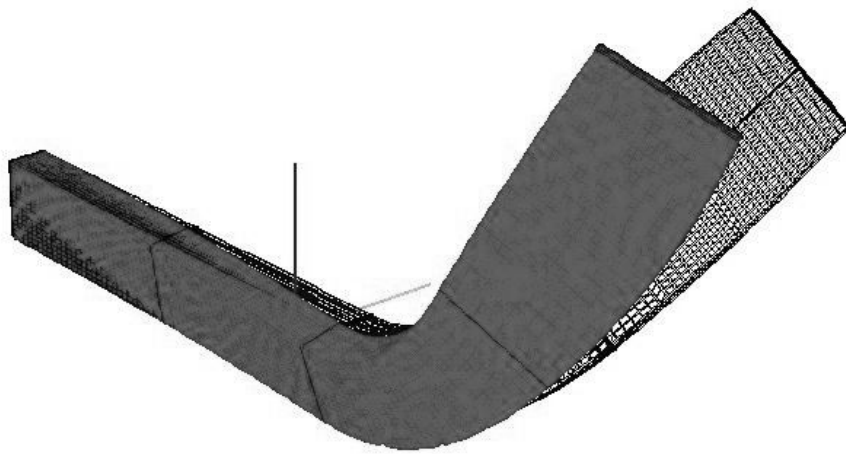
(b) Original (wireframe) and deformed (solid) beams.

Figure 6.1: Sample beam deformation using two elements (with cross-sections shown at the ends and middle of each element).

approximate integrals of the form $\int \chi_{mn}(\tau)f(\tau)\mathrm{d}\tau$ as

$$\int_{\tau=0}^{1} \chi_{mn}(\tau)f(\tau)\mathrm{d}\tau \approx \sum_{i} w_i f(\tau_i) \tag{6.1}$$

In this way, the integral is approximated by a discrete sum of weights w_i multiplied by values of the function $f(\tau)$ evaluated at roots τ_i. For a given function $\chi_{mn}(\tau)$, the roots τ_i and weights w_i must be calculated; a method for doing so is given by Press *et al.* [18]. Although finding the roots and weights is computationally intensive, it only has to be performed once, as a pre-processing step before starting any actual simulation. By splitting the integral in equation (4.60) into separate integrals, each weighted by a different function χ_{mn}, each integral can be approximated as in equation (6.1):

$$
\begin{aligned}
U = \frac{1}{2} \int_{\tau=0}^{1} &\left((\Delta\xi)^2 \left[\frac{E}{\xi^*}\chi_{00} \right] - \Delta\xi\Delta(\xi\kappa_v)\left[\frac{2E}{\xi^*}\chi_{10} \right] + \Delta\xi\Delta(\xi\kappa_u)\left[\frac{2E}{\xi^*}\chi_{01} \right] \right. \\
&+ (\Delta(\xi\kappa_v))^2\left[\frac{E}{\xi^*}\chi_{20} \right] - \Delta(\xi\kappa_v)\Delta(\xi\kappa_u)\left[\frac{2E}{\xi^*}\chi_{11} \right] + (\Delta(\xi\kappa_u))^2\left[\frac{E}{\xi^*}\chi_{02} \right] \\
&\left. + (\Delta(\xi\psi))^2\left[\frac{G}{\xi^*}(\chi_{20}+\chi_{02}) \right] \right) \mathrm{d}\tau \\
= &\int_{\tau=0}^{1} \frac{E\chi_{00}}{2\xi^*}(\Delta\xi)^2\mathrm{d}\tau - \int_{\tau=0}^{1} \frac{E\chi_{10}}{\xi^*}\Delta\xi\Delta(\xi\kappa_v)\mathrm{d}\tau + \int_{\tau=0}^{1} \frac{E\chi_{01}}{\xi^*}\Delta\xi\Delta(\xi\kappa_u)\mathrm{d}\tau \\
&+ \int_{\tau=0}^{1} \frac{E\chi_{20}}{2\xi^*}(\Delta(\xi\kappa_v))^2\mathrm{d}\tau - \int_{\tau=0}^{1} \frac{E\chi_{11}}{\xi^*}\Delta(\xi\kappa_v)\Delta(\xi\kappa_u)\mathrm{d}\tau \\
&+ \int_{\tau=0}^{1} \frac{E\chi_{02}}{2\xi^*}(\Delta(\xi\kappa_u))^2\mathrm{d}\tau + \int_{\tau=0}^{1} \frac{G(\chi_{20}+\chi_{02})}{2\xi^*}(\Delta(\xi\psi))^2\mathrm{d}\tau \\
\approx &\sum_{i} w_{1_i}(\Delta\xi|_{\tau_{1_i}})^2 - \sum_{i} w_{2_i} \Delta\xi|_{\tau_{2_i}} \Delta(\xi\kappa_v)|_{\tau_{2_i}} + \sum_{i} w_{3_i} \Delta\xi|_{\tau_{3_i}} \Delta(\xi\kappa_u)|_{\tau_{3_i}} \\
&+ \sum_{i} w_{4_i}(\Delta(\xi\kappa_v)|_{\tau_{4_i}})^2 - \sum_{i} w_{5_i} \Delta(\xi\kappa_v)|_{\tau_{5_i}} \Delta(\xi\kappa_u)|_{\tau_{5_i}} \\
&+ \sum_{i} w_{6_i}(\Delta(\xi\kappa_u)|_{\tau_{6_i}})^2 + \sum_{i} w_{7_i}(\Delta(\xi\psi)|_{\tau_{7_i}})^2
\end{aligned}
\tag{6.2}
$$

Note that in general, the roots τ_i and weights w_i are different for each summation since the weighting functions are different.

6.2   Kinetic energy

As with strain energy, the integral for kinetic energy in equation (4.72) can be approximated using weighted Gaussian integration:

$$
\begin{aligned}
W &= \frac{1}{2} \int_{\tau=0}^{1} \varrho A (\vec{\nu} \cdot \vec{\nu}) \xi^* \mathrm{d}\tau \\
&= \int_{\tau=0}^{1} \frac{\varrho A \xi^*}{2} (\vec{\nu} \cdot \vec{\nu}) \mathrm{d}\tau \\
&\approx \sum_i w_{8_i} \left. (\vec{\nu} \cdot \vec{\nu}) \right|_{\tau_{8_i}}
\end{aligned}
\tag{6.3}
$$

6.3   Simulation

To simulate the dynamic behaviour of a beam element using a variational finite element approach, it must be possible to find expressions for the derivatives of strain and kinetic energies U and W with respect to independent scalar 'generalized coordinates' q_i [13] and their derivatives (with respect to time) $\dot{q}_i$,

---

q_i Generalized coordinates describing one beam element

$\dot{(\cdot)}$ Derivative of a quantity $(\cdot)$ with respect to time

---

and then solve the Lagrange equations of motion [12, 13]

$$
\frac{\mathrm{d}}{\mathrm{d}t} \left(\frac{\partial L}{\partial \dot{q}_i} \right) - \frac{\partial L}{\partial q_i} = Q_i
\tag{6.4}
$$

where

$$
L = T - U
\tag{6.5}
$$

$$
Q_i = \frac{\partial W}{\partial q_i}
\tag{6.6}
$$

L Lagrangian of one element

W Work done on the element by applied forces and moments

Q_i Generalized force corresponding to coordinate q_i, *i.e.* the partial derivative of work W with respect to that coordinate
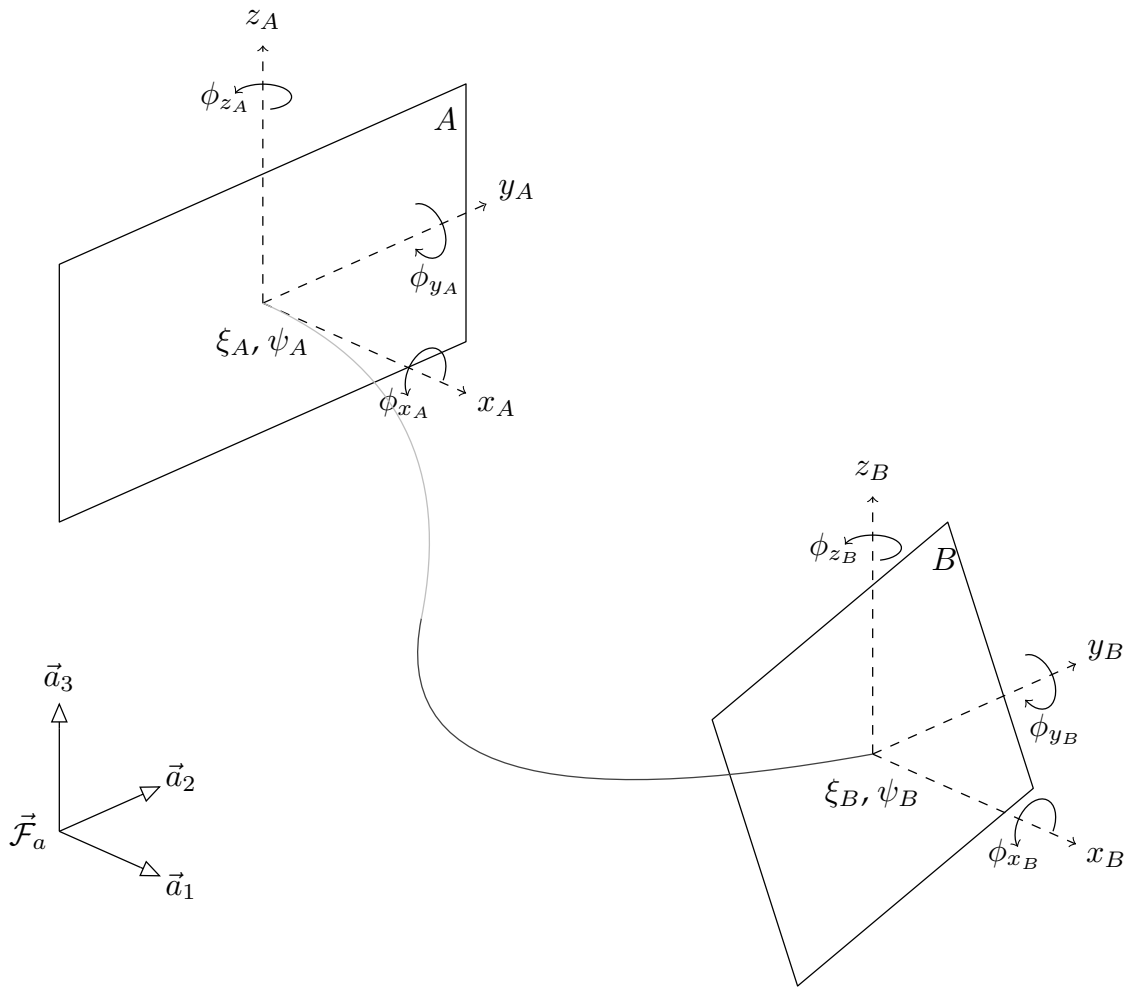

Figure 6.2: Element generalized coordinates.

The motion of each element between cross-sections A and B is defined by the following generalized coordinates, as illustrated in Figure 6.2:

x_A, y_A, z_A	Coordinates of the centroid of cross-section A with respect to the global fixed Cartesian frame $\vec{\mathcal{F}}_a$
$\phi_{x_A}, \phi_{y_A}, \phi_{z_A}$	Rotation angles of cross-section A about the axes of $\vec{\mathcal{F}}_a$
ξ_A, ψ_A	discussed in Chapter 5
x_B, y_B, z_B	Coordinates of the centroid of cross-section B with respect to the global fixed Cartesian frame $\vec{\mathcal{F}}_a$
$\phi_{x_B}, \phi_{y_B}, \phi_{z_B}$	Rotation angles of cross-section B about the axes of $\vec{\mathcal{F}}_a$
ξ_B, ψ_B	discussed in Chapter 5

These sixteen parameters and their derivatives with respect to time collectively make up the q_i and $\dot{q}_i$ for the element.

Note that differential changes $\mathrm{d}x_A$, $\mathrm{d}y_A$, and $\mathrm{d}z_A$ can be interpreted as a differential vector displacement $\mathrm{d}\vec{\rho}_A$:

$$\mathrm{d}\vec{\rho}_A = \mathrm{d}x_A \vec{a}_1 + \mathrm{d}y_A \vec{a}_2 + \mathrm{d}z_A \vec{a}_3 \tag{6.7}$$

$$\frac{\mathrm{d}\vec{\rho}_A}{\mathrm{d}x_A} = \vec{a}_1 \tag{6.8}$$

$$\frac{\mathrm{d}\vec{\rho}_A}{\mathrm{d}y_A} = \vec{a}_2 \tag{6.9}$$

$$\frac{\mathrm{d}\vec{\rho}_A}{\mathrm{d}z_A} = \vec{a}_3 \tag{6.10}$$

Also, the differential changes $\mathrm{d}\phi_{x_A}$, $\mathrm{d}\phi_{y_A}$, and $\mathrm{d}\phi_{z_A}$ can be interpreted as a differential rotation vector $\mathrm{d}\vec{\phi}_A$:

$$\mathrm{d}\vec{\phi}_A = \mathrm{d}\phi_{x_A} \vec{a}_1 + \mathrm{d}\phi_{y_A} \vec{a}_2 + \mathrm{d}\phi_{z_A} \vec{a}_3 \tag{6.11}$$

$$\frac{\mathrm{d}\vec{\phi}_A}{\mathrm{d}\phi_{x_A}} = \vec{a}_1 \tag{6.12}$$

$$\frac{\mathrm{d}\vec{\phi}_A}{\mathrm{d}\phi_{y_A}} = \vec{a}_2 \tag{6.13}$$

$$\frac{\mathrm{d}\vec{\phi}_A}{\mathrm{d}\phi_{z_A}} = \vec{a}_3 \tag{6.14}$$

$\mathrm{d}\vec{\phi}_A$ then acts like an angular velocity vector in determining the change in orientation of vectors attached to cross-section B, *i.e.*

$$\mathrm{d}\vec{t}_A = \mathrm{d}\vec{\phi}_A \times \vec{t}_A \tag{6.15}$$

$$\mathrm{d}\vec{u}_A = \mathrm{d}\vec{\phi}_A \times \vec{u}_A \tag{6.16}$$

$$\mathrm{d}\vec{v}_A = \mathrm{d}\vec{\phi}_A \times \vec{v}_A \tag{6.17}$$

It is convenient to consider each beam element as being composed of two half-elements, each corresponding to one of the two cross-sections defining the element. Each half-element is then defined by a single quadratic spline locus of centroids (plus quadratic splines for angle and shape parameters) instead of a piecewise pair of splines, and is described by its own set of generalized coordinates q_{A_k} and their derivatives $\dot{q}_{A_k}$:

q_{A_k}	Parameters describing the beam half element associated with cross-section A

In this case, the element kinetic energy is $T = T_A + T_B$ and the element strain energy is $U = U_A + U_B$:

T_A	Kinetic energy of the half-element corresponding to cross-section A
T_B	Kinetic energy of the half-element corresponding to cross-section B
U_A	Strain energy of the half-element corresponding to cross-section A
U_B	Strain energy of the half-element corresponding to cross-section B

Each half-element is defined by the following twelve parameters which, along with their derivatives with respect to time, collectively make up the q_{A_k} and $\dot{a}_{A_k}$ for the half-element:

$x_{A_0}, y_{A_0}, z_{A_0}$	Coordinates of the first spline control point with respect to the global fixed Cartesian frame $\vec{\mathcal{F}}_a$
$x_{A_m}, y_{A_m}, z_{A_m}$	Coordinates of the middle spline control point with respect to $\vec{\mathcal{F}}_a$
$x_{A_1}, y_{A_1}, z_{A_1}$	Coordinates of the last spline control point with respect to $\vec{\mathcal{F}}_a$
$\theta_{A_0}, \theta_{A_m}, \theta_{A_1}$	Cross-section angles with respect to spline Frenet frame

The Lagrange equations (6.4) then become (using the convention of summing over repeated indices [14])

$$\frac{\mathrm{d}}{\mathrm{d}t}\left(\frac{\partial L}{\partial \dot{q}_i}\right) - \frac{\partial L}{\partial q_i} = Q_i$$

$$\frac{\mathrm{d}}{\mathrm{d}t}\left(\frac{\partial L_A}{\partial \dot{q}_i} + \frac{\partial L_B}{\partial \dot{q}_i}\right) - \left(\frac{\partial L_A}{\partial q_i} + \frac{\partial L_B}{\partial q_i}\right) = Q_i$$

$$\left[\frac{\mathrm{d}}{\mathrm{d}t}\left(\frac{\partial L_A}{\partial \dot{q}_i}\right) - \frac{\partial L_A}{\partial q_i}\right] + \left[\frac{\mathrm{d}}{\mathrm{d}t}\left(\frac{\partial L_B}{\partial \dot{q}_i}\right) - \frac{\partial L_B}{\partial q_i}\right] = Q_i$$

$$\left[\frac{\mathrm{d}}{\mathrm{d}t}\left(\frac{\partial L_A}{\partial \dot{q}_{A_k}}\frac{\partial \dot{q}_{A_k}}{\partial \dot{q}_i}\right) - \frac{\partial L_A}{\partial q_{A_k}}\frac{\partial q_{A_k}}{\partial q_i}\right] + \left[\frac{\mathrm{d}}{\mathrm{d}t}\left(\frac{\partial L_B}{\partial \dot{q}_{B_k}}\frac{\partial \dot{q}_{B_k}}{\partial \dot{q}_i}\right) - \frac{\partial L_B}{\partial q_{B_k}}\frac{\partial q_{B_k}}{\partial q_i}\right] = Q_i$$

$$\left[\frac{\mathrm{d}}{\mathrm{d}t}\left(\frac{\partial L_A}{\partial \dot{q}_{A_k}}\right)\frac{\partial \dot{q}_{A_k}}{\partial \dot{q}_i} + \frac{\partial L_A}{\partial \dot{q}_{A_k}}\frac{\mathrm{d}}{\mathrm{d}t}\left(\frac{\partial \dot{q}_{A_k}}{\partial \dot{q}_i}\right) - \frac{\partial L_A}{\partial q_{A_k}}\frac{\partial q_{A_k}}{\partial q_i}\right] +$$

$$\left[\frac{\mathrm{d}}{\mathrm{d}t}\left(\frac{\partial L_B}{\partial \dot{q}_{B_k}}\right)\frac{\partial \dot{q}_{B_k}}{\partial \dot{q}_i} + \frac{\partial L_B}{\partial \dot{q}_{B_k}}\frac{\mathrm{d}}{\mathrm{d}t}\left(\frac{\partial \dot{q}_{B_k}}{\partial \dot{q}_i}\right) - \frac{\partial L_B}{\partial q_{B_k}}\frac{\partial q_{B_k}}{\partial q_i}\right] = Q_i \quad (6.18)$$

Therefore, for each half-element, the following quantities must be evaluated:

$\dfrac{\partial L_A}{\partial q_{A_k}}$ Derivatives of strain and kinetic energy of the half-element with respect to the half-element generalized coordinates (*e.g.*, derivative of half-element strain energy with respect to the control point coordinate x_1)

$\dfrac{\partial L_A}{\partial \dot{q}_{A_k}}$ Derivatives of strain and kinetic energy of the half-element with respect to time derivatives of the half-element generalized coordinates (*e.g.*, derivative of half-element kinetic energy with respect to control point velocity component $\dot{x}_1$)

$\dfrac{\partial q_{A_k}}{\partial q_i}$ Derivatives of half-element generalized coordinates with respect to element generalized coordinates (*e.g.*, derivative of control point coordinate x_{A_1} with respect to cross-section centroid coordinate x_A); this can be thought of as a transformation matrix between the two sets of coordinates

$\dfrac{\mathrm{d}}{\mathrm{d}t}\left(\dfrac{\partial \dot{q}_{A_k}}{\partial \dot{q}_i}\right)$ Derivative with respect to time of the above transformation matrix

$\dfrac{\partial \dot{q}_{A_k}}{\partial \dot{q}_i}$ Derivatives of half-element generalized coordinate time deriva-
tives with respect to element generalized coordinate time deriva-
tives (*e.g.*, derivative of control point velocity component $\dot{x}_1$ with
respect to cross-section centroid velocity component $\dot{x}_A$); this can
be thought of as a transformation matrix between the two sets of
coordinate time derivatives

$\dfrac{\mathrm{d}}{\mathrm{d}t}\left(\dfrac{\partial L_A}{\partial \dot{q}_{A_k}}\right)$ Derivative with respect to time of the above transformation matrix

To simplify the current work, however, only the static case will be considered
where all derivatives with respect to time are zero and the kinetic energy $T = 0$. In
this case, the set of equations (6.18) become

$$\left[-\frac{\partial L_A}{\partial q_{A_k}}\frac{\partial q_{A_k}}{\partial q_i}\right] + \left[-\frac{\partial L_B}{\partial q_{B_k}}\frac{\partial q_{B_k}}{\partial q_i}\right] = Q_i$$

$$-\frac{\partial L_A}{\partial q_{A_k}}\frac{\partial q_{A_k}}{\partial q_i} - \frac{\partial L_B}{\partial q_{B_k}}\frac{\partial q_{B_k}}{\partial q_i} = Q_i$$

and since $L = T - U = -U$

$$\frac{\partial U_A}{\partial q_{A_k}}\frac{\partial q_{A_k}}{\partial q_i} + \frac{\partial U_B}{\partial q_{B_k}}\frac{\partial q_{B_k}}{\partial q_i} = Q_i \tag{6.19}$$

To solve the static case, for each half-element it must be possible to evaluate the
12 derivatives $\partial U_A/\partial q_{A_k}$ and the $12 \times 16 = 192$ derivatives $\partial q_{A_k}/\partial q_i$. These can all
be found using the chain rule and the equations from Chapters 4 and 5, as well as
equations (6.8) − (6.10) and (6.12) − (6.14).

6.3.1 Derivative examples

Half-element coordinate with respect to element coordinate

As an example of one of the derivatives $\partial q_{A_k}/\partial q_i$ that must be evaluated to perform
a static simulation, consider $\partial y_{B_m}/\partial \phi_{x_B}$, the derivative of the y coordinate of the
middle control point of the second quadratic spline of an element with respect to
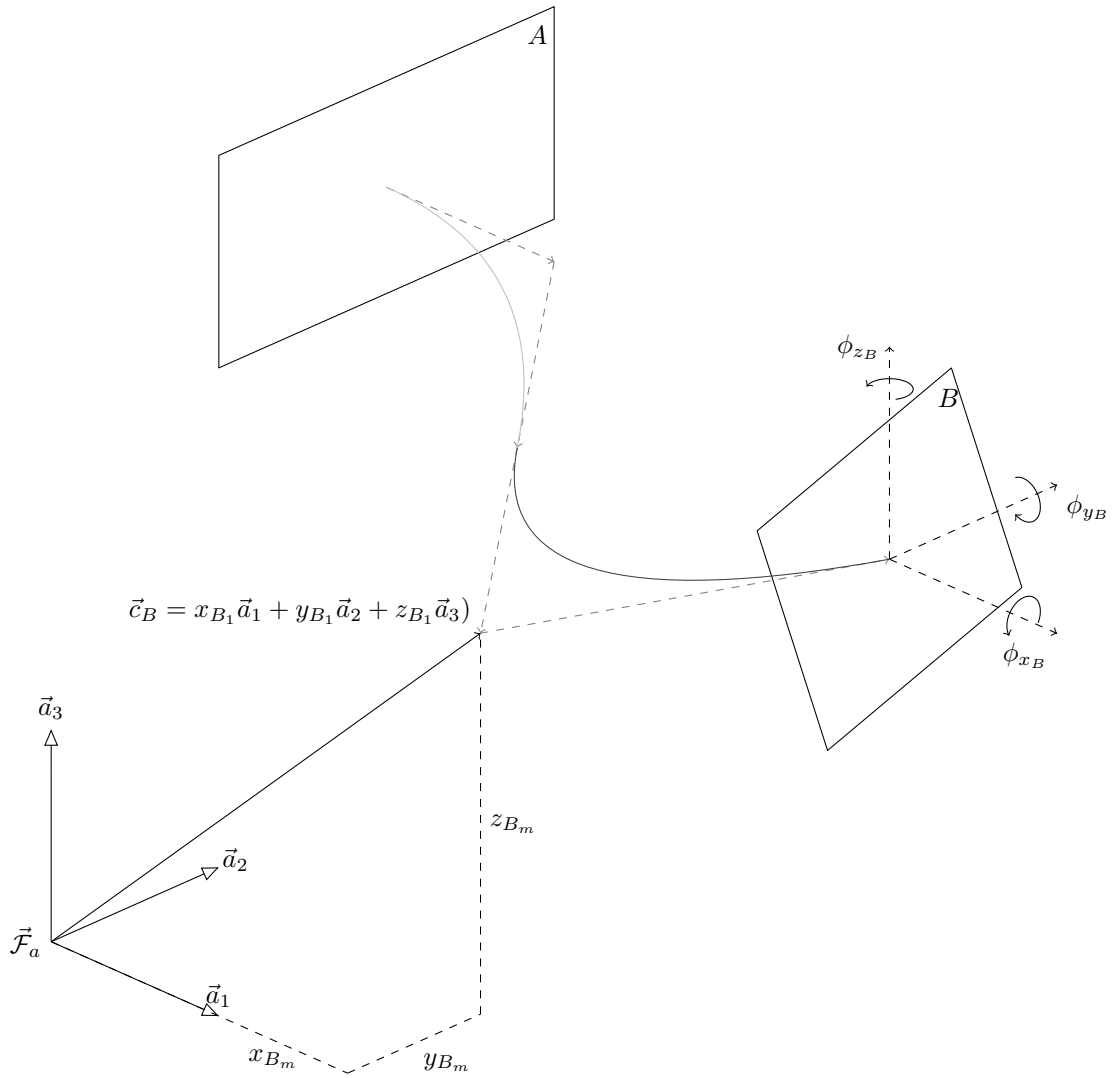
Figure 6.3: Example element and half-element coordinates.

the rotation angle ϕ_{x_B} of the second cross-section B defining the element, as shown in Figure 6.3. First, note that

$$y_{B_m} = \vec{c}_B \cdot \vec{a}_2 \tag{6.20}$$

so that

$$\frac{\partial y_{B_m}}{\partial \phi_{x_B}} = \frac{\partial \vec{c}_B}{\partial \phi_{x_B}} \cdot \vec{a}_2 \tag{6.21}$$

From equation (5.15),

$$\vec{c}_B = \vec{\rho}_B - \frac{1}{2}\xi_B \vec{t}_B$$

so that

$$\frac{\partial \vec{c}_B}{\partial \phi_{x_B}} = \frac{\partial \vec{\rho}_B}{\partial \phi_{x_B}} - \frac{1}{2}\left(\frac{\partial \xi_B}{\partial \phi_{x_B}}\vec{t}_B + \xi_B \frac{\partial \vec{t}_B}{\partial \phi_{x_B}}\right) \tag{6.22}$$

However, ξ_B and ϕ_{x_B} are independent generalized coordinates, so $\partial \xi_B / \partial \phi_{x_B} = 0$; also, by inspection of equation (6.7), $\partial \vec{\rho}_B / \partial \phi_{x_B} = 0$. Therefore,

$$\frac{\partial y_{B_m}}{\partial \phi_{x_B}} = -\frac{1}{2}\xi_B \frac{\partial \vec{t}_B}{\partial \phi_{x_B}} \cdot \vec{a}_2 \tag{6.23}$$

Finally, using equations (6.15) and (6.11),

$$\begin{aligned}
\frac{\partial y_{B_m}}{\partial \phi_{x_B}} &= -\frac{1}{2}\xi_B \left(\frac{\partial \vec{\phi}_B}{\partial \phi_{x_B}} \times \vec{t}_B\right) \cdot \vec{a}_2 \\
&= -\frac{1}{2}\xi_B(\vec{a}_1 \times \vec{t}_B) \cdot \vec{a}_2 \\
&= \frac{1}{2}\xi_B(\vec{t}_B \times \vec{a}_1) \cdot \vec{a}_2
\end{aligned} \tag{6.24}$$

Half-element strain energy with respect to half-element coordinate

As an example of one of the derivatives $\partial U_A / \partial q_{A_k}$, consider $\partial U_A / \partial \theta_{A_1}$, the derivative of the strain energy of the first half-element with respect to the last cross-sectional angle control point of the half-element. From equation (4.60),

$$\begin{aligned}
U_A = \frac{1}{2}\int_{\tau_A=0}^{1} &\left((\Delta \xi)^2\left[\frac{E}{\xi^*}\chi_{00}\right] - \Delta \xi \Delta(\xi \kappa_v)\left[\frac{2E}{\xi^*}\chi_{10}\right] + \Delta \xi \Delta(\xi \kappa_u)\left[\frac{2E}{\xi^*}\chi_{01}\right]\right. \\
&+ (\Delta(\xi \kappa_v))^2\left[\frac{E}{\xi^*}\chi_{20}\right] - \Delta(\xi \kappa_v)\Delta(\xi \kappa_u)\left[\frac{2E}{\xi^*}\chi_{11}\right] + (\Delta(\xi \kappa_u))^2\left[\frac{E}{\xi^*}\chi_{02}\right] \\
&\left.+ (\Delta(\xi \psi))^2\left[\frac{G}{\xi^*}(\chi_{20} + \chi_{02})\right]\right) d\tau_A
\end{aligned}$$

so that

$$\frac{\partial U_A}{\partial \theta_{A_1}} = \frac{1}{2} \int_{\tau_A=0}^{1} \left(\frac{\partial}{\partial \theta_{A_1}} \left((\Delta \xi)^2 \right) \left[\frac{E}{\xi^*} \chi_{00} \right] - \frac{\partial}{\partial \theta_{A_1}} \left(\Delta \xi \Delta(\xi \kappa_v) \right) \left[\frac{2E}{\xi^*} \chi_{10} \right] \right.$$

$$+ \frac{\partial}{\partial \theta_{A_1}} \left(\Delta \xi \Delta(\xi \kappa_u) \right) \left[\frac{2E}{\xi^*} \chi_{01} \right] + \frac{\partial}{\partial \theta_{A_1}} \left((\Delta(\xi \kappa_v))^2 \right) \left[\frac{E}{\xi^*} \chi_{20} \right]$$

$$- \frac{\partial}{\partial \theta_{A_1}} \left(\Delta(\xi \kappa_v) \Delta(\xi \kappa_u) \right) \left[\frac{2E}{\xi^*} \chi_{11} \right] + \frac{\partial}{\partial \theta_{A_1}} \left((\Delta(\xi \kappa_u))^2 \right) \left[\frac{E}{\xi^*} \chi_{02} \right]$$

$$\left. + \frac{\partial}{\partial \theta_{A_1}} \left((\Delta(\xi \psi))^2 \right) \left[\frac{G}{\xi^*} (\chi_{20} + \chi_{02}) \right] \right) \mathrm{d}\tau_A \qquad (6.25)$$

However, ξ, κ_u, and κ_v all do not depend on the orientation angle, so

$$\frac{\partial U_A}{\partial \theta_{A_1}} = \frac{1}{2} \int_{\tau_A=0}^{1} \frac{\partial}{\partial \theta_{A_1}} \left((\Delta(\xi \psi))^2 \right) \left[\frac{G}{\xi^*} (\chi_{20} + \chi_{02}) \right] \mathrm{d}\tau_A$$

$$= \frac{1}{2} \int_{\tau_A=0}^{1} 2 \Delta(\xi \psi) \frac{\partial}{\partial \theta_{A_1}} \left(\Delta(\xi \psi) \right) \left[\frac{G}{\xi^*} (\chi_{20} + \chi_{02}) \right] \mathrm{d}\tau_A$$

using $\Delta(\xi \psi) = \xi \psi - \xi^* \psi^*$,

$$\frac{\partial U_A}{\partial \theta_{A_1}} = \frac{1}{2} \int_{\tau_A=0}^{1} 2 \Delta(\xi \psi) \left(\frac{\partial \xi}{\partial \theta_{A_1}} \psi + \xi \frac{\partial \psi}{\partial \theta_{A_1}} \right) \left[\frac{G}{\xi^*} (\chi_{20} + \chi_{02}) \right] \mathrm{d}\tau_A$$

but again ξ does not depend on θ_{A_1}, so

$$= \frac{1}{2} \int_{\tau_A=0}^{1} 2 \Delta(\xi \psi) \xi \frac{\partial \psi}{\partial \theta_{A_1}} \left[\frac{G}{\xi^*} (\chi_{20} + \chi_{02}) \right] \mathrm{d}\tau_A$$

and using equation (5.39),

$$\frac{\partial U_A}{\partial \theta_{A_1}} = \frac{1}{2} \int_{\tau_A=0}^{1} 2 \Delta(\xi \psi) \xi \frac{\partial}{\partial \theta_{A_1}} \left((1 - \tau_A)^2 \theta_{A_0} + 2\tau_A (1 - \tau_A) \theta_{A_m} + \tau^2 \theta_{A_1} \right)$$

$$\left[\frac{G}{\xi^*} (\chi_{20} + \chi_{02}) \right] \mathrm{d}\tau_A$$

$$= \frac{1}{2} \int_{\tau_A=0}^{1} 2 \Delta(\xi \psi) \xi \tau^2 \left[\frac{G}{\xi^*} (\chi_{20} + \chi_{02}) \right] \mathrm{d}\tau_A$$

$$= \int_{\tau_A=0}^{1} \left[\frac{G(\chi_{20} + \chi_{02})}{2\xi^*} \right] 2 \Delta(\xi \psi) \xi \tau^2 \mathrm{d}\tau_A \qquad (6.26)$$

Note that since the weighting function $G(\chi_{20} + \chi_{02})/2\xi^*$ is the same, this integral can be evaluated using the same Gaussian integration roots τ_{7_i} and weights w_{7_i} as equation (6.2):

$$\frac{\partial U_A}{\partial \theta_{A_1}} \approx \sum_i w_{7_i} 2 \left. \Delta(\xi \psi) \right|_{\tau_{7_i}} \left. \xi \right|_{\tau_{7_i}} \tau_{7_i}^2 \qquad (6.27)$$

6.3.2 Solution

Equations (6.24) and (6.26) are two examples of the expressions that make up the system of equations (6.19). This system of equations (for one element) is then combined with those of every other element to form one large system of nonlinear equations that must be solved. Note that the systems of equations for individual elements are not independent, since the parameters defined at any interior cross-section will appear in the Lagrange equations for the elements on both sides of that cross-section.

Since the equations are nonlinear, they cannot be solved (as in the linear case) by a simple matrix inversion. Instead, a method such as Newton-Raphson [17, 18] must be used. For a system of nonlinear equations in the q_i for each element, the Newton-Raphson method requires that the derivatives of each equation with respect to each of the q_i are known; this means, for instance, that the derivatives in equations (6.24) and (6.26) must be again differentiated with respect to q_i. Then, having formed a square matrix of second derivatives (n derivatives with respect to each of the q_i, of each of the n equations), this matrix is inverted and used to increment the values of q_i towards a solution. The implications of this approach are discussed in Chapter 8; for simplicity, the simulation described in Chapter 7 used a numerical method to approximate the various second derivatives.

7

Implementation and Results

A sample program was written in C++ [19] to compute the strain energy of a beam given a specific deformation, to calculate the internal bending forces and moments, and also to simulate the deformed shape of a beam under a given loading. Gaussian integration with three nodes, as described in section 6.1, was used to evaluate all of the quantities and their derivatives needed for the solution approach described in section 6.3.2.

In all figures, the wire-frame version of the body denotes the original, undeformed configuration and the solid version denotes the deformed configuration. When force/moment plots are shown, take care to note the scale on each; frequently there will appear to be some insignificant numerical noise which may appear as large internal forces or moments since the plot scale is on the order of 10^{-6} or smaller.

The cross-sections at the ends of each element are highlighted, along with the cross-sections at the middle of each element (where the two quadratic splines making up the element meet). All numerical values given can be assumed to be in any consistent system of units.

Where orientations of cross-sections are discussed, they are specified as rotation matrices (which define the orientation of the cross-section's frame, as discussed in Appendix A). The shorthand notation $\mathbf{R}_1(\theta)$, $\mathbf{R}_2(\theta)$, $\mathbf{R}_3(\theta)$ is used for rotations

Table 7.1: Symbolic Equivalents to Textual Labels

XA0	x_A	XB1	x_B
YA0	y_A	YB1	y_B
ZA0	z_A	ZB1	z_B
PHXA0	ϕ_{x_A}	PHXB1	ϕ_{x_B}
PHYA0	ϕ_{y_A}	PHYB1	ϕ_{y_B}
PHZA0	ϕ_{z_A}	PHZB1	ϕ_{z_B}
XIA0	ξ_A	XIB1	ξ_B
PSA0	ψ_A	PSB1	ψ_B

about the three coordinate axes:

$$\mathbf{R}_1(\theta) = \begin{bmatrix} 1 & 0 & 0 \\ 0 & \cos(\theta) & \sin(\theta) \\ 0 & -\sin(\theta) & \cos(\theta) \end{bmatrix} \tag{7.1}$$

$$\mathbf{R}_2(\theta) = \begin{bmatrix} \cos(\theta) & 0 & -\sin(\theta) \\ 0 & 1 & 0 \\ \sin(\theta) & 0 & \cos(\theta) \end{bmatrix} \tag{7.2}$$

$$\mathbf{R}_3(\theta) = \begin{bmatrix} \cos(\theta) & \sin(\theta) & 0 \\ -\sin(\theta) & \cos(\theta) & 0 \\ 0 & 0 & 1 \end{bmatrix} \tag{7.3}$$

If no orientation matrix is given, it is assumed to be the identity matrix, so that the normal vector to the cross-section is aligned with the global x axis and the cross-section principal axes are aligned with the global y and z axes.

Some of the screenshots in this chapter show numerical values for the derivatives $\partial U/\partial q_i$; the labels used correspond to the symbols used in section 6.3, as shown in Table 7.1.
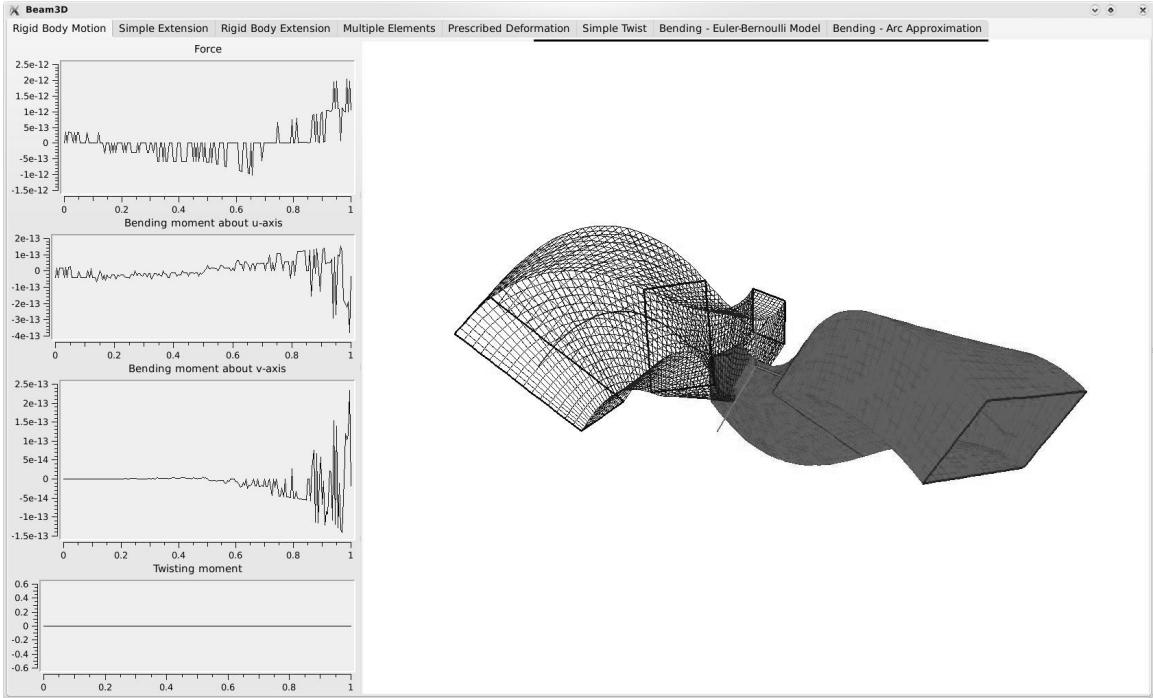
Figure 7.1: Rigid body motion.

7.1 Prescribed deformation

7.1.1 Rigid body motion

Figure 7.1 shows a single curved and twisted beam element with varying cross-section being put through a rigid body motion. In this case, as summarized in Table 7.2, the width and height of the cross-section increase over the length of the element, and the cross-sections twist about the locus of centroids (since the second cross-section is given an extra rotation about its own normal vector). The rigid body motion is a simple rotation about a vertical axis. As expected, all internal forces and moments are zero (within a small amount of numerical noise, on the order of 10^{-12}).

Table 7.2: Rigid Body Motion Example Parameters

Parameter	Value
Start position	(-5, -2, -5)
Start width	1
Start height	2
Start extension ξ	5
Start twist ψ	0
End position	(5, -2, 5)
End width	2
End height	3
End extension ξ	5
End twist ψ	0
End orientation	$\mathbf{R}_1(1)$
Elastic modulus E	1000

Table 7.3: Simple Extension Example Parameters

(a) Undeformed		(b) Deformed	
Parameter	Value	Parameter	Value
Length L	10	Start position	(-5.25, 0.6, 0)
Start position	(-5, -0.6, 0)	Start extension ξ	5.25
Start extension ξ	5	End position	(5.25, 0.6, 0)
End position	(5, -0.6, 0)	End extension ξ	5.25
End extension ξ	5		
Width w	1		
Height h	2		
Elastic modulus E	1000		
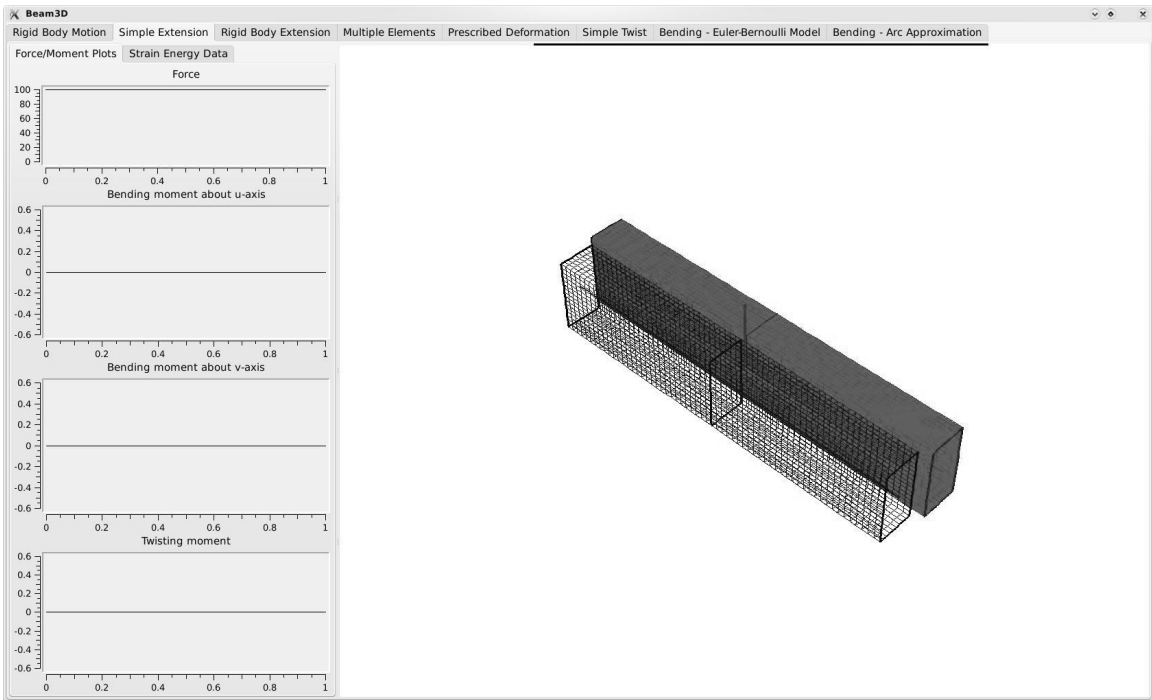
(a) Force and moment plots
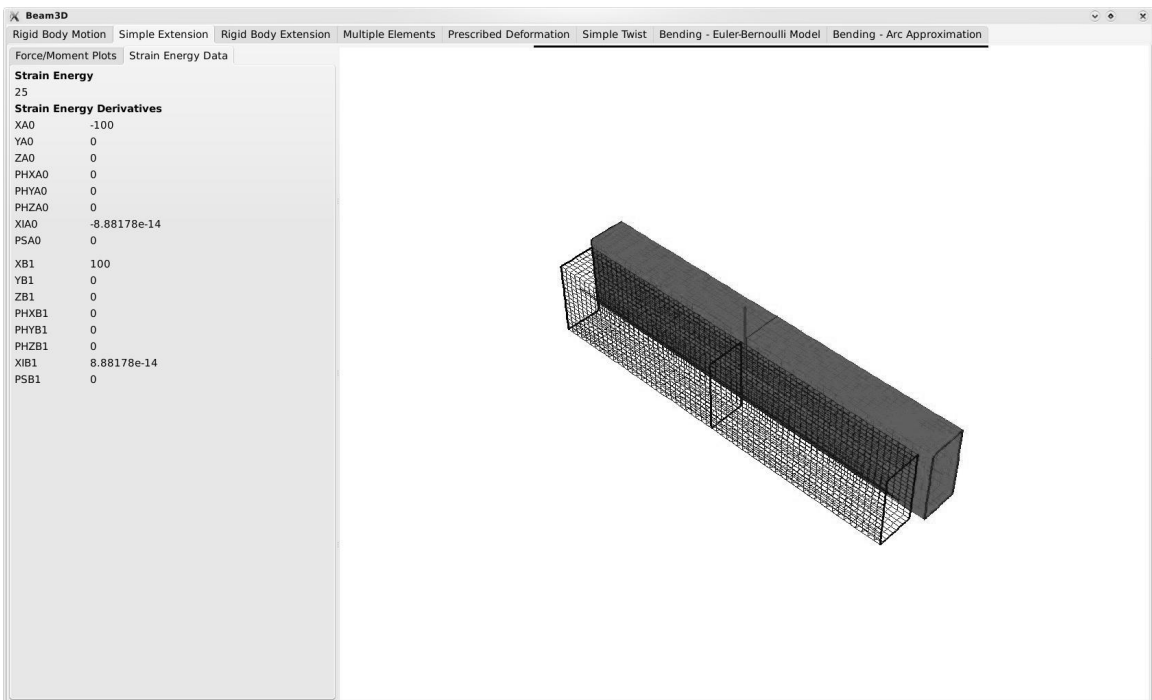
(b) Strain energy and derivatives

Figure 7.2: Simple extension.

7.1.2 Extension

Figure 7.2 illustrates the simple case of a straight beam being stretched (a pre-scribed axial displacement), combined with a rigid-body translation. Note that to stretch the beam linearly, the cross-sections must be translated outwards *and* the rate of extension ξ must be increased, as shown in Table 7.3.

As expected, all internal moments are zero and the the internal force has a magnitude of 100, as expected from linear elasticity:

$$
\begin{aligned}
F &= \sigma A \\
&= E\epsilon A \\
&= E\left(\frac{\Delta L}{L}\right) A \\
&= (1000)\left(\frac{0.5}{10}\right)(1)(2) \\
&= 100
\end{aligned}
$$

Also, the only non-zero derivatives $\partial U/\partial q_i$ are those with respect to axial displacements at the ends, which is correct since this type of deformation corresponds to equal and opposite extensional forces at the ends of the beam.

Figure 7.3 shows the same case as illustrated in Figure 7.2, but adds a rigid body rotation about both the y and z axes; again only the internal extensional force is non-zero and has a magnitude of 100 as expected. Here, all three displacements at both ends of the beam have non-zero corresponding $\partial U/\partial q_i$, as the force at each end would in this case have components in all three coordinate directions.

7.1.3 Twist

Figure 7.4 shows an example of a beam going through a prescribed constant twist of 0.1 radians per unit length; as expected, only the internal twisting moment and the derivatives of strain energy with respect to twist angle at the two ends are non-zero. The computed internal twisting moment has a magnitude of 83.333, which
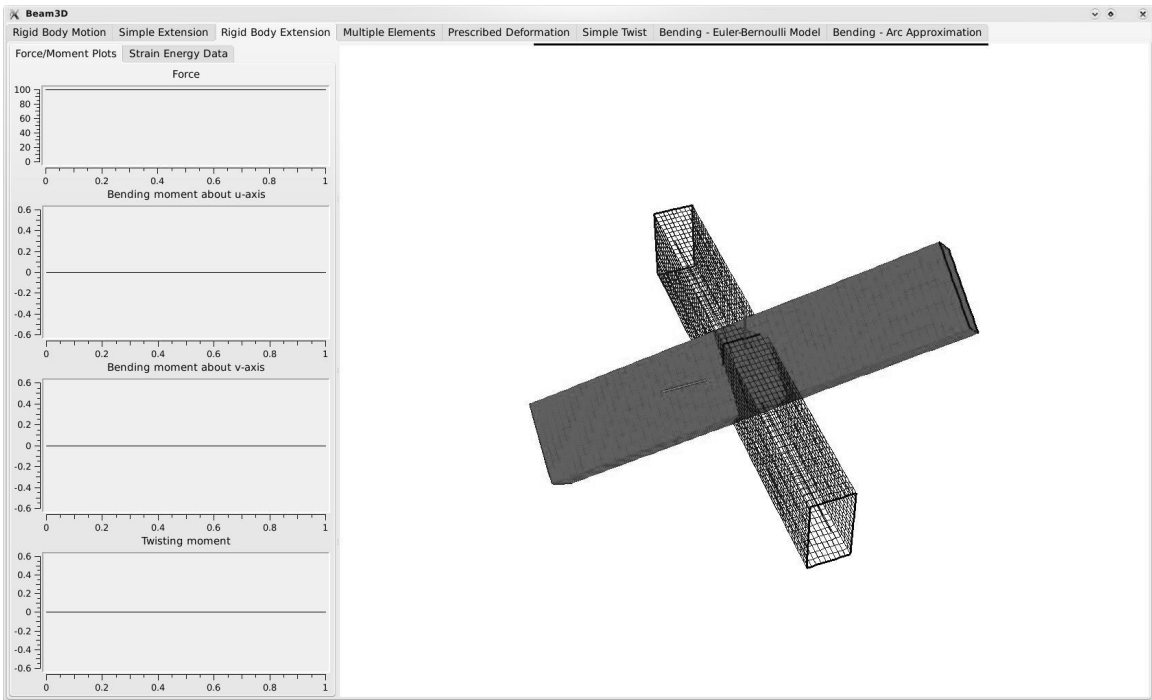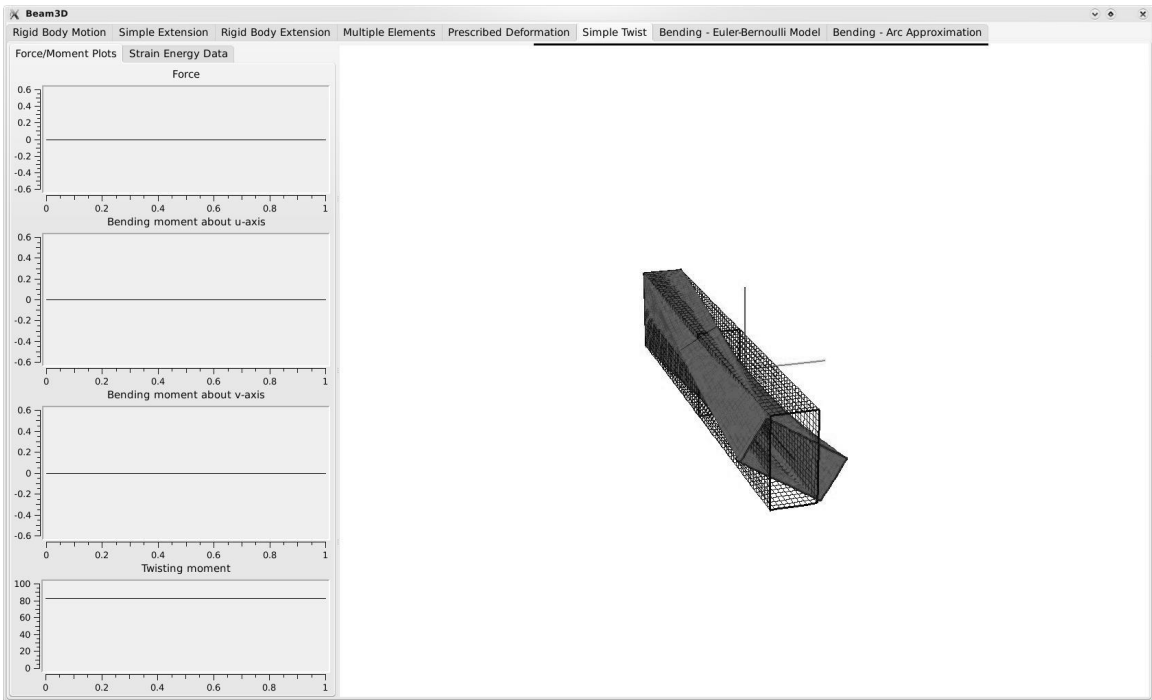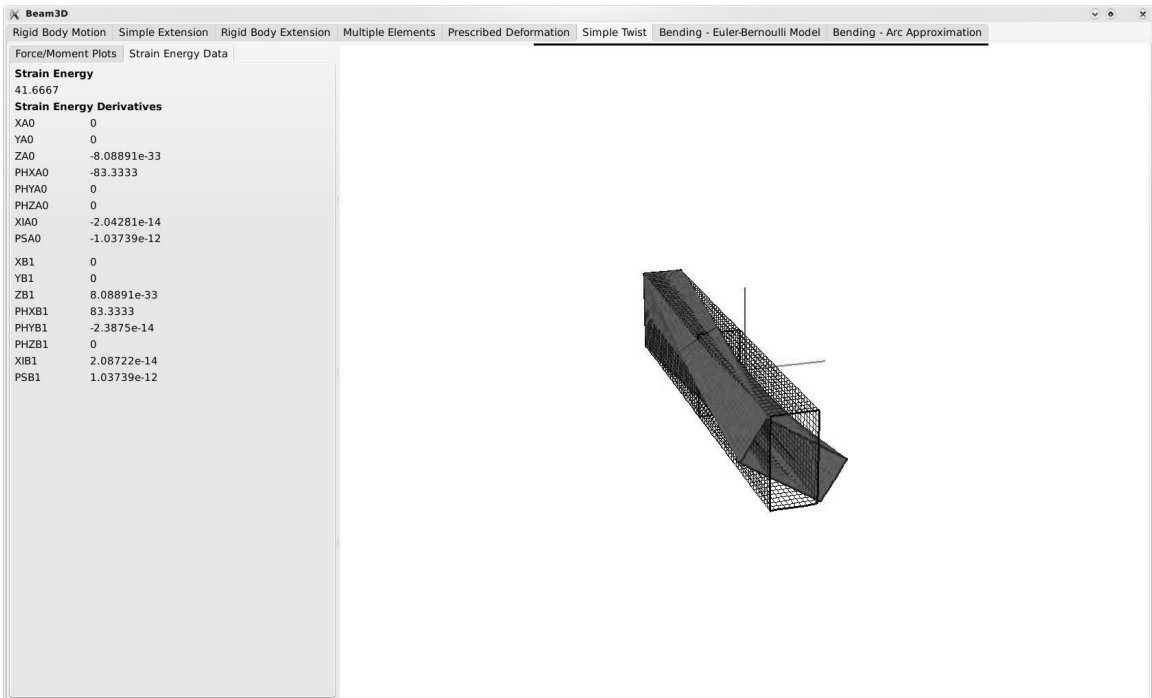
(a) Force and moment plots
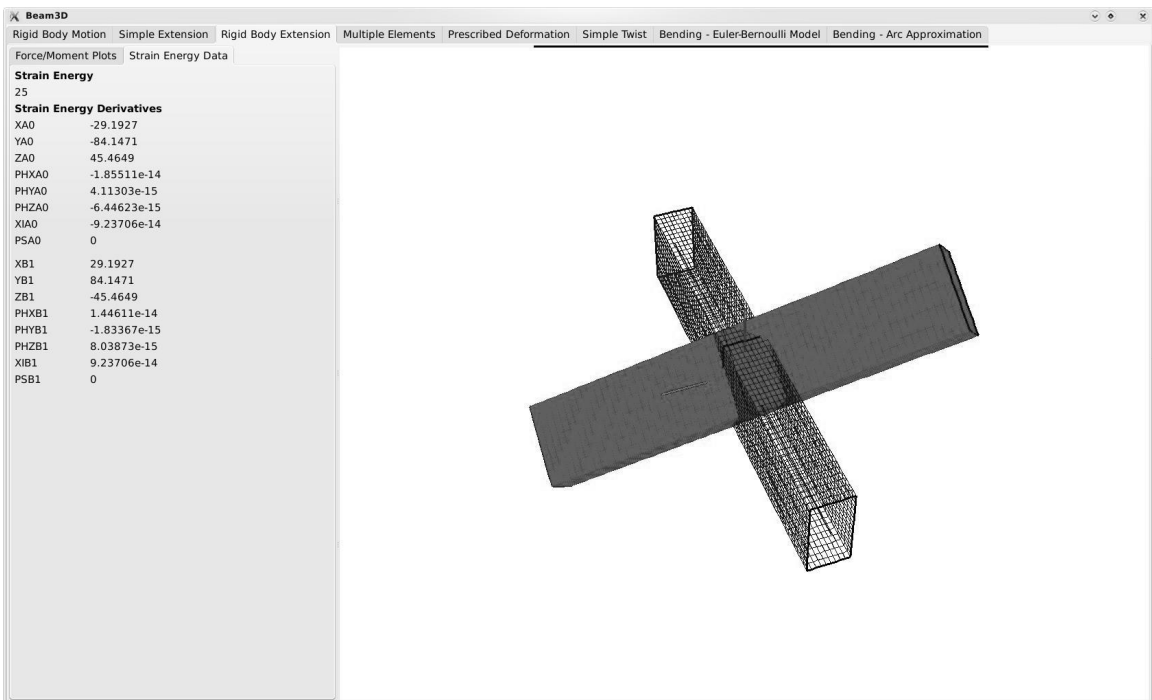
(b) Strain energy and derivatives

Figure 7.3: Extension combined with rigid body motion.

(a) Force and moment plots

(b) Strain energy and derivatives

Figure 7.4: Simple twist.

Table 7.4: Simple Twist Example Parameters

(a) Undeformed		(b) Deformed	
Parameter	**Value**	**Parameter**	**Value**
Length L	10	Start twist rate ψ	0.1
Start position	(-5, -0.6, 0)	End twist rate ψ	0.1
Start extension ξ	5	End orientation	$\mathbf{R}_1(1)$
Start twist rate ψ	0		
End position	(5, -0.6, 0)		
End extension ξ	5		
End twist rate ψ	0		
Width w	1		
Height h	2		
Shear modulus G	1000		

agrees with the expected result for the simple torsion model used [1]:

$$
\begin{aligned}
M &= \frac{GJ\Delta\theta}{L} \\
&= \frac{G\left(\frac{1}{12}wh(w^2 + h^2)\right)\Delta\theta}{L} \\
&= \frac{Gwh(w^2 + h^2)\Delta\theta}{12L} \\
&= \frac{(1000)(2)(1)\left(2^2 + 1^2\right)(1)}{12(10)} \\
&= 83.3
\end{aligned}
$$

Note that this uses the polar moment J directly in the computation of twisting moment; to accommodate for warping, an adjusted value of J should be used, as discussed in section 1.2.
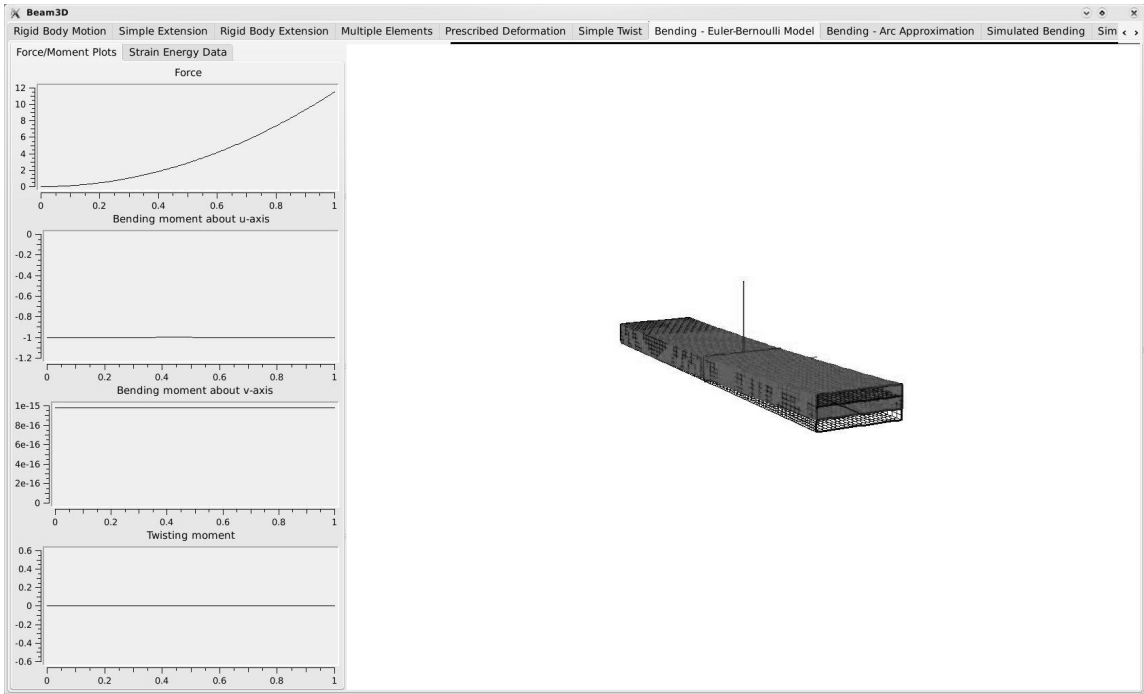
(a) Euler-Bernoulli model
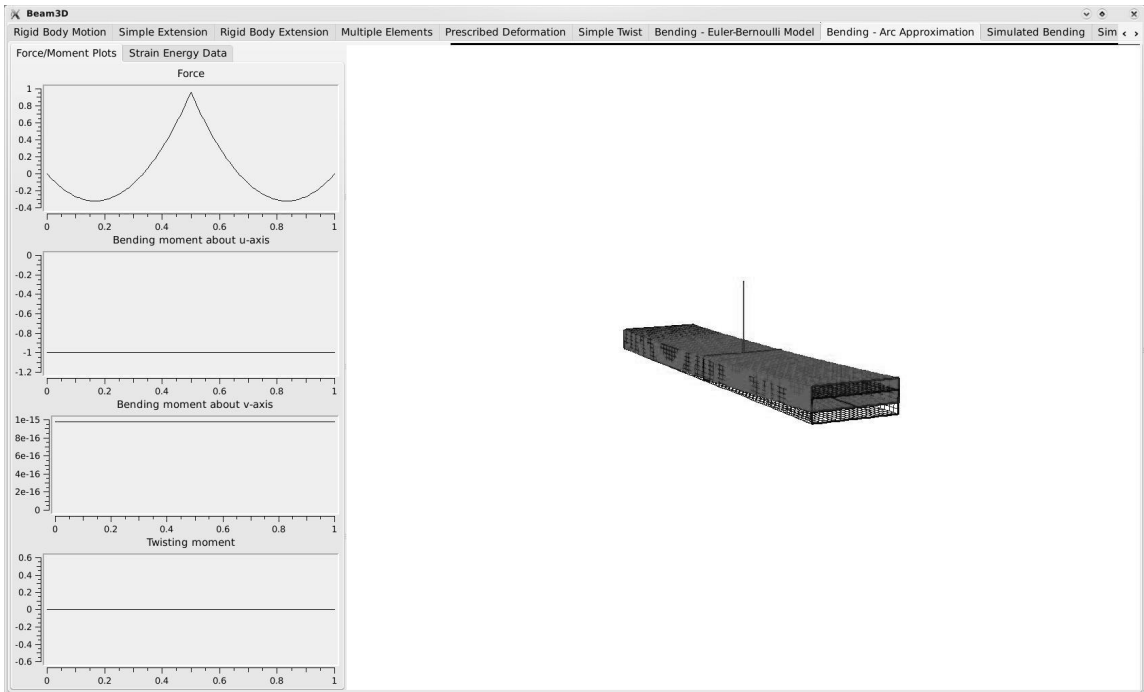
(b) Arc approximation

Figure 7.5: Bending.

Table 7.5: Bending Example Parameters (Undeformed)

Parameter	Value
Length L	10
Start position	(-5, 0, 0)
Start extension ξ	5
Start twist rate ψ	0
End position	(5, 0, 0)
End extension ξ	5
End twist rate ψ	0
Width w	2
Height h	0.5
Elastic modulus E	10000
Applied bending moment M	1

7.1.4 Bending

Figure 7.5 compares an Euler-Bernoulli model of pure beam bending with equal and opposite moments applied at each end (for which the solution is a quadratic curve) to the analytical solution of a circular arc. For both cases, the original beam and applied moment was as specified in Table 7.5.

The Euler-Bernoulli solution for simple beam bending predicts a purely vertical tip deflection w, as well as a change in angle ϕ at the tip of the beam [1]:

$$
\begin{aligned}
w &= \frac{ML^2}{2EI} \\
&= \frac{ML^2}{2E\left(\frac{1}{12}wh^3\right)} \\
&= \frac{6ML^2}{Ewh^3} \\
&= \frac{6(1)(10^2)}{(10000)(2)(0.5)^3} \\
&= 0.24
\end{aligned}
$$

Table 7.6: Bending Example Parameters (Deformed Euler-Bernoulli beam)

Parameter	Value
End position	$(5, 0, 0.24)$
End orientation	$\mathbf{R}_2(-0.048)$
End extension ξ	$5/\cos(0.048)$

$$
\begin{aligned}
\phi &= \frac{ML}{EI} \\
&= \frac{ML}{E\left(\frac{1}{12}wh^3\right)} \\
&= \frac{12ML}{Ewh^3} \\
&= \frac{12(1)(10)}{(10000)(2)(0.5)^3} \\
&= 0.048
\end{aligned}
$$

The deformed Euler-Bernoulli beam is then as described in Table 7.6; note that since the Euler-Bernoulli model assumes a constant rate of extension along the horizontal x axis (as opposed to along the curved, deformed beam locus of centroids), the end extension of the element must be adjusted slightly since the locus of centroids is not horizontal at that point.

For large deformations such as the one shown, the fact that the Euler-Bernoulli model in Figure 7.5(a) assumes zero deformation in the axial direction of points along the locus of centroids leads to a large, spurious internal force. Also, since a simple quadratic does not have constant curvature, the internal moment is not quite constant. (Note that since the Euler-Bernoulli solution for a single applied moment is a single quadratic curve, a single element formed of quadratic splines is able to replicate the Euler-Bernoulli solution exactly.)

In contrast, taking large-deformation effects into consideration by approximating the analytical arc solution leads to much better results. Here, as illustrated in
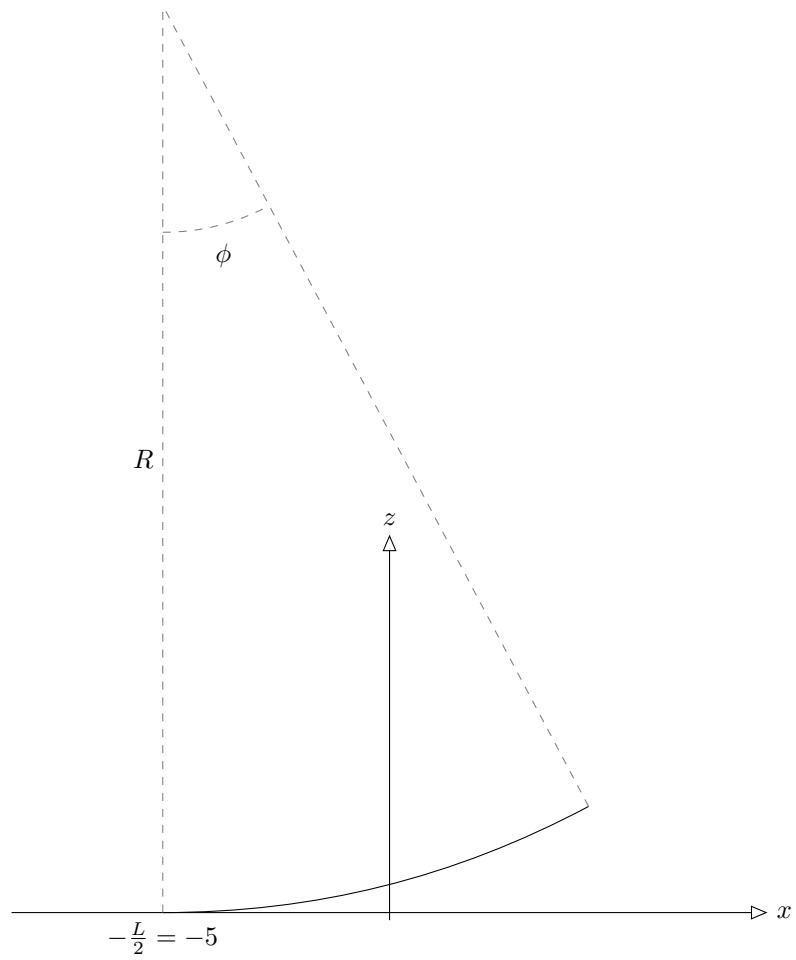
Figure 7.6: Deformed circular arc shape of locus of centroids.

Figure 7.6 (not to scale), the deformed radius R is given by

$$M = EI\kappa$$

$$M = \frac{EI}{R}$$

$$R = \frac{E\left(\frac{1}{12}wh^3\right)}{M}$$

$$= \frac{Ewh^3}{12M}$$

$$= \frac{(10000)(2)(0.5)^3}{12(1)}$$

$$= 208.3$$

the sweep angle ϕ (equal to the rotation of the tip cross-section) is

$$\phi = \frac{L}{R}$$

$$= \frac{10}{208.3}$$

$$= 0.048$$

the deformed position of the tip of the beam is given by

$$x = -\frac{L}{2} + R\sin\phi \qquad\qquad z = R(1 - \cos\phi)$$

$$= -5 + (208.3)\sin(0.048) \qquad\qquad = (208.3)\left(1 - \cos(0.048)\right)$$

$$= 4.9962 \qquad\qquad = 0.23995$$

Although still not perfect (since quadratic splines cannot reproduce arcs exactly) the resulting internal moment as shown in Figure 7.5(b) is nearly constant and the spurious internal force is much lower.

7.1.5 Multiple Elements

Figure 7.7 demonstrates how multiple elements can be joined together to make complex shapes, while still remaining strain-free (computed internal forces and moments in the order of 10^{-12}) under rigid body motion (in this case, a single rotation about a vertical axis). Unsurprisingly, the first element (which is completely
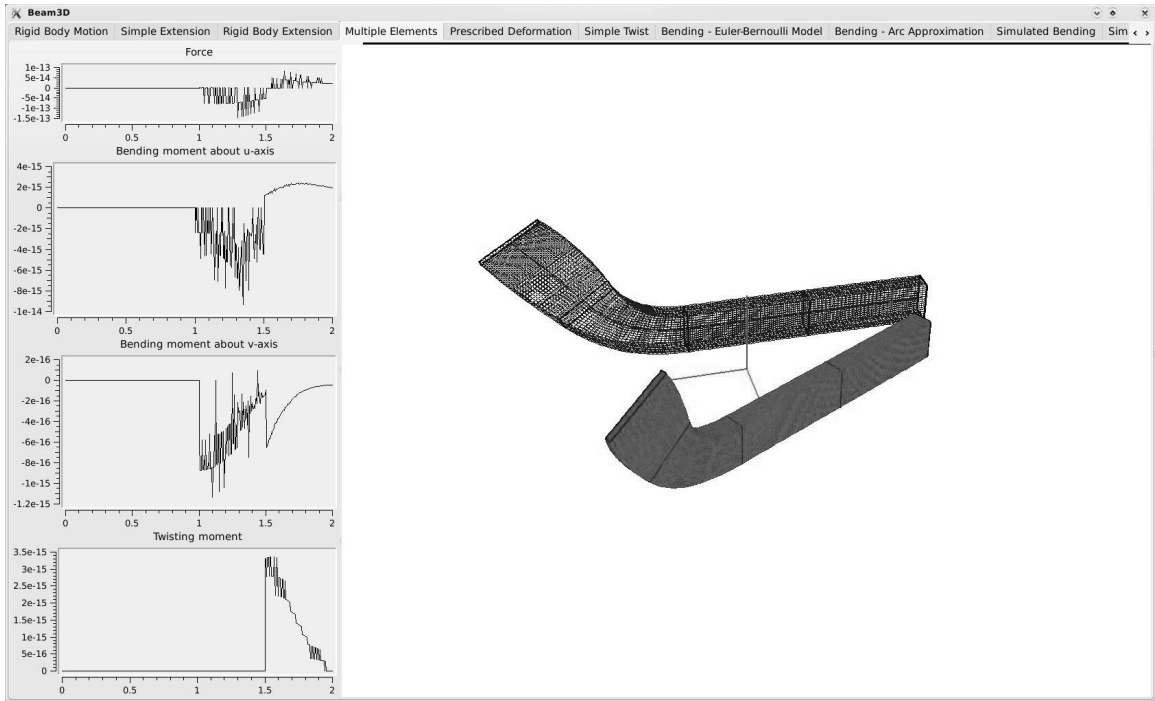
Figure 7.7: Multiple elements.

straight, and corresponds to the range 0-1 on the plots) has no numerical noise at all while the second (curved and twisted) element does.

7.2   Simulation

All of the previous examples showed cases where the deformation of the beam was prescribed and the resulting forces and moments were computed. Using the approach described in Chapter 6, it is also possible to specify a particular force/-moment loading and compute the resulting deformation. In all cases, for simplicity, the beam is assumed to be fixed at one end and have a single load at the other end.
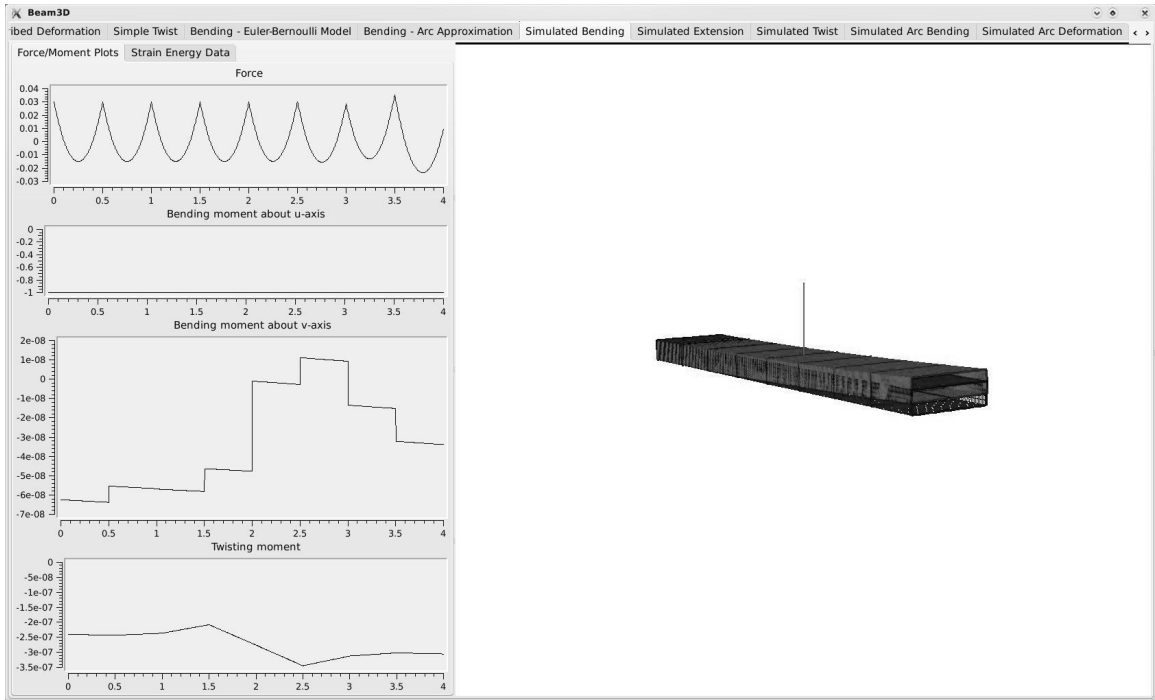
Figure 7.8: Simulated bending of a straight beam.

Table 7.7: Comparison of Tip Deflections

Beam Type	x	y	z
Euler-Bernoulli	0	0	0.24
Arc	-0.00383956	0	0.239954
Simulation	-0.00384024	-5.92898×10^{-10}	0.239952
ANSYS	0.23714 (only total displacement given)		

7.2.1 Straight beam bending

Figure 7.8 illustrates a straight beam with a moment applied at the end, as in Figure 7.5 and with the same parameters as given in Table 7.5. In this case, four elements are used, which allows the final shape to more closely approximate an arc; the computed solution indeed has much lower spurious internal force than either of the solutions described earlier. The simulated beam very closely approximates the analytical solution of an arc.

Table 7.7 compares the tip deflections for the Euler-Bernoulli approximation, the analytical arc solution, and the simulated beam, as well as the solution computed by the Stress Analysis tool of Autodesk Inventor [20], which internally uses ANSYS [21]. The latter result is also shown in Figure 7.9. Note that the beam simulation is much closer to the analytical solution than the solution computed using ANSYS. Also note how the horizontal displacement predicted by the beam model (-0.00384024) is almost exactly the same as the arc solution (-0.00383956); this illustrates how the curved beam model can effectively simulate the kinds of nonlinear effects that are ignored by the Euler-Bernoulli model.

7.2.2 Curved beam bending

Figure 7.10 demonstrates how the beam model can be used to analyze beams with large initial curvatures. The shape and loading are the same as those specified in Table 7.5, except that the beam has initial curvature about its u axis with a radius of curvature of 10 units. Note that as expected, the internal moment from Figure 7.10 is nearly constant, although as before there is some small spurious internal force.

Figure 7.11 shows the same case simulated in Inventor/ANSYS. This gave a total tip displacement of 0.2346, while the beam simulation gave a total tip displacement of 0.2310 (-0.1463 in the x direction and 0.1793 in the z direction). The difference can be attributed largely to the discrepancy from theory of the ANSYS solution noted in the previous section, as well as the fact that Autodesk Inventor reports maximum deflection of any point on the beam, which in this case may
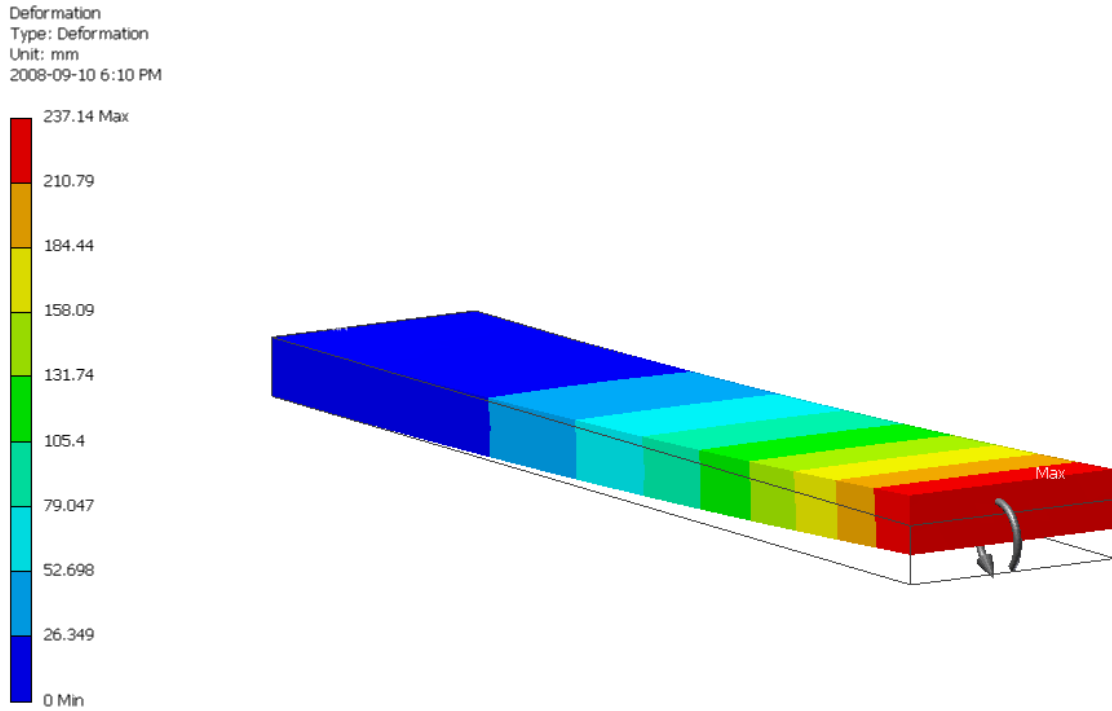
Figure 7.9: ANSYS simulation of straight beam bending.
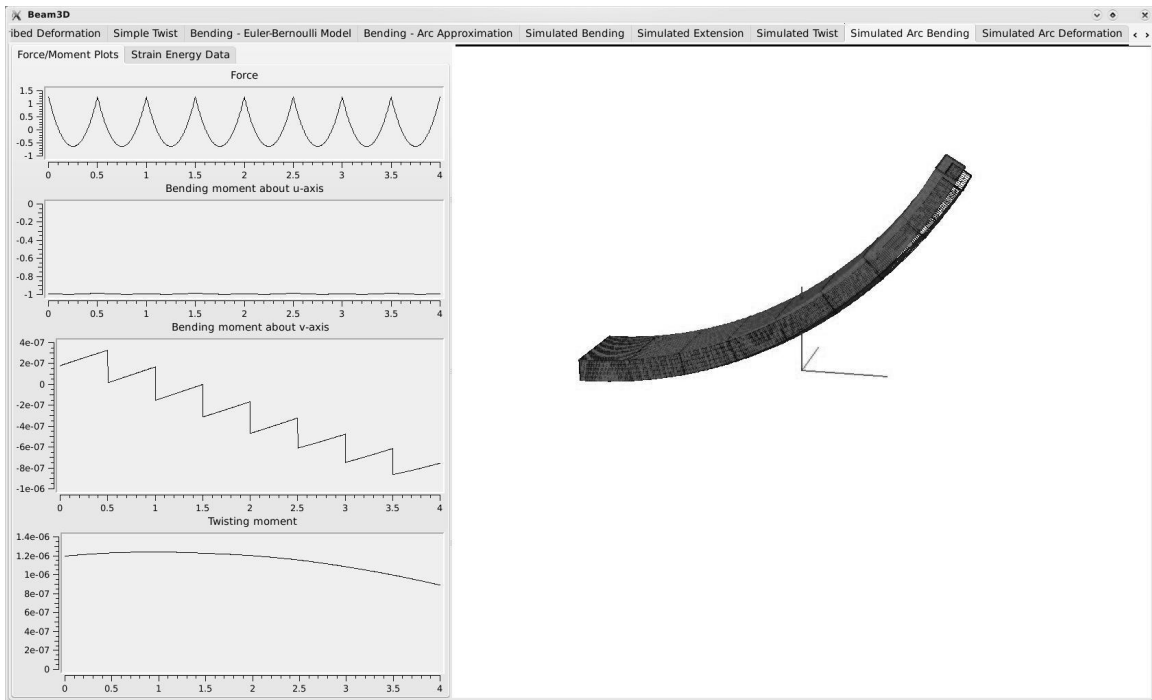
Figure 7.10: Simulated bending of a beam in the shape of a circular arc.
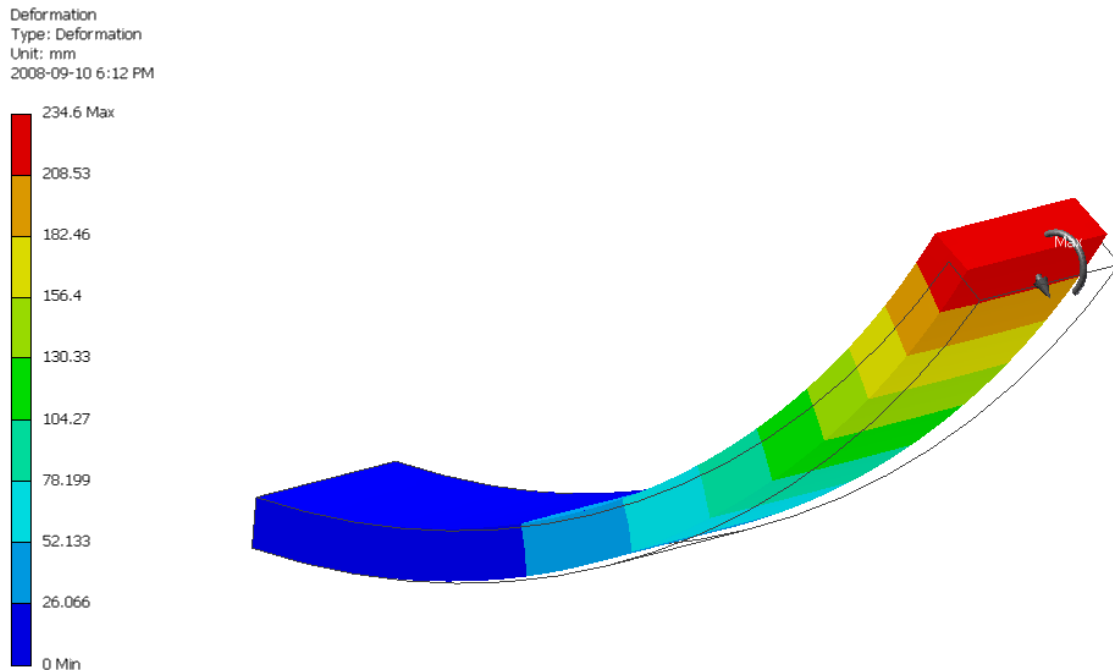
Figure 7.11: ANSYS simulation of curved beam bending.

be at some point along the outside edge of the tip cross-section instead of the tip cross-section's centroid.

7.2.3 Curved beam combined bending and torsion

Finally, Figure 7.12 illustrates a non-planar case of a beam in the shape of a circular arc (initially in the global xy plane) with a downwards ($-z$ direction) force acting at the tip; the shape and loading parameters are given in Table 7.8. Poisson's ratio is used only to compute the shear modulus G, given by [1]:

$$
\begin{aligned}
G &= \frac{E}{2(1+\nu)} \\
&= \frac{10000}{2(1+0.3)} \\
&= 3846
\end{aligned}
$$

(Changes in cross-section shape due to Poisson's effect are still ignored.)
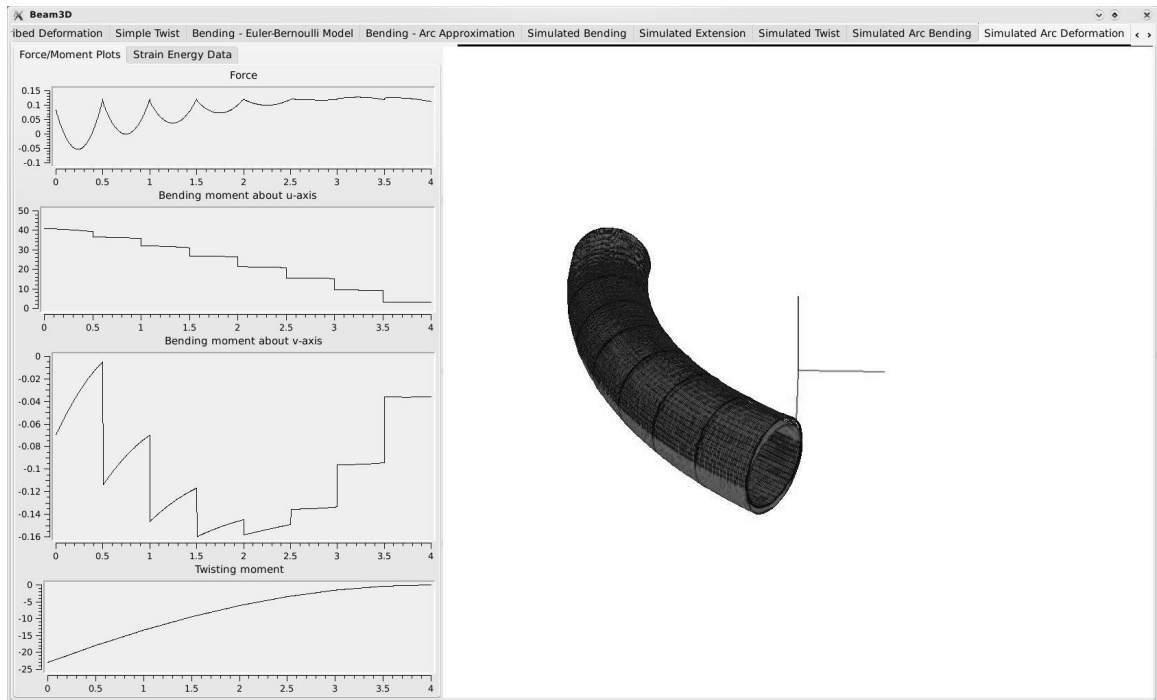
Figure 7.12: Simulated deformation of a beam in the shape of a circular arc.

Table 7.8: Combined Bending and Torsion Example Parameters

Parameter	Value
Length L	10
Start extension ξ	5
End extension ξ	5
Cross-section radius r	1
Radius of curvature R	10
Elastic modulus E	10000
Poisson's ratio ν	0.3
Applied force	(0, 0, -1)
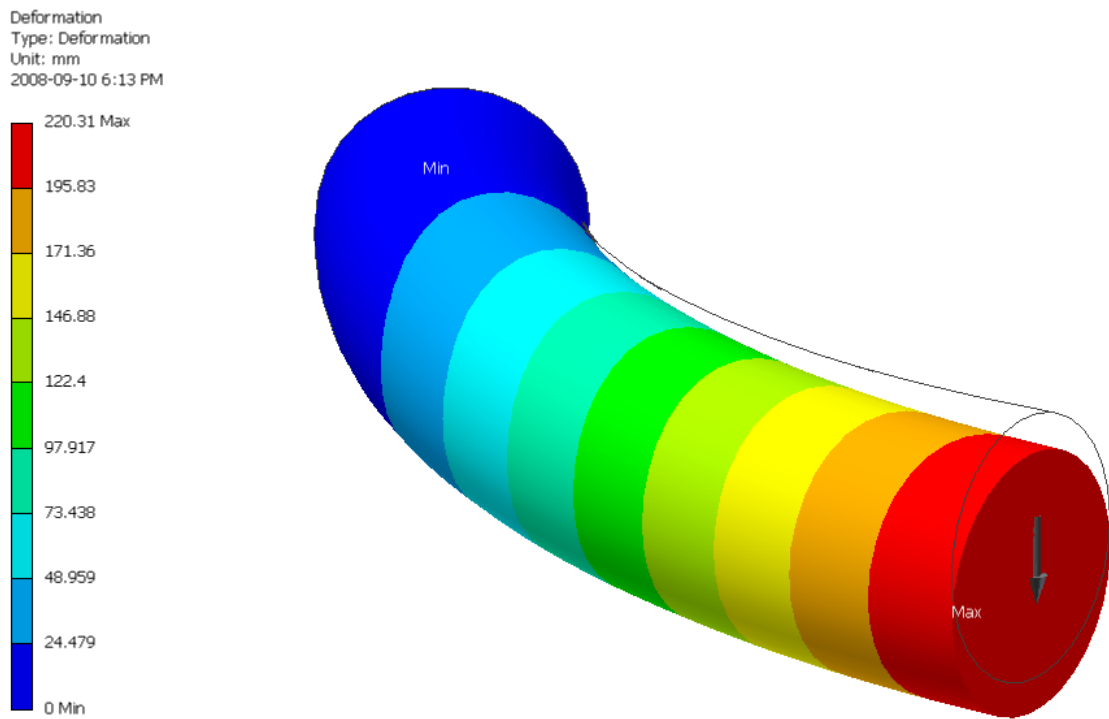
Figure 7.13: ANSYS simulation of curved beam combined bending and torsion.

As expected, the bending moments about the horizontal u-axis and the twisting moment are both at a maximum at the base of the beam and are zero at the tip. Figure 7.13 shows the same beam being simulated in Inventor/ANSYS; this gave a tip deflection of 0.2201 as compared to the beam simulation result of 0.2094. (Note that Inventor automatically applies scaling to the displayed deformations, so the deformations in the two figures look slightly different.)

8

Conclusions and Recommendations

As discussed in Chapters 1–3, forming a finite element model of a beam requires that its strain energy be defined in terms of discrete nodal parameters. This was then split into two independent problems: deriving an expression for the strain energy of an arbitrary curved and twisted beam, and then describing how to describe a curved beam efficiently in terms of discrete parameters.

Chapter 4 derives a strain energy integral for an arbitrary curved and twisted beam in terms of rotation-invariant quantities ξ (extension of the locus of centroids), κ_u and κ_v (curvatures about cross-sectional principal axes) and ψ (twist). As discussed in section 6.1, this integral lends itself well to being evaluated by weighted Gaussian integration. As long as the four properties of the locus of centroids could be evaluated, the strain energy integral in equation (4.60) could be applied to any choice of parametric curve defining the beam's locus of centroids.

Chapter 5 then presents a method for describing the shape of a curved and twisted beam in terms of quadratic spline curves. Although quadratic splines are a convenient choice due to their planar nature and their representation as polynomials, for specialized beam shapes the strain energy integral described above could easily be used with a different choice of curve. Chapter 6 shows how to combine the curved beam model with the piecewise quadratic element to form a finite element simulation of a curved and twisted beam.

8.1 Future Work

As demonstrated in Chapter 7, the beam model that was developed can be used to simulate a wide range of types of deformation involving large displacements of curved and twisted beams, and could be used directly to simulate the static behaviour of long and slender curved beams. The beam model is effective at simulating nonlinear effects such as the beam contraction discussed in section 7.2.1, and can be used in non-planar cases involving both bending and torsion, as shown in section 7.2.3. As a result, the simulation program that was written could be used directly to simulate the static deformation of isotropic beams where the nonlinear behaviour due to large deformations is significant, *e.g.*, a case where the horizontal deflection of beam loaded vertically is important.

To fully simulate cases such as the hockey stick mentioned earlier, several refinements would have to be made to the simulation in order to support:

- Orthotropic materials (such as wood or fibre composites)

- Trapezoidal cross-sections

- Dynamic behaviour

- Greater efficiency

Currently, the beam model assumes an isotropic material; as a result, equation (4.60) is based solely on modulus of elasticity E and shear modulus G. To allow for orthotropic materials such as wood or fiberglass, equation (4.40) would have to be modified to use a different constitutive matrix. The derivation of equation (4.60) would then follow in exactly the same way, although the end result would be more complex.

To simulate a beam with a given type of cross-section, the various indexed moments I_{mn} defined by equation (4.45) must be calculated for that cross-sectional shape. Currently, the simulation only supports rectangular and circular cross-sections; to accurately simulate a hockey stick blade, where the cross-section is

better approximated by a trapezoid, an expression for I_{mn} for a trapezoid must be derived. This would likely be most easily done by determining I_{mn} for a single triangle with one vertex at the origin, and then forming a trapezoid by a combination of four triangles. This approach would also have the advantage of allowing I_{mn} to be evaluated for any other polygonal cross-sectional shape, which would in turn allow I_{mn} to be approximated to arbitrary accuracy for other shapes by approximating them with polygons.

By implementing the various derivatives described in section 6.3, the model could be adapted to handle dynamic simulations of beams where the kinetic energy and momentum of the beam are significant. In this case, it would also be important to improve the efficiency of the simulation; for simplicity, many of the required derivatives are calculated numerically, so a method would have to be developed to automatically and efficiently evaluate the various derivatives. However, note that the derivatives for any one element can be calculated completely independently from all others. Therefore, efficiency gains could also be achieved by modifying the simulation to take advantage of multi-processor systems. Finally, it would be valuable to optimize the solution of the large, sparse linear system described in section 6.3.2; the current implementation simply calls a generic third-party solver.

By implementing the four improvements just described, the model would be effective at simulating the dynamic behaviour of curved beams which go through large displacements. The strength of the model comes from its ability to correctly compute strain under conditions of large displacement, as well as being able to robustly and efficiently define the shape of a beam as it goes through arbitrarily complex 3D motions.

References

[1] Anthony Bedford and Kenneth M. Liechti. *Mechanics of Materials*. Prentice Hall, 2000.

[2] S. Timoshenko. *Strength of Materials*. Van Nostrand Reinhold Company, 1958.

[3] Ahmed K. Noor, William H. Greene, and Stephen J. Hartley. Nonlinear finite element analysis of curved beams. *Computer Methods in Applied Mechanics and Engineering*, 12:289–307, 1997.

[4] D. Zupan and M. Saje. The linearized three-dimensional beam theory of naturally curved and twisted beams: The strain vectors formulation. *Computer Methods in Applied Mechanics and Engineering*, 195:4557–4578, 2006.

[5] B. Tabarrok, M. Farshad, and H. Yi. Finite element formulation of spatially curved and twisted rods. *Computer Methods in Applied Mechanics and Engineering*, 70:275–299, 1988.

[6] J. S. Sandhu, K. A. Stevens, and G. A. O. Davies. A 3-d, co-rotational, curved and twisted beam element. *Computers & Structures*, 35(1):69–79, 1990.

[7] Ken Shoemake. Animating rotation with quaternion curves. *Computer Graphics*, 19(3):245–254, 1985.

[8] Myung-Soo Kim and Kee-Won Nam. Interpolating solid orientations with circular blending quaternion curves. *Computer-Aided Design*, 27(5):385–398, 1995.

[9] Myoung-Jun Kim, Myung-Soo Kim, and Sung Yong Shin. A general construction scheme for unit quaternion curves with simple high order derivatives. In *Proceedings of SIGGRAPH'95*, pages 369–376, 1995.

[10] F. C. Park and Bahram Navani. Smooth invariant interpolation of rotations. *ACM Transactions on Graphics*, 16(3):277–295, July 1997.

[11] Victor N. Kaliakin. *Introduction to Approximate Solution Techniques, Numerical Modeling, and Finite Element Methods*. Marcel Dekker, Inc., 2002.

[12] Irving H. Shames and Clive L. Dym. *Energy and Finite Element Methods in Structural Mechanics*. Hemisphere Publishing Corporation, 1985.

[13] Henry L. Langhaar. *Energy Methods in Applied Mechanics*. John Wiley and Sons, Inc., 1962.

[14] George E. Mase. *Continuum Mechanics*. Schaum's Outline Series. McGraw-Hill, 1970.

[15] Eric W. Weisstein. "Negative Binomial Series". From *MathWorld*–A Wolfram Web Resource.
http://mathworld.wolfram.com/NegativeBinomialSeries.html.

[16] Gerald Farin. *Curves and Surfaces for CAGD*. Academic Press, 5th edition, 2002.

[17] Kendall Atkinson and Weimin Han. *Elementary Numerical Analysis*. Wiley, 3rd edition, 2003.

[18] William H. Press, Saul A. Teukolsky, William T. Vetterling, and Brian P. Flannery. *Numerical Recipes in C*. Cambridge University Press, 2nd edition, 1992.

[19] Bjarne Stroustrup. *The C++ Programming Language*. Addison-Wesley, special edition, 2000.

[20] Autodesk. http://www.autodesk.com.

[21] ANSYS. http://www.ansys.com.

[22] Peter C. Hughes. *Spacecraft Attitude Dynamics*. John Wiley and Sons, Inc., 1986.

Appendix A

Vectrices

Vectrix notation provides a concise and convenient way of expressing the relationships between different frames of reference. A 'vectrix' represents a frame of reference as a column matrix of unit vectors, i.e.,

$$\vec{\mathcal{F}}_a = \begin{bmatrix} \vec{a}_1 \\ \vec{a}_2 \\ \vec{a}_3 \end{bmatrix} \tag{A.1}$$

In this way, $\vec{a}_1$ defines the '1-axis' or '1-direction' of $\vec{\mathcal{F}}_a$, and similarly for the other two vectors.

A vector can then be defined as the product of $\vec{\mathcal{F}}_a^T$ and a column matrix of components $\mathbf{v}_a = [v_{a_1} \ v_{a_2} \ v_{a_3}]^T$, following standard rules of matrix arithmetic:

$$\vec{v} = \vec{\mathcal{F}}_a^T \mathbf{v}_a \tag{A.2}$$

$$= \begin{bmatrix} \vec{a}_1 & \vec{a}_2 & \vec{a}_3 \end{bmatrix} \begin{bmatrix} v_{a_1} \\ v_{a_2} \\ v_{a_3} \end{bmatrix} \tag{A.3}$$

$$= v_{a_1}\vec{a}_1 + v_{a_2}\vec{a}_2 + v_{a_3}\vec{a}_3 \tag{A.4}$$

where v_{a_1}, v_{a_2} and v_{a_3} are the components of vector $\vec{v}$ as expressed in the frame $\vec{\mathcal{F}}_a$.

Having defined frames this way, it becomes simple to define new frames with specified orientation relative to existing frames. For example, consider multiplying

$\vec{\mathcal{F}}_a$ (as defined above) by the standard rotation matrix describing a rotation by an angle θ around the 1-axis, once again following standard rules of matrix arithmetic:

$$\begin{bmatrix} 1 & 0 & 0 \\ 0 & \cos(\theta) & \sin(\theta) \\ 0 & -\sin(\theta) & \cos(\theta) \end{bmatrix} \begin{bmatrix} \vec{a}_1 \\ \vec{a}_2 \\ \vec{a}_3 \end{bmatrix} = \begin{bmatrix} \vec{a}_1 \\ \vec{a}_2 \cos\theta + \vec{a}_3 \sin\theta \\ \vec{a}_3 \cos\theta - \vec{a}_2 \sin(\theta) \end{bmatrix} \quad \text{(A.5)}$$

The result is a vectrix describing a second frame, rotated about the 1-axis of the original frame $\vec{\mathcal{F}}_a$ by an angle θ; call this new frame $\vec{\mathcal{F}}_b$:

$$\vec{\mathcal{F}}_b = \mathbf{R}\vec{\mathcal{F}}_a \quad \text{(A.6)}$$

where in this case

$$\mathbf{R} = \begin{bmatrix} 1 & 0 & 0 \\ 0 & \cos(\theta) & \sin(\theta) \\ 0 & -\sin(\theta) & \cos(\theta) \end{bmatrix} \quad \text{(A.7)}$$

but in general $\mathbf{R}$ could by any rotation matrix. The rotation matrix $\mathbf{R}$ can also be expressed as a dot product of the two frames. First, note that for any frame $\vec{\mathcal{F}}_i$, $\vec{\mathcal{F}}_i \cdot \vec{\mathcal{F}}_i^T = \mathbf{I}$ where $\mathbf{I}$ is the 3×3 identity matrix:

$$\vec{\mathcal{F}}_i \cdot \vec{\mathcal{F}}_i^T = \begin{bmatrix} \vec{i}_1 \\ \vec{i}_2 \\ \vec{i}_3 \end{bmatrix} \cdot \begin{bmatrix} \vec{i}_1 & \vec{i}_2 & \vec{i}_3 \end{bmatrix} = \begin{bmatrix} \vec{i}_1 \cdot \vec{i}_1 & \vec{i}_1 \cdot \vec{i}_2 & \vec{i}_1 \cdot \vec{i}_3 \\ \vec{i}_2 \cdot \vec{i}_1 & \vec{i}_2 \cdot \vec{i}_2 & \vec{i}_2 \cdot \vec{i}_3 \\ \vec{i}_3 \cdot \vec{i}_1 & \vec{i}_3 \cdot \vec{i}_2 & \vec{i}_3 \cdot \vec{i}_3 \end{bmatrix} = \begin{bmatrix} 1 & 0 & 0 \\ 0 & 1 & 0 \\ 0 & 0 & 1 \end{bmatrix} = \mathbf{I} \quad \text{(A.8)}$$

then

$$\vec{\mathcal{F}}_b = \mathbf{R}\vec{\mathcal{F}}_a$$
$$\vec{\mathcal{F}}_b \cdot \vec{\mathcal{F}}_a^T = \mathbf{R}\vec{\mathcal{F}}_a \cdot \vec{\mathcal{F}}_a^T$$
$$\vec{\mathcal{F}}_b \cdot \vec{\mathcal{F}}_a^T = \mathbf{R}\mathbf{I}$$
$$\mathbf{R} = \vec{\mathcal{F}}_b \cdot \vec{\mathcal{F}}_a^T \quad \text{(A.9)}$$

It is now possible to determine the coefficients $\mathbf{v}_b$ of $\vec{v}$ as expressed in $\vec{\mathcal{F}}_b$.

$$\vec{v} = \vec{\mathcal{F}}_a^T \mathbf{v}_a \quad \text{(A.10)}$$
$$\vec{v} = \vec{\mathcal{F}}_b^T \mathbf{v}_b \quad \text{(A.11)}$$

Therefore,

$$\vec{\mathcal{F}}_a^T \mathbf{v}_a = \vec{\mathcal{F}}_b^T \mathbf{v}_b$$

Using the matrix transpose property $(\mathbf{AB})^T = \mathbf{B}^T \mathbf{A}^T$,

$$\mathbf{v}_a^T \vec{\mathcal{F}}_a = \mathbf{v}_b^T \vec{\mathcal{F}}_b$$
$$\mathbf{v}_a^T \vec{\mathcal{F}}_a \cdot \vec{\mathcal{F}}_a^T = \mathbf{v}_b^T \vec{\mathcal{F}}_b \cdot \vec{\mathcal{F}}_a^T$$
$$\mathbf{v}_a^T \mathbf{I} = \mathbf{v}_b^T \mathbf{R}$$
$$\mathbf{v}_a = \mathbf{R}^T \mathbf{v}_b$$

And since the transpose of any rotation matrix $\mathbf{R}$ is its own inverse,

$$\mathbf{v}_b = \mathbf{R}\mathbf{v}_a \tag{A.12}$$

For a more detailed description of vectrices, see Hughes [22].

Appendix B

Spline Curvature

Differentiating equation (5.2), the second derivative of a quadratic spline (with respect to τ) is

$$\frac{\mathrm{d}^2\vec{\ell}}{\mathrm{d}\tau^2} = 2(\vec{d_1} - \vec{d_0}) \tag{B.1}$$

The second derivative of a quadratic spline with respect to s is

$$
\begin{aligned}
\frac{\mathrm{d}^2\vec{\ell}}{\mathrm{d}s^2} &= \frac{\mathrm{d}}{\mathrm{d}s}\left(\frac{\mathrm{d}\vec{\ell}}{\mathrm{d}s}\right) \\[2mm]
&= \frac{\mathrm{d}}{\mathrm{d}s}\left(\frac{\mathrm{d}\vec{\ell}}{\mathrm{d}\tau}\frac{\mathrm{d}\tau}{\mathrm{d}s}\right) \\[2mm]
&= \frac{\mathrm{d}}{\mathrm{d}s}\left(\frac{\frac{\mathrm{d}\vec{\ell}}{\mathrm{d}\tau}}{\frac{\mathrm{d}s}{\mathrm{d}\tau}}\right) \\[2mm]
&= \frac{\mathrm{d}}{\mathrm{d}s}\left(\frac{\frac{\mathrm{d}\vec{\ell}}{\mathrm{d}\tau}}{\left|\frac{\mathrm{d}\vec{\ell}}{\mathrm{d}\tau}\right|}\right) \\[2mm]
&= \frac{\frac{\mathrm{d}}{\mathrm{d}s}\left(\frac{\mathrm{d}\vec{\ell}}{\mathrm{d}\tau}\right)\left|\frac{\mathrm{d}\vec{\ell}}{\mathrm{d}\tau}\right| - \frac{\mathrm{d}\vec{\ell}}{\mathrm{d}\tau}\frac{\mathrm{d}}{\mathrm{d}s}\left|\frac{\mathrm{d}\vec{\ell}}{\mathrm{d}\tau}\right|}{\left|\frac{\mathrm{d}\vec{\ell}}{\mathrm{d}\tau}\right|^2} \\[2mm]
&= \frac{\frac{\mathrm{d}}{\mathrm{d}\tau}\left(\frac{\mathrm{d}\vec{\ell}}{\mathrm{d}\tau}\right)\frac{\mathrm{d}\tau}{\mathrm{d}s}\left|\frac{\mathrm{d}\vec{\ell}}{\mathrm{d}\tau}\right| - \frac{\mathrm{d}\vec{\ell}}{\mathrm{d}\tau}\frac{\mathrm{d}}{\mathrm{d}s}\sqrt{\frac{\mathrm{d}\vec{\ell}}{\mathrm{d}\tau}\cdot\frac{\mathrm{d}\vec{\ell}}{\mathrm{d}\tau}}}{\frac{\mathrm{d}\vec{\ell}}{\mathrm{d}\tau}\cdot\frac{\mathrm{d}\vec{\ell}}{\mathrm{d}\tau}} \\[2mm]
&= \frac{\frac{\mathrm{d}^2\vec{\ell}}{\mathrm{d}\tau^2}\frac{\mathrm{d}\tau}{\mathrm{d}s}\frac{\mathrm{d}s}{\mathrm{d}\tau} - \frac{\mathrm{d}\vec{\ell}}{\mathrm{d}\tau}\left(\frac{1}{2}\left(\frac{\mathrm{d}\vec{\ell}}{\mathrm{d}\tau}\cdot\frac{\mathrm{d}\vec{\ell}}{\mathrm{d}\tau}\right)^{-1/2}\left(2\left(\frac{\mathrm{d}}{\mathrm{d}s}\frac{\mathrm{d}\vec{\ell}}{\mathrm{d}\tau}\right)\cdot\frac{\mathrm{d}\vec{\ell}}{\mathrm{d}\tau}\right)\right)}{\frac{\mathrm{d}\vec{\ell}}{\mathrm{d}\tau}\cdot\frac{\mathrm{d}\vec{\ell}}{\mathrm{d}\tau}}
\end{aligned}
$$

Simplifying,

$$\frac{\mathrm{d}^2\vec{\ell}}{\mathrm{d}s^2} = \frac{\frac{\mathrm{d}^2\vec{\ell}}{\mathrm{d}\tau^2} - \frac{\mathrm{d}\vec{\ell}}{\mathrm{d}\tau}\left(\frac{\frac{\mathrm{d}}{\mathrm{d}\tau}\frac{\mathrm{d}\vec{\ell}}{\mathrm{d}\tau}\frac{\mathrm{d}\tau}{\mathrm{d}s}\cdot\frac{\mathrm{d}\vec{\ell}}{\mathrm{d}\tau}}{\sqrt{\frac{\mathrm{d}\vec{\ell}}{\mathrm{d}\tau}\cdot\frac{\mathrm{d}\vec{\ell}}{\mathrm{d}\tau}}}\right)}{\frac{\mathrm{d}\vec{\ell}}{\mathrm{d}\tau}\cdot\frac{\mathrm{d}\vec{\ell}}{\mathrm{d}\tau}}$$

$$= \frac{\frac{\mathrm{d}^2\vec{\ell}}{\mathrm{d}\tau^2} - \frac{\mathrm{d}\vec{\ell}}{\mathrm{d}\tau}\left(\frac{\frac{\mathrm{d}^2\vec{\ell}}{\mathrm{d}\tau^2}\cdot\frac{\mathrm{d}\vec{\ell}}{\mathrm{d}\tau}}{\frac{\mathrm{d}s}{\mathrm{d}\tau}\sqrt{\frac{\mathrm{d}\vec{\ell}}{\mathrm{d}\tau}\cdot\frac{\mathrm{d}\vec{\ell}}{\mathrm{d}\tau}}}\right)}{\frac{\mathrm{d}\vec{\ell}}{\mathrm{d}\tau}\cdot\frac{\mathrm{d}\vec{\ell}}{\mathrm{d}\tau}}$$

$$= \frac{\frac{\mathrm{d}^2\vec{\ell}}{\mathrm{d}\tau^2} - \frac{\mathrm{d}\vec{\ell}}{\mathrm{d}\tau}\left(\frac{\frac{\mathrm{d}^2\vec{\ell}}{\mathrm{d}\tau^2}\cdot\frac{\mathrm{d}\vec{\ell}}{\mathrm{d}\tau}}{\frac{\mathrm{d}\vec{\ell}}{\mathrm{d}\tau}\cdot\frac{\mathrm{d}\vec{\ell}}{\mathrm{d}\tau}}\right)}{\frac{\mathrm{d}\vec{\ell}}{\mathrm{d}\tau}\cdot\frac{\mathrm{d}\vec{\ell}}{\mathrm{d}\tau}}$$

$$= \frac{\frac{\mathrm{d}^2\vec{\ell}}{\mathrm{d}\tau^2}\left(\frac{\mathrm{d}\vec{\ell}}{\mathrm{d}\tau}\cdot\frac{\mathrm{d}\vec{\ell}}{\mathrm{d}\tau}\right) - \frac{\mathrm{d}\vec{\ell}}{\mathrm{d}\tau}\left(\frac{\mathrm{d}^2\vec{\ell}}{\mathrm{d}\tau^2}\cdot\frac{\mathrm{d}\vec{\ell}}{\mathrm{d}\tau}\right)}{\left(\frac{\mathrm{d}\vec{\ell}}{\mathrm{d}\tau}\cdot\frac{\mathrm{d}\vec{\ell}}{\mathrm{d}\tau}\right)^2}$$

Using (5.2) and (B.1),

$$\frac{\mathrm{d}^2\vec{\ell}}{\mathrm{d}s^2} = \left(\frac{8(\vec{d_1} - \vec{d_0})\big((1-\tau)^2 d_{00} + 2\tau(1-\tau)d_{01} + \tau^2 d_{11}\big)}{16\big((1-\tau)^2 d_{00} + 2\tau(1-\tau)d_{01} + \tau^2 d_{11}\big)^2}\right)$$

$$- \left(\frac{8\big((1-\tau)\vec{d_0} + \tau\vec{d_1}\big)\big((\vec{d_1} - \vec{d_0})\cdot((1-\tau)\vec{d_0} + \tau\vec{d_1})\big)}{16\big((1-\tau)^2 d_{00} + 2\tau(1-\tau)d_{01} + \tau^2 d_{11}\big)^2}\right)$$

$$= \left(\frac{(\vec{d_1} - \vec{d_0})\big((1-\tau)^2 d_{00} + 2\tau(1-\tau)d_{01} + \tau^2 d_{11}\big)}{2\big((1-\tau)^2 d_{00} + 2\tau(1-\tau)d_{01} + \tau^2 d_{11}\big)^2}\right)$$

$$- \left(\frac{\big((1-\tau)\vec{d_0} + \tau\vec{d_1}\big)\big(-(1-\tau)d_{00} + (1-2t)d_{01} - \tau d_{11}\big)}{2\big((1-\tau)^2 d_{00} + 2\tau(1-\tau)d_{01} + \tau^2 d_{11}\big)^2}\right)$$

$$= \frac{\vec{d_1}\big((1-\tau)d_{00} + \tau d_{01}\big) - \vec{d_0}\big((1-\tau)d_{01} + \tau d_{11}\big)}{2\big((1-\tau)^2 d_{00} + 2\tau(1-\tau)d_{01} + \tau^2 d_{11}\big)^2} \tag{B.2}$$

The curvature κ of the spline is then equal to the magnitude of $\frac{\mathrm{d}^2\vec{\ell}}{\mathrm{d}s^2}$:

$$
\begin{aligned}
\kappa &= \left|\frac{\mathrm{d}^2\vec{\ell}}{\mathrm{d}s^2}\right| \\
&= \sqrt{\frac{\mathrm{d}^2\vec{\ell}}{\mathrm{d}s^2} \cdot \frac{\mathrm{d}^2\vec{\ell}}{\mathrm{d}s^2}} \\
&= \frac{\sqrt{\begin{aligned}&\left(\vec{d_1}\big((1-\tau)d_{00}+\tau d_{01}\big) - \vec{d_0}\big((1-\tau)d_{01}+\tau d_{11}\big)\right) \\ &\cdot \left(\vec{d_1}\big((1-\tau)d_{00}+\tau d_{01}\big) - \vec{d_0}\big((1-\tau)d_{01}+\tau d_{11}\big)\right)\end{aligned}}}{2\big((1-\tau)^2 d_{00} + 2\tau(1-\tau)d_{01} + \tau^2 d_{11}\big)^2} \\
&= \frac{\sqrt{\begin{aligned}&\big((1-\tau)d_{01}+\tau d_{11}\big)^2 d_{00} \\ &- 2\big((1-\tau)d_{01}+\tau d_{11}\big)\big((1-\tau)d_{00}+\tau d_{01}\big)d_{01} \\ &+ \big((1-\tau)d_{00}+\tau d_{01}\big)^2 d_{11}\end{aligned}}}{2\big((1-\tau)^2 d_{00} + 2\tau(1-\tau)d_{01} + \tau^2 d_{11}\big)^2} \\
&= \frac{\sqrt{(1-\tau)^2(d_{00}^2 d_{11} - d_{01}^2 d_{00}) + 2\tau(1-\tau)(d_{00}d_{01}d_{11} - d_{01}^3) + \tau^2(d_{00}^2 d_{11} - d_{11}d_{01}^2)}}{2\big((1-\tau)^2 d_{00} + 2\tau(1-\tau)d_{01} + \tau^2 d_{11}\big)^2} \\
&= \frac{\sqrt{(1-\tau)^2 d_{00}(d_{00}d_{11} - d_{01}^2) + 2\tau(1-\tau)d_{01}(d_{00}d_{11} - d_{01}^2) + \tau^2 d_{11}(d_{00}d_{11} - d_{01}^2)}}{2\big((1-\tau)^2 d_{00} + 2\tau(1-\tau)d_{01} + \tau^2 d_{11}\big)^2} \\
&= \frac{\sqrt{\big(d_{00}d_{11} - d_{01}^2\big)\big((1-\tau)^2 d_{00} + 2\tau(1-\tau)d_{01} + \tau^2 d_{11}\big)}}{2\big((1-\tau)^2 d_{00} + 2\tau(1-\tau)d_{01} + \tau^2 d_{11}\big)^2} \\
&= \frac{1}{2}\sqrt{\frac{(d_{00}d_{11} - d_{01}^2)}{\big((1-\tau)^2 d_{00} + 2\tau(1-\tau)d_{01} + \tau^2 d_{11}\big)^3}}
\end{aligned}
$$

Using equation (5.5),

$$\kappa = \frac{4\sqrt{d_{00}d_{11} - d_{01}^2}}{\xi^3} \tag{B.3}$$